

**NONLINEAR STRAIN-DISPLACEMENT RELATIONS IN THE  
DYNAMICS OF A TWO-LINK FLEXIBLE MANIPULATOR**

by

Carlos Eduardo Padilla Santos

B.S. in Mechanical and Aerospace Engineering  
Princeton University  
(1986)

SUBMITTED TO THE DEPARTMENT OF AERONAUTICS AND  
ASTRONAUTICS IN PARTIAL FULFILLMENT OF THE  
REQUIREMENTS FOR THE DEGREE OF

MASTER OF SCIENCE IN AERONAUTICS AND ASTRONAUTICS  
at the

MASSACHUSETTS INSTITUTE OF TECHNOLOGY  
May 1989

© Carlos E. Padilla 1989. All rights reserved

The author hereby grants to MIT permission to reproduce and to distribute  
copies of this thesis document in whole or in part.

Signature of Author \_\_\_\_\_  
Department of Aeronautics and Astronautics  
May 12, 1989

Certified by \_\_\_\_\_  
Prof. Andreas von Flotow  
Assistant Professor of Aeronautics and Astronautics  
Thesis Supervisor

Accepted by \_\_\_\_\_  
Prof. Harold Y. Wachman  
Chairman, Departmental Graduate Committee

ARCHIVES  
MASSACHUSETTS INSTITUTE  
OF TECHNOLOGY

JUN 07 1989

# ABSTRACT

The equations of motion of a flexible, two-link, planar manipulator are derived via the Kane formalism, correctly linearized in small elastic deflections and speeds through the use of nonlinear strain-displacement relations. Ordinary differential equations are obtained as a result of modelling the links as Bernoulli-Euler beams and expanding the elastic deflections in terms of cantilever modes. A simulation is implemented that allows the determination of the manipulator's dynamic response to desired forcing functions in the form of joint torques. Slew maneuver simulation results are then compared for models with and without the properly modelled kinematics of deformation, in order to quantify the relative significance of certain nonlinear terms in the motion equations. It is found that rigid body motion limits exist below which elastic nonlinear terms are negligible. These are nonlinear terms that involve the generalized elastic coordinates and their time derivatives. These rigid body motion limits are set by the requirement that inconsistently linearized equations of motion (those derived using linear strain-displacement or linear kinematics of deformation) yield accurate results. Within these limits, it is found that equations derived ignoring all elastic nonlinear terms produce simulation results that are as good as the inconsistently and consistently linearized equations.

# ACKNOWLEDGEMENTS

This research work was made possible by a National Science Foundation Minority Graduate Fellowship. The author wishes to thank the people at NSF who made the award possible.

Special thanks go to Prof. Andy von Flotow for his invaluable support and guidance. His accessibility, interest, and quick insight helped create an enjoyable and challenging environment.

The author also wishes to thank the many friends and relatives whose unfaltering support and caring made the work bearable; in particular Dave for his timely advice, and Javier for pushing to the limit.

Finally, I want to continue thanking my father, mother, sister, and brother for always being there.

# TABLE OF CONTENTS

Abstract .....	2
Acknowledgements .....	3
List of Figures .....	7
List of Tables .....	9
Chapter 1: Introduction .....	10
Chapter 2: Dynamics .....	13
2.1 System Model .....	13
2.1.1 List of Assumptions .....	14
2.2 System Kinematics .....	15
2.2.1 Shoulder Body .....	15
2.2.2 Inboard Link .....	16
2.2.3 Elbow Joint .....	17
2.2.4 Outboard Link .....	20
2.2.5 Tip Mass .....	21
2.3 Linearized Dynamics - Assumed-Modes Method .....	23
2.3.1 Linearized Velocities .....	26
2.3.2 Linearized Angular Velocities .....	27
2.4 Kane's Dynamical Equations .....	27
2.4.1 Generalized Inertia Forces .....	28
2.4.2 Generalized Active Forces .....	31
2.4.3 Equations of Motion .....	34
Chapter 3: Dynamic Analysis .....	36
3.1 Form of the Equations of Motion for a Chain of Elastic Bodies .....	36
3.2 Comparison Models .....	39
3.3 Single Flexible Body Example .....	40
3.3.1 Pure Rotation .....	40
3.3.2 Pure Linear Acceleration .....	43

3.3.3 General Stability Boundary of the Consistent Model .....	44
3.4 Predictions .....	46
3.5 Eigenanalysis of the Two-link Manipulator .....	46
Chapter 4: Simulation Results .....	55
4.1 Numerical Simulation .....	55
4.2 Time Scaling of Trajectories .....	57
4.3 Results .....	58
4.3.1 Spinning of the Outboard Link .....	58
4.3.2 First Smooth Trajectory .....	59
4.3.3 Second Smooth Trajectory .....	65
4.3.4 Minimum-Time Trajectory .....	70
4.4 Discussion .....	74
Chapter 5: Conclusions .....	77
References .....	79
Appendix A: Nonlinear Strain-Displacement and Linearization .....	82
A.1 General Discussion .....	82
A.2 A Simple Example .....	84
A.2.1 Lagrange's Equations of Motion .....	85
A.2.2 Kane's Dynamical Equations .....	89
Appendix B: Calculation of Modal Integrals and Constants .....	91
B.1 Constants Independent of Mode Shape .....	91
B.2 Mode Shape Dependent Constants .....	92
B.2.1 Constants obtained using linear strain-displacement relations .....	93
B.2.2 Constants obtained through proper linearization .....	95
Appendix C: Equations of Motion .....	97
C.1 Entries in the Stiffness Matrix .....	98

C.2 Entries in the Mass Matrix .....	98
C.3 Entries in the Vector of Nonlinear Forces .....	101
Appendix D: FORTRAN Simulation Code .....	104

# LIST OF FIGURES

2.1	Schematic of the Two-link Flexible Manipulator .....	14
2.2	Definitions for Link Kinematics .....	16
2.3	Schematic of Internal Forces and Elbow Joint Definitions .....	32
3.1	Fundamental Bending Frequency of Spinning Beam v.s. Spin Rate .....	42
3.2	Stability Boundary for Axial Acceleration Below Critical .....	45
3.3	Stability Boundary for Axial Acceleration Above Critical .....	45
3.4	s-plane Plot of Manipulator Frequencies with Locked Joints	
	a) For Elbow Angle equal to 0 deg. ....	48
	b) Close-up of Lower Frequency Range for Different values of Elbow Angle ..	48
3.5	First Four Manipulator Mode Shapes with Joints Free .....	49
3.6	First Four Manipulator Mode Shapes with Joints Locked ( $\beta=0$ deg) .....	50
3.7	First Four Manipulator Mode Shapes with Joints Locked ( $\beta=45$ deg).....	51
3.8	First Four Manipulator Mode Shapes with Joints Locked ( $\beta=90$ deg).....	52
3.9	First Four Manipulator Mode Shapes with Joints Locked ( $\beta=135$ deg) .....	53
3.10	First Four Manipulator Mode Shapes with Joints Locked ( $\beta=180$ deg) .....	54
4.1	Smooth Spin-up Maneuver of the Outboard Link .....	59
4.2	Computed Torques for First Smooth Trajectory .....	61
4.3	First Smooth Trajectory with $\alpha=0.2865$ .....	62
4.4	First Smooth Trajectory with $\alpha=0.4197$ .....	63
4.5	First Smooth Trajectory with $\alpha=2.0$ .....	64
4.6	Computed Torques for Second Smooth Trajectory.....	66
4.7	Second Smooth Trajectory with $\alpha=1.0$ .....	67
4.8	Second Smooth Trajectory with $\alpha=0.1685$ .....	68
4.9	Second Smooth Trajectory with $\alpha=1.2$ .....	69

4.10	Time-Optimal Trajectory for Two-link Rigid Manipulator.....	72
4.11	Time-Optimal Trajectory for Two-link Flexible Manipulator.....	73
4.12	Comparison of Right Singular Vectors for the Mass Matrix at Failure.....	75
A.1	Single Beam Attached to a Moving Base .....	84



# LIST OF TABLES

2.1	Linearized Partial Velocities .....	29
2.2	Linearized Partial Angular Velocities .....	31
3.1	Configuration Dependent Manipulator Frequencies .....	47
3.2	Frequencies for Each Link when the Other is Rigid and Joints are Locked .....	48
4.1	Physical Properties of the Two-link Manipulator .....	57
A.1	Linearized Partial Velocities and Angular Velocities.....	90

# CHAPTER 1: INTRODUCTION

Manipulators for space applications need to be lightweight for economical reasons. It is also desirable that they be faster and more autonomous than the SRMS (Space Shuttle Remote Manipulator System), which moves relatively slowly (0.1 deg/sec) in order to minimize elastic excitation, and is teleoperated. The first of these requirements results in manipulators with significant structural flexibility (the SRMS has a natural vibration frequency of 0.3 Hz unloaded and with extended and locked links); while the need to expand the performance/operational envelope requires that this flexibility be modelled accurately.

Much work has been done on the dynamic modelling of open chains of rigid and elastic bodies (see references in [25],[12]). The heightened interest in multibody simulation, particularly flexible multibody simulation, prompted a workshop on the subject sponsored by the Jet Propulsion Laboratory late last year [15]. As stated in the preface to the Proceedings of the Workshop, this interest is being driven by mission requirements put forth by NASA and the SDIO that call for high angular rate and acceleration articulation of complex arrangements of interconnected rigid and flexible bodies.

A review of this literature shows that it is common practice to assume small elastic deflections and beam-like links when modelling structural flexibility in appendages or robotic links. Small rigid body motions and velocities (translations and relative angular motion of the links) have sometimes been assumed to simplify the equations of motion. In particular, so-called "rate-linear" equations have been proposed to yield tractable motion equations when the rigid body rates are assumed small enough so that second order terms can be neglected [8]. It has been pointed out by Hollerbach [4], however, that gyroscopic terms (which are second order in rigid body rates) are as important as inertia terms in the motion equations for open chains of rigid links. For this reason, it would seem desirable to obtain motion equations that do not ignore these gyroscopic terms and are in consequence valid for rigid body motions. Some work has been done in this respect for the case of a manipulator, using finite element modelling for the small elastic deflections but allowing large rigid body motion and high velocities [29]. This results in a large number of equations that are reduced using Guyan model reduction.

In recent years a fundamental limitation of linear finite element formulations of flexible deformations in flexible multibody simulation programs such as TREETOPS[31], DISCOS[3], etc. has been pointed out [23,24,27]. This limitation could be characterized as a premature linearization of velocity expressions that is implicit in a linear finite element or modal formulation of the motion equations for flexible bodies [24]. Kane et al. [11] demonstrated this flaw of the traditional approach numerically by simulating a simple system consisting of a flexible beam attached to a rigid base spinning in the plane. This simulation yielded the surprising and intuitively wrong result of the beam diverging during a spin up maneuver [23]. Probably because of this simple example the "prematurely linearized" equations of motion are said to lack the "spin-stiffening effect."

The purpose of this thesis is to provide the equations of motion of a flexible, two-link, planar manipulator, correctly linearized in small elastic deflection and speeds, but fully nonlinear in rigid body motions. The links are modelled as Bernoulli-Euler beams and the elastic deflections are expanded in terms of cantilever (clamped-free) modes. This results in a small number of equations that can be derived analytically. The equations of motion are desired to provide the capability to determine the dynamic response of a two-link manipulator to desired forcing functions for control experiments purposes. It is further desired that the developed simulation allow for the use of a variable number of modes in order to test effects such as spillover when reduced-order controllers are tested.

In view of the limitation of certain linear finite element multibody programs, it is further desired to investigate the relative significance of "elastic" nonlinear terms in the equations of motion. These are nonlinear terms that involve the generalized elastic coordinates and their time derivatives. For this purpose, the simulation is developed with the capability of ignoring select elastic nonlinear terms, or all elastic nonlinear terms.

## **THESIS OVERVIEW**

Chapter two presents the derivation of the linearized equations of motion for the two-link manipulator. Using Kane's formalism [9] the correctly linearized equations are obtained through the proper use of nonlinear strain-displacement relations.

In chapter three, a dynamic analysis of a simplified single beam example is used to investigate the relative significance of elastic nonlinear terms. Three levels of increasing simplification of the linearized motion equations are proposed for this investigation.

The results of the previous chapter are compared to the results of numerical simulation of the two-link manipulator in chapter four. Four different open loop trajectories are investigated and conclusions about the dynamic modelling and relative significance of nonlinear terms are drawn.

# CHAPTER 2: DYNAMICS

## INTRODUCTION

The equations of motion of a planar, flexible, two-link manipulator, linearized in small elastic coordinates and speeds, are developed in this chapter. After describing the system model and stating the assumptions made, the system kinematics are presented. In section 2.2, the kinematics of the system are derived without making any assumptions as to the size of generalized elastic coordinates. It is in section 2.3 that the kinematic expressions are linearized assuming small elastic coordinates and speeds. In the last section of this chapter the dynamic equations for the nonlinear system, correct to first order in elastic coordinates and speeds, are derived using Kane's formalism.

## 2.1 SYSTEM MODEL

The dynamics of a planar, two-link, flexible arm with revolute joints, composed of three rigid bodies connected by two slender uniform beams (see Fig. 2.1) are to be investigated. The equations of motion for this system are derived using Kane's formalism [9] together with second order strain-displacement relations. The equations are thus exact to first order in the beams' elastic generalized coordinates and speeds, but fully nonlinear in rigid body coordinates and rates. The normal to the plane of motion is parallel to the local acceleration of gravity, so gravity can be ignored. Independent axial extensions of the beams are ignored (i.e., the axial strain at the neutral axis is assumed zero for each beam). The elbow joint is actually modelled as two bodies: one attached to link 1 in a cantilevered way and the other, free to rotate with respect to the first, with link 2 attached to it in a cantilevered way also. Both elbow bodies are rigid and share the hinge point but their mass centers are allowed to be offset from the hinge point. One percent modal damping is added to the model to represent material damping. Actuation is assumed in the form of shoulder and elbow torques. The equations of motion for this system are available in Appendix C.

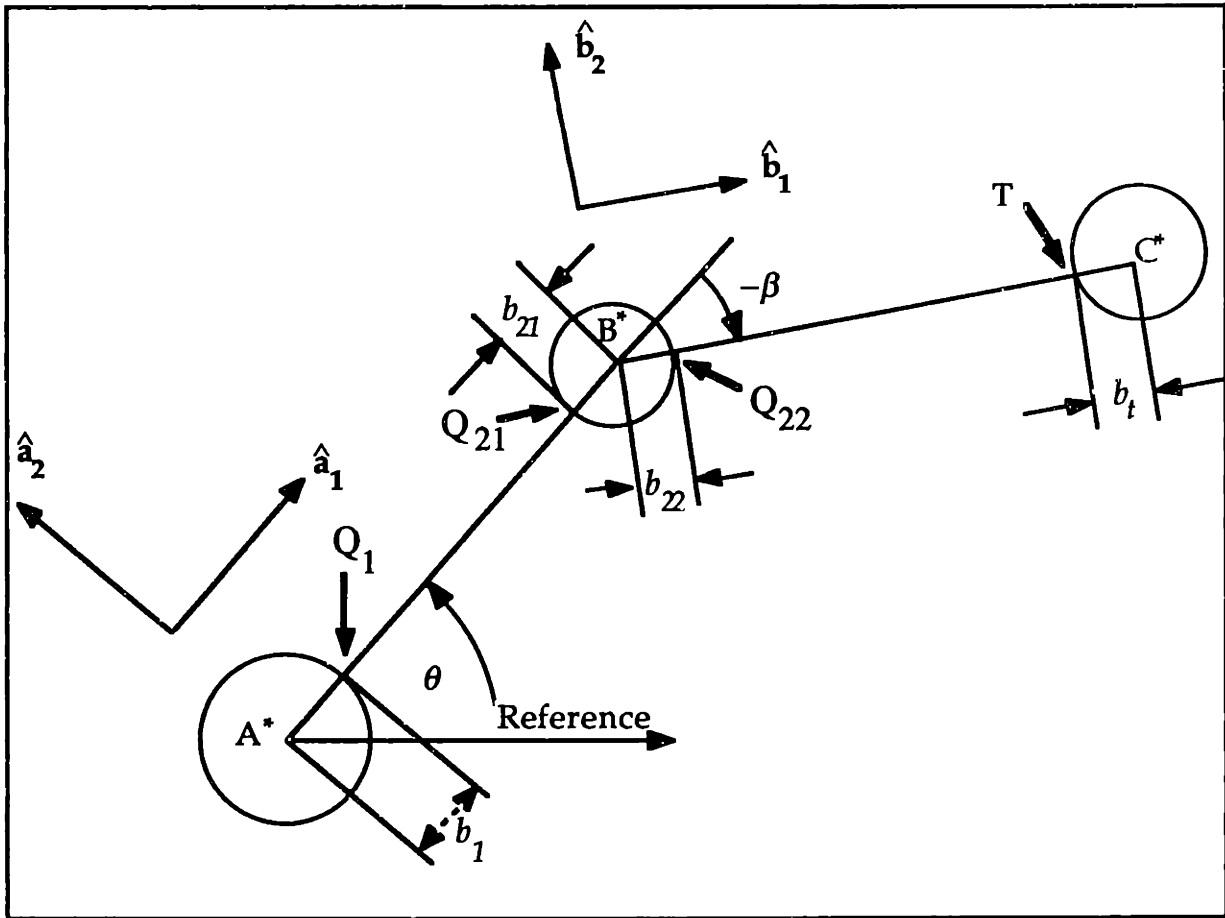


**Figure 2.1: Schematic of the Two-link Flexible Manipulator**

The rigid body generalized coordinates, the shoulder angle,  $\theta$ , and the relative elbow angle,  $\beta$ , are defined in Figure 2.1. In Figure 2.2 it is anticipated that the transverse deflection of the inboard link,  $u_2$ , will be expanded in a series of assumed mode shapes. The time-dependent coefficients of these assumed modes,  $q_i$  ( $i=1, \dots, n$ ), are the generalized elastic coordinates for the beam. An analogous definition for the outboard link results in generalized elastic coordinates  $p_j$  ( $j=1, \dots, m$ ). This set of  $2+n+m$  generalized coordinates uniquely specifies the configuration of the two-link manipulator.

### 2.1.1 List of Assumptions

The following is a list of the assumptions made in the derivation of the linearized equations of motion presented in the rest of this chapter.

1. The links are modelled as nominally straight, uniform beams, with symmetric cross-sections about axes  $a_2$  and  $a_3$  ( $b_2$  and  $b_3$ ) when undeformed.
2. The cross-sectional dimensions of the beams are much smaller than the lengths, so that rotary inertia and shear effects are negligible [18].

3. Torsion is ignored.
4. No relative motion is allowed between links and points of attachment to the rigid bodies.
5. Friction, damping, and flexibility have been assumed negligible at the joints.
6. Actuators are assumed to apply torques. Other actuator dynamics are not taken into consideration.
7. All rigid bodies are modelled as a lumped mass, situated at the mass center, and lumped moment of inertia, but the mass centers can be offset from the point of attachment of the links to account for planar dimensions of the same bodies.
8. The shoulder body rotates in inertial frame, but undergoes no translation.
9. The elbow joint is made up of two bodies that share the hinge point, but have mass centers that can be offset from the hinge point (see Fig. 2.3).
10. The relative elbow angle,  $\beta$ , is measured between the tangent to the neutral axis of link two (outboard) at its point of attachment to the elbow ( $y=0$ ), and the tangent to the neutral axis of link one (inboard) at the end of link one attached to the elbow (i.e.,  $x=l_1$ ).
11. Elastic deformation coordinates and rates for both links are assumed small enough so that second order terms can be ignored.

## 2.2 SYSTEM KINEMATICS

### 2.2.1 Shoulder Body

Following Kane [9,10], an embedded reference frame is associated with each rigid body (see Fig. 2.1). Frame  $(\mathbf{a}_1, \mathbf{a}_2, \mathbf{a}_3)$  is associated with the shoulder body, denoted as body A, and its origin coincides with the body's center of mass. The  $\mathbf{a}_1$  axis extends along the line  $b_1$  and thus along the neutral axis of the undeformed link 1. Axis  $\mathbf{a}_2$  is perpendicular to this one in the plane of motion, and  $\mathbf{a}_3$  is such that A is a right-handed, Cartesian coordinate system. Body A is free to rotate in the plane but pinned at its mass center  $A^*$ , so that frame A can only rotate and undergoes no translation. The motion of A in the inertial frame N  $(\mathbf{n}_1, \mathbf{n}_2, \mathbf{n}_3)$  is pure rotation, where the angular velocity of A in N is given by

$${}^N \underline{\omega}^A = \omega_3 \hat{a}_3 \quad (1)$$

and  $\omega_3$  uniquely defines the motion of body A. This quantity is termed a generalized speed in Kane's formalism.

### 2.2.2 Inboard Link

Following [11], the motion of link 1 in the inertial reference frame N is described by introducing a rigid differential element  $P_1$  of link 1, with centroid  $C_1$  and elastic center  $E_1$  located at a distance  $x$  from  $Q_1$ , when the link is undeformed (see Fig. 2.2). No relative motion is allowed between body A and link 1 at  $Q_1$ , i.e., link 1 is attached to A in a cantilevered way. The position of point  $E_1$  (which coincides with  $C_1$  under the stated assumptions) in the frame A after deformation is found by applying the translations

$$u_1 \hat{a}_1 \quad \text{and} \quad u_2 \hat{a}_2.$$

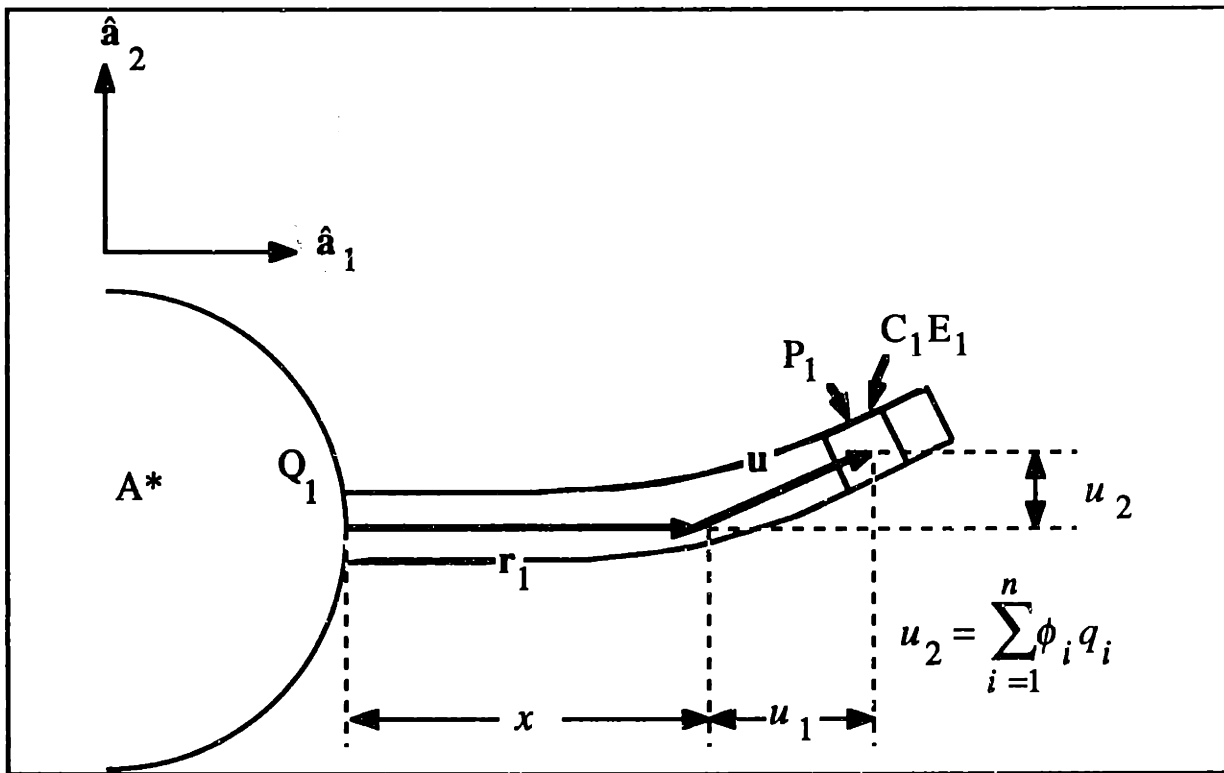


Figure 2.2: Definitions for Link Kinematics

Defining  $r_1$  and  $u$  as



$$\begin{aligned}\mathbf{r}_1 &\equiv x \hat{\mathbf{a}}_1 \\ \mathbf{u}(x, t) &\equiv u_1(x, t) \hat{\mathbf{a}}_1 + u_2(x, t) \hat{\mathbf{a}}_2\end{aligned}\quad (1)$$

the position vector from  $Q_1$  to  $E_1$  (see Fig. 2.2) can be expressed as

$$\mathbf{p}^{Q_1 E_1} = \mathbf{r}_1 + \mathbf{u}(x, t). \quad (2)$$

Further, since

$$\mathbf{p}^{E_1 C_1} = 0,$$

$$\mathbf{p}^{Q_1 C_1} = \mathbf{p}^{Q_1 E_1} = \mathbf{r}_1 + \mathbf{u}(x, t) = (x + u_1) \hat{\mathbf{a}}_1 + u_2 \hat{\mathbf{a}}_2. \quad (3)$$

Finally, the position vector for  $C_1$  in frame A is obtained:

$$\mathbf{p}^{A^* C_1} = \mathbf{p}^{A^* Q_1} + \mathbf{p}^{Q_1 C_1} = (b_1 + x + u_1) \hat{\mathbf{a}}_1 + u_2 \hat{\mathbf{a}}_2. \quad (4)$$

Now it is possible to write down the velocities of  $Q_1$  and  $P_1$  in N:

$$\begin{aligned}N_{\mathbf{v}}^{Q_1} &= N_{\mathbf{v}^{A^*}} + N_{\underline{\omega}^A} \times \mathbf{p}^{A^* Q_1} + {}^A \mathbf{v}^{Q_1} \\ &= b_1 \omega_3 \hat{\mathbf{a}}_2 \\ N_{\mathbf{v}}^{C_1} &= N_{\mathbf{v}^{A^*}} + N_{\underline{\omega}^A} \times \mathbf{p}^{A^* C_1} + {}^A \mathbf{v}^{C_1} \\ &= (\dot{u}_1 - \omega_3 u_2) \hat{\mathbf{a}}_1 + [\dot{u}_2 + \omega_3 (b_1 + x + u_1)] \hat{\mathbf{a}}_2\end{aligned}\quad (5)$$

where

$$N_{\mathbf{v}^{A^*}} = {}^A \mathbf{v}^{Q_1} = 0. \quad (6)$$

### 2.2.3 Elbow Joint

As mentioned in section 2.1, it is assumed that the elbow consists of two rigid bodies (see Fig. 2.3). Body  $B_1$  is attached to link 1 at point  $Q_{21}$ , while body  $B_2$  is connected to  $B_1$  at the hinge point H. No relative motion is allowed between link 1 and body  $B_1$  at  $Q_{21}$ . The mass center of  $B_1$ ,  $B_1^*$ , can be offset from the hinge point. This

configuration of elbow bodies was chosen to allow the simulation maximum flexibility, as it is easier to align hardware hinge points than to place mass centers.

To characterize the motion of  $B_1$  in  $N$ , it is convenient to first obtain the velocity of  $H$  in  $N$ :

$${}^N \mathbf{v}^H = {}^N \mathbf{v}^{A^*} + {}^N \underline{\boldsymbol{\omega}}^A \times \mathbf{p}^{A^*H} + {}^A \mathbf{v}^H. \quad (1)$$

To be able to write down the distance from  $A^*$  to  $H$ , note that the angle between the normal to the cross-section of the beam at  $x$  after deformation, and the neutral axis before deformation, is, for a Bernoulli-Euler beam (where distortion due to shear is ignored-see [18])

$$\frac{\partial}{\partial x} u_2(x, t)$$

and defining

$$\alpha_1 = \left. \frac{\partial u_2}{\partial x} \right|_{x=l_1}, \quad (2)$$

the position vector results:

$$\mathbf{p}^{A^*H} = [b_1 + l_1 + u_1(l_1, t) + b_{21} \cos(\alpha_1)] \hat{\mathbf{a}}_1 + [u_2(l_1, t) + b_{21} \sin(\alpha_1)] \hat{\mathbf{a}}_2. \quad (3)$$

This yields for the desired hinge point velocity vector

$$\begin{aligned} {}^N \mathbf{v}^H = & \{\dot{u}_1(l_1, t) - b_{21} \dot{\alpha}_1 \sin \alpha_1 - \omega_3 [u_2(l_1, t) + b_{21} \sin \alpha_1]\} \hat{\mathbf{a}}_1 \\ & + \{\dot{u}_2(l_1, t) + b_{21} \dot{\alpha}_1 \cos \alpha_1 + \omega_3 [b_1 + l_1 + u_1(l_1, t) + b_{21} \cos \alpha_1]\} \hat{\mathbf{a}}_2 \end{aligned} \quad (4)$$

where the following convention has been used:

$$\dot{\alpha}_1 = \frac{\partial}{\partial t} \left[ \left. \frac{\partial u_2}{\partial x} \right|_{x=l_1} \right] \quad (5)$$

The angular velocity of  $B_1$  is then

$${}^N \underline{\boldsymbol{\omega}}^{B_1} = (\dot{\alpha}_1 + \omega_3) \hat{\mathbf{a}}_3 \quad (6)$$

and it is possible to write the velocity of  $B_1^*$  in N as

$$\begin{aligned} {}^N \mathbf{v}^{B_1^*} &= {}^N \mathbf{v}^H + {}^N \underline{\omega}^{B_1} \times \mathbf{p}^{HB_1^*} + {}^{B_1} \mathbf{v}^{B_1^*} \\ &= {}^N \mathbf{v}^H - e_1(\dot{\alpha}_1 + \omega_3) \sin(\gamma_1 + \alpha_1) \hat{\mathbf{a}}_1 + e_1(\dot{\alpha}_1 + \omega_3) \cos(\gamma_1 + \alpha_1) \hat{\mathbf{a}}_2 \end{aligned} \quad (7)$$

where the following expression has been used for the distance from the hinge point to the mass center of  $B_1$

$$\begin{aligned} \mathbf{p}^{HB_1^*} &= e_1 \cos(\gamma_1 + \alpha_1) \hat{\mathbf{a}}_1 + e_1 \sin(\gamma_1 + \alpha_1) \hat{\mathbf{a}}_2 \\ {}^{B_1} \mathbf{v}^{B_1^*} &= 0. \end{aligned} \quad (8)$$

The velocity of point  $Q_{21}$  in body  $B_1$  will be needed in the determination of the generalized active forces (see section 2.4.2), and so it is written down here for the sake of completeness:

$$\begin{aligned} {}^N \mathbf{v}^{Q_{21}} &= {}^N \mathbf{v}^{C_1} \Big|_{x=l_1} \\ &= [\dot{u}_1(l_1, t) - \omega_3 u_2(l_1, t)] \hat{\mathbf{a}}_1 + \{\dot{u}_2(l_1, t) + \omega_3 [b_1 + l_1 + u_1(l_1, t)]\} \hat{\mathbf{a}}_2. \end{aligned} \quad (9)$$

The second elbow body,  $B_2$ , is free to rotate with respect to body  $B_1$  about the hinge point H. Frame B ( $\mathbf{b}_1, \mathbf{b}_2, \mathbf{b}_3$ ) is associated with body  $B_2$ , and the origin of the coordinate frame coincides with the hinge point. The axis  $\mathbf{b}_1$  lies along line  $b_{22}$ , that is, also along the neutral axis of the undeformed link 2;  $\mathbf{b}_2$  is perpendicular to  $\mathbf{b}_1$  in the plane of motion;  $\mathbf{b}_3$  completes a right-handed rectangular coordinate system. As in the case of  $B_1$ ,  $B_2^*$  can be offset from the hinge point. The rotational motion of  $B_2$  in N is characterized by

$$\Omega_3 = \dot{\beta} \quad (10)$$

where  $\beta$  is the relative angle between bodies  $B_1$  and  $B_2$ , and the angular velocity of  $B_2$  in the inertial frame is given by:

$${}^N \underline{\omega}^B = {}^N \underline{\omega}^{B_2} = (\omega_3 + \dot{\alpha}_1 + \Omega_3) \hat{\mathbf{a}}_3. \quad (11)$$

The velocity of  $B_2^*$  in N can be written down immediately as

$$\begin{aligned}
{}^N \mathbf{v}^{B_2^*} &= {}^N \mathbf{v}^H + {}^N \boldsymbol{\omega}^{B_2} \times \mathbf{p}^{HB_2^*} + {}^B \mathbf{v}^{B_2^*} \\
&= {}^N \mathbf{v}^H - e_2 {}^N \omega^{B_2} \sin \gamma_2 \hat{\mathbf{b}}_1 + e_2 {}^N \omega^{B_2} \cos \gamma_2 \hat{\mathbf{b}}_2
\end{aligned} \tag{12}$$

where the following facts have been used:

$$\begin{aligned}
\mathbf{p}^{HB_2^*} &= e_2 \cos \gamma_2 \hat{\mathbf{b}}_1 + e_2 \sin \gamma_2 \hat{\mathbf{b}}_2 \\
{}^B \mathbf{v}^{B_2^*} &= 0
\end{aligned} \tag{13}$$

and the following definition has been made:

$${}^N \omega^{B_2} = \omega_3 + \dot{\alpha}_1 + \Omega_3. \tag{14}$$

## 2.2.4 Outboard Link

Using a similar approach to that of section 2.2.2, the motion of link 2 in N is described by introducing a rigid differential element  $P_2$  of link 2, with centroid  $C_2$  and elastic center  $E_2$ , located at a distance  $y$  from point  $Q_{22}$  when the link is undeformed. Again relative motion is disallowed between body  $B_2$  and link 2 at the point  $Q_{22}$  (see Fig. 2.1). Defining  $\mathbf{r}_2$  and  $\mathbf{v}$  as

$$\begin{aligned}
\mathbf{r}_2 &\equiv y \hat{\mathbf{b}}_1 \\
\mathbf{v} &\equiv v_1(y, t) \hat{\mathbf{b}}_1 + v_2(y, t) \hat{\mathbf{b}}_2,
\end{aligned} \tag{1}$$

and following the set of assumptions described in section 2.1, the position vector from H to  $C_2$  results:

$$\begin{aligned}
\mathbf{p}^{E_2 C_2} &= 0 \\
\mathbf{p}^{Q_{22} C_2} &= \mathbf{p}^{Q_{22} E_2} = \mathbf{r}_2 + \mathbf{v}(y, t) = (y + v_1) \hat{\mathbf{b}}_1 + v_2 \hat{\mathbf{b}}_2 \\
\mathbf{p}^{H C_2} &= \mathbf{p}^{H Q_{22}} + \mathbf{p}^{Q_{22} C_2} = (b_{22} + y + v_1) \hat{\mathbf{b}}_1 + v_2 \hat{\mathbf{b}}_2.
\end{aligned} \tag{2}$$

In equation (2),  $\mathbf{v}$  is the vector that describes the change in position of  $E_2$  due to the deformation.

It is now possible to write the velocities of  $Q_{22}$  and  $P_2$  in the inertial reference frame:

$$\begin{aligned}
N_{\mathbf{v}}^{Q_{22}} &= N_{\mathbf{v}}^H + N_{\underline{\omega}}^B \times \mathbf{p}^{HQ_{22}} + {}^B \mathbf{v}^{Q_{22}} \\
&= N_{\mathbf{v}}^H + N_{\omega}^B b_{22} \hat{\mathbf{b}}_2 \\
N_{\mathbf{v}}^{C_2} &= N_{\mathbf{v}}^H + N_{\underline{\omega}}^B \times \mathbf{p}^{HC_2} + {}^B \mathbf{v}^{C_2} \\
&= N_{\mathbf{v}}^H + (\dot{v}_1 - N_{\omega}^B v_2) \hat{\mathbf{b}}_1 + [\dot{v}_2 + N_{\omega}^B (b_{22} + y + v_1)] \hat{\mathbf{b}}_2
\end{aligned} \tag{3}$$

where

$$\begin{aligned}
\mathbf{p}^{HQ_{22}} &= b_{22} \hat{\mathbf{b}}_1 \\
{}^B \mathbf{v}^{C_2} &= \left( \frac{d}{dt} \right)_B \mathbf{p}^{HC_2}.
\end{aligned} \tag{4}$$

### 2.2.5 Tip Mass

Finally, the kinematics of the "end effector," or tip body, are determined. Again it is assumed that the tip rigid body C is attached rigidly to link 2 at point T. As in the case of link 1, the angle between the normal to the cross-section of the beam at  $y$  after deformation and the neutral axis before deformation is given by:

$$\frac{\partial}{\partial y} v_2(y, t).$$

Note that as before, the above equation is true due to the assumption of Bernoulli-Euler beams. Defining

$$\alpha_2 = \left. \frac{\partial v_2}{\partial y} \right|_{y=l_2}, \tag{1}$$

the distance from H to C\* is:

$$\mathbf{p}^{HC^*} = [b_{22} + l_2 + v_1(l_2, t) + b_t \cos(\alpha_2)] \hat{\mathbf{b}}_1 + [v_2(l_2, t) + b_t \sin(\alpha_2)] \hat{\mathbf{b}}_2. \tag{2}$$

Then the velocity in the inertial reference frame of the mass center  $C^*$  of body C is given by:

$$\begin{aligned}
{}^N \mathbf{v}^{C^*} &= {}^N \mathbf{v}^H + {}^N \underline{\boldsymbol{\omega}}^B \times \mathbf{p}^{HC^*} + {}^B \mathbf{v}^{C^*} \\
&= {}^N \mathbf{v}^H + \{\dot{v}_1(l_2, t) - b_l \dot{\alpha}_2 \sin \alpha_2 - {}^N \omega^B [v_2(l_2, t) + b_l \sin \alpha_2]\} \hat{\mathbf{b}}_1 \\
&+ \{\dot{v}_2(l_2, t) + b_l \dot{\alpha}_2 \cos \alpha_2 + {}^N \omega^B [b_{22} + l_2 + v_1(l_2, t) + b_l \cos \alpha_2]\} \hat{\mathbf{b}}_2 \quad (3)
\end{aligned}$$

where

$${}^B \mathbf{v}^{C^*} = \left. \frac{d}{dt} \right)_B \mathbf{p}^{HC^*}. \quad (4)$$

The angular velocity of C in the inertial frame is

$${}^N \underline{\boldsymbol{\omega}}^C = (\omega_3 + \dot{\alpha}_1 + \Omega_3 + \dot{\alpha}_2) \hat{\mathbf{a}}_3. \quad (5)$$

The velocity of point T in N is

$$\begin{aligned}
{}^N \mathbf{v}^T &= {}^N \mathbf{v}^{C_2} \Big|_{y=l_2} \\
&= {}^N \mathbf{v}^H + [\dot{v}_1(l_2, t) - {}^N \omega^B v_2(l_2, t)] \hat{\mathbf{b}}_1 \\
&+ \{\dot{v}_2(l_2, t) + {}^N \omega^B [b_{22} + l_2 + v_1(l_2, t)]\} \hat{\mathbf{b}}_2. \quad (6)
\end{aligned}$$

Together with the relation

$$\omega_3 = \dot{\theta}, \quad (7)$$

the above completes the kinematic description of the model. The transformation matrix to go from frame B ( $\mathbf{b}_1, \mathbf{b}_2, \mathbf{b}_3$ ) to frame A ( $\mathbf{a}_1, \mathbf{a}_2, \mathbf{a}_3$ ) is

$${}^A \mathbf{T}^B = \begin{bmatrix} \cos(\alpha_1 + \beta) & -\sin(\alpha_1 + \beta) & 0 \\ \sin(\alpha_1 + \beta) & \cos(\alpha_1 + \beta) & 0 \\ 0 & 0 & 1 \end{bmatrix} \quad (8)$$

## 2.3 LINEARIZED DYNAMICS - ASSUMED-MODES METHOD

Following the development outlined in section A.1 (see Appendix A), a solution to the free vibration problem is assumed in the form of a series composed of a linear combination of admissible functions of the spatial coordinates, multiplied by time-dependent generalized coordinates [19]. This is equivalent to treating the continuous system as a discrete many-degrees-of-freedom system and will result in the motion equations being ordinary differential equations instead of partial differential equations. As pointed out in [19], the assumed-modes method is well suited to the case of systems with both distributed and discrete properties.

For the system model under consideration, and taking into account the assumptions stated at the beginning of the chapter, independent axial extensions of both links are ignored, as in the example of section A.2. The correct condition for this assumption is

$$\dot{\epsilon}_{xx} = 0 \quad (1)$$

This results in the following expressions for the axial displacements of both link 1 and 2 in frames A and B respectively:

$$\begin{aligned} u_1(x, t) &= -\int_0^x \frac{1}{2} \left( \frac{\partial u_2}{\partial \sigma} \right)^2 d\sigma \\ v_1(y, t) &= -\int_0^y \frac{1}{2} \left( \frac{\partial v_2}{\partial \sigma} \right)^2 d\sigma \end{aligned} \quad (2)$$

which are correct to second order in the transverse displacement gradients.

Assuming now the following solutions for the transverse displacements of both links in frames A and B respectively

$$\begin{aligned} u_2(x, t) &= \sum_{i=1}^n \phi_i(x) q_i(t) \\ v_2(y, t) &= \sum_{i=1}^m \psi_i(y) p_i(t) \end{aligned} \quad (3)$$

expressions for  $u_1$  and  $v_1$  correct to second order in the generalized elastic coordinates  $q_i$ ,  $p_i$  are obtained

$$\begin{aligned}
u_1(x,t) &= -\frac{1}{2} \sum_{i=1}^n \sum_{j=1}^n \int_0^x \phi_i(\sigma) \phi_j'(\sigma) d\sigma q_i q_j \\
v_1(y,t) &= -\frac{1}{2} \sum_{i=1}^m \sum_{j=1}^m \int_0^y \psi_i(\sigma) \psi_j'(\sigma) d\sigma p_i p_j
\end{aligned} \tag{4}$$

Note that the hybrid continuous and discrete system has been transformed into a  $2+n+m$  degrees of freedom system. The admissible functions  $\phi(x)$  and  $\psi(y)$  are chosen to be cantilevered (clamped-free) mode shapes for uniform beams of lengths  $l_1$  and  $l_2$  respectively. These are given explicitly as the following functions of spatial coordinates [2]:

$$\begin{aligned}
\tilde{y}_i(s) &= \cosh\left(\frac{\lambda_i s}{l_j}\right) - \cos\left(\frac{\lambda_i s}{l_j}\right) - \sigma_i \left( \sinh\left(\frac{\lambda_i s}{l_j}\right) - \sin\left(\frac{\lambda_i s}{l_j}\right) \right) \\
\tilde{y}_i &= \begin{cases} \phi_i \\ \psi_i \end{cases}, \quad s = \begin{cases} x \\ y \end{cases}, \quad i = \begin{cases} 1, \dots, n & , j = 1 \\ 1, \dots, m & , j = 2 \end{cases}
\end{aligned} \tag{5}$$

where

$$\sigma_i = \frac{\sinh \lambda_i - \sin \lambda_i}{\cosh \lambda_i + \cos \lambda_i} \tag{6}$$

and  $\lambda_i$  are the solutions, arranged in increasing order, of the transcendental equation:

$$\cos \lambda \cosh \lambda + 1 = 0. \tag{7}$$

These mode shapes satisfy the following orthogonality conditions

$$\int_0^l \tilde{y}_i(s) \tilde{y}_j(s) ds = \int_0^l \tilde{y}_i''(s) \tilde{y}_j''(s) ds = \begin{cases} 0, & i \neq j \\ l, & i = j \end{cases} \tag{8}$$

where

$$\tilde{y}_i''(s) = \left(\frac{l}{\lambda_i}\right)^2 \frac{d^2 \tilde{y}_i}{ds^2}$$



$$\frac{d^n}{d\left(\frac{\lambda_i s}{l}\right)^n} \tilde{y}_i = \frac{d^{n+4}}{d\left(\frac{\lambda_i s}{l}\right)^{n+4}} \tilde{y}_i. \quad (9)$$

Requiring now that the elastic generalized coordinates,  $q_i$  and  $p_j$ , and the elastic generalized speeds,  $dq_i/dt$  and  $dp_j/dt$  ( $i=1,\dots,n$ ;  $j=1,\dots,m$ ), be infinitesimally small, it should be possible to obtain equations of motion for the system model under consideration that are linear in these elastic coordinates and speeds. Heeding the lessons of Appendix A, the expressions for velocities and angular velocities obtained in section 2.2 are not linearized until after the formation of partial velocities and partial angular velocities but previous to the formation of the accelerations (see section 2.4). The velocities and angular velocities linearized in the elastic coordinates and speeds are presented below.

In what follows, a  $\sim$  represents a quantity that has been linearized with respect to the small elastic deflections and speeds. The following definitions will be used throughout the next two sub-sections to simplify the equations.

$$u_1(x, t) = \dot{u}_1(x, t) = 0$$

$$v_1(y, t) = \dot{v}_1(y, t) = 0$$

$$u_2(x, t) = \sum_{i=1}^n \phi_i(x) q_i(t)$$

$$v_2(y, t) = \sum_{i=1}^m \psi_i(y) p_i(t)$$

$$\dot{u}_2(x, t) = \sum_{i=1}^n \phi_i(x) \dot{q}_i(t)$$

$$\dot{v}_2(y, t) = \sum_{i=1}^m \psi_i(y) \dot{p}_i(t)$$

$$\alpha_1(t) = \sum_{i=1}^n \phi_i(l_1) q_i(t)$$

$$\alpha_2(t) = \sum_{i=1}^m \psi_i(l_2) p_i(t)$$

$$\dot{\alpha}_1(t) = \sum_{i=1}^n \phi_i(l_1) \dot{q}_i(t)$$

$$\dot{\alpha}_2(t) = \sum_{i=1}^m \psi_i(l_2) \dot{p}_i(t)$$

$$L_1 = b_1 + l_1 + b_{21}$$

$$L_2 = b_{22} + l_2 + b_t$$

$$\tilde{c}_{\gamma_1} = \cos \gamma_1 - \sin \gamma_1 \cdot \alpha_1$$

$$\tilde{s}_{\gamma_1} = \sin \gamma_1 + \cos \gamma_1 \cdot \alpha_1$$

$$\begin{aligned}
{}^N\tilde{\omega}^B{}_2 &= \omega_3 + \Omega_3 \\
\tilde{c}_{\gamma_2} &= \cos(\gamma_2 + \beta) - \sin(\gamma_2 + \beta) \cdot \alpha_1 & \tilde{s}_{\gamma_2} &= \sin(\gamma_2 + \beta) + \cos(\gamma_2 + \beta) \cdot \alpha_1 \\
\tilde{c}_{\beta} &= \cos \beta - \sin \beta \cdot \alpha_1 & \tilde{s}_{\beta} &= \sin \beta + \cos \beta \cdot \alpha_1
\end{aligned} \tag{10}$$

### 2.3.1 Linearized Velocities

$$\begin{aligned}
{}^N\tilde{v}^Q &= b_1\omega_3\hat{a}_2 \\
{}^N\tilde{v}^C{}_1 &= -\omega_3u_2\hat{a}_1 + [u_2 + \omega_3(b_1 + x)]\hat{a}_2 \\
{}^N\tilde{v}^H &= [-\omega_3(u_2(l_1, t) + b_{21}\alpha_1)]\hat{a}_1 + [u_2(l_1) + b_{21}\dot{\alpha}_1 + \omega_3L_1]\hat{a}_2
\end{aligned} \tag{1}$$

$$\begin{aligned}
{}^N\tilde{v}^{B^*}_1 &= {}^N\tilde{v}^H - [e_1\dot{\alpha}_1 \sin \gamma_1 + e_1\omega_3\tilde{s}_{\gamma_1}]\hat{a}_1 + [e_1\dot{\alpha}_1 \cos \gamma_1 + e_1\omega_3\tilde{c}_{\gamma_1}]\hat{a}_2 \\
{}^N\tilde{v}^{Q21} &= -\omega_3u_2(l_1, t)\hat{a}_1 + [u_2(l_1, t) + \omega_3(b_1 + l_1)]\hat{a}_2 \\
{}^N\tilde{v}^{B^*}_2 &= {}^N\tilde{v}^H - \left[ {}^N\tilde{\omega}^B{}_2 e_2 \tilde{s}_{\gamma_2} + \dot{\alpha}_1 e_2 \sin(\beta + \gamma_2) \right] \hat{a}_1 \\
&\quad + \left[ {}^N\tilde{\omega}^B{}_2 e_2 \tilde{c}_{\gamma_2} + \dot{\alpha}_1 e_2 \cos(\beta + \gamma_2) \right] \hat{a}_2
\end{aligned} \tag{2}$$

$$\begin{aligned}
{}^N\tilde{v}^{Q22} &= {}^N\tilde{v}^H + b_{22} \left\{ \left[ -{}^N\tilde{\omega}^B{}_2 \tilde{s}_{\beta} - \dot{\alpha}_1 \sin \beta \right] \hat{a}_1 + \left[ {}^N\tilde{\omega}^B{}_2 \tilde{c}_{\beta} + \dot{\alpha}_1 \cos \beta \right] \hat{a}_2 \right\} \\
{}^N\tilde{v}^C{}_2 &= {}^N\tilde{v}^H - \left\{ {}^N\tilde{\omega}^B{}_2 [v_2 \cos \beta + (b_{22} + y)\tilde{s}_{\beta}] + [v_2 + \dot{\alpha}_1(b_{22} + y)] \sin \beta \right\} \hat{a}_1 \\
&\quad + \left\{ {}^N\tilde{\omega}^B{}_2 [-v_2 \sin \beta + (b_{22} + y)\tilde{c}_{\beta}] + [v_2 + \dot{\alpha}_1(b_{22} + y)] \cos \beta \right\} \hat{a}_2
\end{aligned} \tag{3}$$

$$\begin{aligned}
{}^N\tilde{v}^{C^*} &= {}^N\tilde{v}^H \\
&\quad - \left\{ {}^N\tilde{\omega}^B{}_2 [(v_2(l_2) + b_t\alpha_2)\cos \beta + L_2\tilde{s}_{\beta}] + [\dot{v}_2(l_2) + \dot{\alpha}_1L_2 + \dot{\alpha}_2b_t] \sin \beta \right\} \hat{a}_1 \\
&\quad + \left\{ {}^N\tilde{\omega}^B{}_2 [-(v_2(l_2) + b_t\alpha_2)\sin \beta + L_2\tilde{c}_{\beta}] + [\dot{v}_2(l_2) + \dot{\alpha}_1L_2 + \dot{\alpha}_2b_t] \cos \beta \right\} \hat{a}_2
\end{aligned} \tag{4}$$

$$\begin{aligned}
{}^N \underline{\dot{v}}^T &= {}^N \underline{\dot{v}}^H \\
&- \left\{ {}^N \tilde{\omega}^B \left[ v_2(l_2) \cos \beta + (b_{22} + l_2) \tilde{s}_\beta \right] + [\dot{v}_2(l_2) + \dot{\alpha}_1(b_{22} + l_2)] \sin \beta \right\} \hat{a}_1 \\
&+ \left\{ {}^N \tilde{\omega}^B \left[ -v_2(l_2) \sin \beta + (b_{22} + l_2) \tilde{c}_\beta \right] + [\dot{v}_2(l_2) + \dot{\alpha}_1(b_{22} + l_2)] \cos \beta \right\} \hat{a}_2 \quad (5)
\end{aligned}$$

### 2.3.2 Linearized Angular Velocities

$$\begin{aligned}
{}^N \underline{\omega}^A &= \omega_3 \hat{a}_3 \\
{}^N \underline{\omega}^{B_1} &= (\omega_3 + \dot{\alpha}_1) \hat{a}_3 \\
{}^N \underline{\omega}^{B_2} &= (\omega_3 + \dot{\alpha}_1 + \Omega_3) \hat{a}_3 \\
{}^N \underline{\omega}^C &= (\omega_3 + \dot{\alpha}_1 + \Omega_3 + \dot{\alpha}_2) \hat{a}_3 \quad (1)
\end{aligned}$$

## 2.4 KANE'S DYNAMICAL EQUATIONS

In this section, Kane's dynamical equations are used to assemble the equations of motion for the system model, linearized in small generalized elastic coordinates and speeds.

According to the Kane formalism, the dynamic equations are given by

$$\begin{aligned}
\tilde{F}_r^* + \tilde{F}_r &= 0 \\
r &= \omega_3, \Omega_3, q_i, p_j \quad (i = 1, \dots, n; j = 1, \dots, m) \quad (1)
\end{aligned}$$

where  $F_r^*$  is the generalized inertia force corresponding to the generalized speed  $r$ , while  $F_r$  is the associated generalized active force. Note that as in the previous section, a  $\sim$  signifies that the indicated quantity has been linearized with respect to the small elastic deflections and speeds.

For a collection of rigid bodies, the generalized inertia force is equal to the sum over all the bodies of the d'Alembert force dot multiplied by the partial velocity of each body's mass center with respect to a particular generalized speed, plus the inertial time derivative of the bodies' angular momenta, about their respective mass centers, dot multiplied by the corresponding partial angular velocity. The generalized active force is equal to the sum over all the forces and torques acting on the system of the forces and torques themselves

dot multiplied by the appropriate partial velocities and partial angular velocities, respectively, at the points or bodies of application. These definitions will become clearer when they are applied in the following sections.

The selected generalized speeds

$$\omega_3, \Omega_3, q_i, p_j \quad (i = 1, \dots, n; j = 1, \dots, m)$$

together with the kinematic relationships

$$\begin{aligned} \omega_3 &= \dot{\theta} & \Omega_3 &= \dot{\beta} \\ q_i &= \frac{d}{dt} q_i & p_j &= \frac{d}{dt} p_j \quad (i = 1, \dots, n; j = 1, \dots, m) \end{aligned} \quad (2)$$

completely characterize the  $2+n+m$  degree of freedom system.

Define  $m_X$  to be the mass of body X, and  $J_X$  to be the moment of inertia of body X about an axis passing through its mass center,  $X^*$ , and parallel to  $\mathbf{n}_3$  ( $X=A, B_1, B_2, C$ ).  $\rho_i$  ( $i=1,2$ ) is the mass per unit length of link  $i$ .  ${}^N \tilde{\mathbf{a}}^P$  is the linearized acceleration of point P in the inertial reference frame, while  ${}^N \underline{\alpha}^X$  is the angular acceleration of body X in the same frame. Further, following Kane, the partial velocity of point P, and the partial angular velocity of frame/body X, with respect to the generalized speed  $r$  are defined as

$$\begin{aligned} {}^N \tilde{\mathbf{v}}_r^P &= \frac{\partial}{\partial \dot{r}} [{}^N \tilde{\mathbf{v}}^P] \\ {}^N \underline{\omega}_r^X &= \frac{\partial}{\partial \dot{r}} [{}^N \underline{\omega}^X] \end{aligned} \quad (3)$$

respectively.

### 2.4.1 Generalized Inertia Forces

With the above definitions, the generalized inertia force for the system under consideration is given by

$$\begin{aligned} \tilde{F}_r^* &= -J_A {}^N \underline{\omega}_r^A \cdot {}^N \underline{\alpha}^A - \int_0^{l_1} {}^N \tilde{\mathbf{v}}_r^{C_1} \cdot {}^N \tilde{\mathbf{a}}^{C_1} \rho_1 dx - J_{B_1} {}^N \underline{\omega}_r^{B_1} \cdot {}^N \underline{\alpha}^{B_1} \\ &\quad - J_{B_2} {}^N \underline{\omega}_r^{B_2} \cdot {}^N \underline{\alpha}^{B_2} - m_{B_1} {}^N \tilde{\mathbf{v}}_r^{B_1^*} \cdot {}^N \tilde{\mathbf{a}}^{B_1^*} - m_{B_2} {}^N \tilde{\mathbf{v}}_r^{B_2^*} \cdot {}^N \tilde{\mathbf{a}}^{B_2^*} \end{aligned}$$

$$-\int_0^{l_2} N \bar{v}_r^{C_2} \cdot N \bar{a}^{C_2} \rho_2 dy - J_C N \bar{\omega}_r^C \cdot N \bar{\alpha}^C - m_C N \bar{v}_r^{C^*} \cdot N \bar{a}^{C^*} \quad (1)$$

where as before

$$r = \omega_3, \Omega_3, q_i, p_j \quad (i = 1, \dots, n; j = 1, \dots, m)$$

The partial velocities are obtained from the velocity expressions which are correct to second order in elastic generalized coordinates and speeds (see section 2.2), and are then linearized in these same coordinates and speeds. The linearized partial velocities are given in Table 2.1, and the partial angular velocities are presented in Table 2.2. The linearized accelerations are obtained by differentiating the linearized velocity expressions at the end of section 2.4, and ignoring terms of second order or higher in the elastic deflections and speeds.

$r$	$N \bar{v}_r^{Q_1}$	$N \bar{v}_r^{C_1}$	$N \bar{v}_r^{Q_{21}}$
$\omega_3$	$b_1 \hat{a}_2$	$-\sum_{i=1}^n \phi_i q_i \hat{a}_1 + (x + b_1) \hat{a}_2$	$-\sum_{i=1}^n \phi_i(l_1) q_i \hat{a}_1 + (l_1 + b_1) \hat{a}_2$
$\dot{q}_j$	0	$-\sum_{i=1}^n \beta_{ij}(x) q_i \hat{a}_1 + \phi_j(x) \hat{a}_2$	$-\sum_{i=1}^n \beta_{ij}(l_1) q_i \hat{a}_1 + \phi_j(l_1) \hat{a}_2$

Table 2.1a: Linearized Partial Velocities

$r$	$N \bar{v}_r^H$	$N \bar{v}_r^{B_1^*}$
$\omega_3$	$-\sum_{i=1}^n A_i(l_1) q_i \hat{a}_1 + L_1 \hat{a}_2$	$\left[ -\sum_{i=1}^n A_i(l_1) q_i - e_1 \tilde{\gamma}_1 \right] \hat{a}_1 + [L_1 + e_1 \tilde{\gamma}_1] \hat{a}_2$
$\dot{q}_j$	$-\sum_{i=1}^n C_{ij}(l_1) q_i \hat{a}_1 + A_j(l_1) \hat{a}_2$	$\left[ -\sum_{i=1}^n C_{ij}(l_1) q_i - \phi_j(l_1) e_1 \tilde{\gamma}_1 \right] \hat{a}_1$ $+ [A_j(l_1) + \phi_j(l_1) e_1 \tilde{\gamma}_1] \hat{a}_2$

Table 2.1b: Linearized Partial Velocities (cont.)

$r$	$N \bar{v}_r^{B_2^*}$	$N \bar{v}_r^{Q_{22}}$
$\omega_3$	$N \bar{v}_{\omega_3}^H - e_2 \sin \gamma_2 \hat{\mathbf{b}}_1 + e_2 \cos \gamma_2 \hat{\mathbf{b}}_2$	$N \bar{v}_{\omega_3}^H + b_{22} \hat{\mathbf{b}}_2$
$\dot{q}_j$	$N \bar{v}_{\dot{q}_j}^H - \phi_j(l_1) e_2 \sin \gamma_2 \hat{\mathbf{b}}_1 + \phi_j(l_1) e_2 \cos \gamma_2 \hat{\mathbf{b}}_2$	$N \bar{v}_{\dot{q}_j}^H + \phi_j(l_1) b_{22} \hat{\mathbf{b}}_2$
$\Omega_3$	$- e_2 \sin \gamma_2 \hat{\mathbf{b}}_1 + e_2 \cos \gamma_2 \hat{\mathbf{b}}_2$	$b_{22} \hat{\mathbf{b}}_2$

Table 2.1c: Linearized Partial Velocities (cont.)

The symbols in Table 2.1 that have not been defined previously are the modal integrals and constants that depend on the mode shapes. These are defined in Appendix B, where they are also evaluated for the physical manipulator parameters chosen (see Table 4.1), and assuming cantilever mode shapes.

$r$	$N \bar{v}_r^{C_2}$	$N \bar{v}_r^T$
$\omega_3$	$N \bar{v}_{\omega_3}^H - \sum_{i=1}^m \psi_i p_i \hat{\mathbf{b}}_1 + (y + b_{22}) \hat{\mathbf{b}}_2$	$N \bar{v}_{\omega_3}^H - \sum_{i=1}^m \psi_i(l_2) p_i \hat{\mathbf{b}}_1 + (l_2 + b_{22}) \hat{\mathbf{b}}_2$
$\dot{q}_j$	$N \bar{v}_{\dot{q}_j}^H - \phi_j(l_1) \sum_{i=1}^m \psi_i p_i \hat{\mathbf{b}}_1$ $+ \phi_j(l_1) (y + b_{22}) \hat{\mathbf{b}}_2$	$N \bar{v}_{\dot{q}_j}^H - \phi_j(l_1) \sum_{i=1}^m \psi_i(l_2) p_i \hat{\mathbf{b}}_1$ $+ \phi_j(l_1) (l_2 + b_{22}) \hat{\mathbf{b}}_2$
$\Omega_3$	$- \sum_{i=1}^m \psi_i p_i \hat{\mathbf{b}}_1 + (y + b_{22}) \hat{\mathbf{b}}_2$	$- \sum_{i=1}^m \psi_i(l_2) p_i \hat{\mathbf{b}}_1 + (l_2 + b_{22}) \hat{\mathbf{b}}_2$
$\dot{p}_j$	$- \sum_{i=1}^m \beta_{ij}^*(y) p_i \hat{\mathbf{b}}_1 + \psi_j(y) \hat{\mathbf{b}}_2$	$- \sum_{i=1}^m \beta_{ij}^*(l_2) p_i \hat{\mathbf{b}}_1 + \psi_j(l_2) \hat{\mathbf{b}}_2$

Table 2.1d: Linearized Partial Velocities (cont.)

$r$	${}^N \hat{v}_r^{C^*}$
$\omega_3$	${}^N \hat{v}_{\omega_3}^H - \sum_{i=1}^m B_i(l_2) p_i \hat{\mathbf{b}}_1 + L_2 \hat{\mathbf{b}}_2$
$\dot{q}_j$	${}^N \hat{v}_{\dot{q}_j}^H - \phi_j(l_1) \sum_{i=1}^m B_i(l_2) p_i \hat{\mathbf{b}}_1 + \phi_j(l_1) L_2 \hat{\mathbf{b}}_2$
$\Omega_3$	$-\sum_{i=1}^m B_i(l_2) p_i \hat{\mathbf{b}}_1 + L_2 \hat{\mathbf{b}}_2$
$\dot{p}_j$	$-\sum_{i=1}^m C_{ij}^*(l_2) p_i \hat{\mathbf{b}}_1 + B_j(l_2) \hat{\mathbf{b}}_2$

Table 2.1e: Linearized Partial Velocities (cont.)

$r$	${}^N \hat{\omega}_r^A$	${}^N \hat{\omega}_r^{B_1}$	${}^N \hat{\omega}_r^{B_2}$	${}^N \hat{\omega}_r^C$
$\omega_3$	$\hat{\mathbf{a}}_3$	$\hat{\mathbf{a}}_3$	$\hat{\mathbf{a}}_3$	$\hat{\mathbf{a}}_3$
$\dot{q}_j$	0	$\phi_j(l_1) \hat{\mathbf{a}}_3$	$\phi_j(l_1) \hat{\mathbf{a}}_3$	$\phi_j(l_1) \hat{\mathbf{a}}_3$
$\Omega_3$	0	0	$\hat{\mathbf{a}}_3$	$\hat{\mathbf{a}}_3$
$\dot{p}_j$	0	0	0	$\psi_j(l_2) \hat{\mathbf{a}}_3$

Table 2.2: Linearized Partial Angular Velocities

## 2.4.2 Generalized Active Forces

The generalized active force can be written as

$$\begin{aligned} \hat{F}_r &= (\hat{F}_r)_I + (\hat{F}_r)_C \\ r = \omega_3, \Omega_3, \dot{q}_i, \dot{p}_j \quad (i = 1, \dots, n; j = 1, \dots, m) \end{aligned} \quad (1)$$

where  $(\hat{F}_r)_I$  consists of those contributions to the generalized active forces due to internal forces; and  $(\hat{F}_r)_C$  are those contributions due to external or "control" forces. Taking into

account the definitions given at the beginning of this section, and referring to Fig. 2.3, the expression for the  $(\bar{F}_r)_I$  is

$$\begin{aligned}
 (\bar{F}_r)_I = & {}^N \underline{\omega}_r^A \cdot [M_1(0) \hat{a}_3] + {}^N \underline{v}_r^{Q_1} \cdot [-V_1(0) \hat{a}_2] + \int_0^{l_1} {}^N \underline{v}_r^{C_1} \cdot \left[ -\frac{\partial V_1}{\partial x} \hat{a}_2 \right] dx \\
 & + {}^N \underline{v}_r^{Q_{21}} \cdot [V_1(l_1) \hat{a}_2] + {}^N \underline{\omega}_r^{B_1} \cdot [-M_1(l_1) \hat{a}_3] + {}^N \underline{\omega}_r^{B_2} \cdot [M_2(0) \hat{a}_3] \\
 & + {}^N \underline{v}_r^{Q_{22}} \cdot [-V_2(0) \hat{b}_2] + \int_0^{l_2} {}^N \underline{v}_r^{C_2} \cdot \left[ -\frac{\partial V_2}{\partial y} \hat{b}_2 \right] dy + {}^N \underline{v}_r^T \cdot [V_2(l_2) \hat{b}_2] \\
 & + {}^N \underline{\omega}_r^C \cdot [-M_2(l_2) \hat{a}_3]
 \end{aligned}$$

$$r = \omega_3, \Omega_3, q_i, p_j \quad (i = 1, \dots, n; j = 1, \dots, m) \quad (2)$$

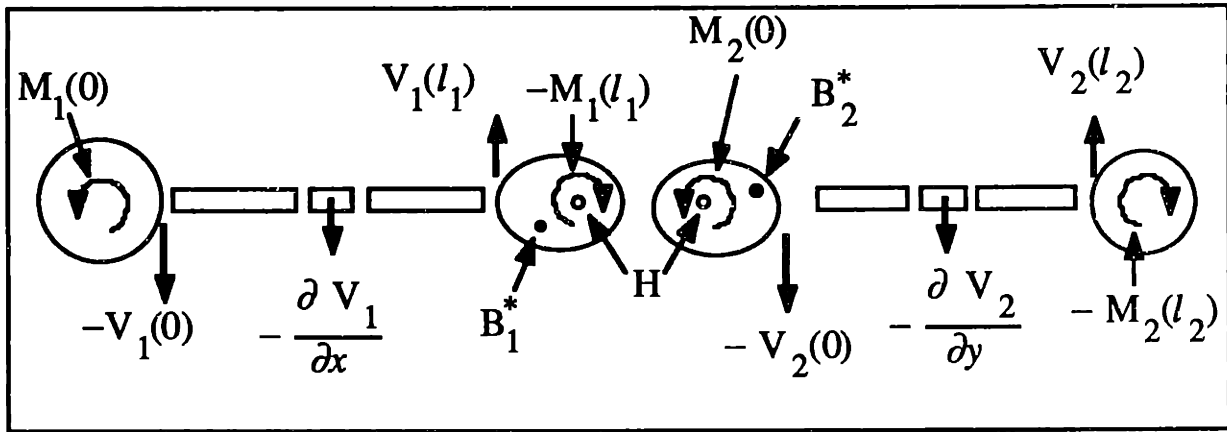


Figure 2.3: Schematic of Internal Forces and Elbow Joint Definitions

For a Bernoulli-Euler beam, under the governing assumptions presented in section 2.1,

$$\begin{aligned}
 M_1(x) &= (EI)_1 \frac{\partial^2 u_2}{\partial x^2} & M_2(y) &= (EI)_2 \frac{\partial^2 v_2}{\partial y^2} \\
 V_1(x) &= \frac{\partial}{\partial x} M_1(x) & V_2(y) &= \frac{\partial}{\partial y} M_2(y)
 \end{aligned} \quad (3)$$

where  $(EI)_i$  ( $i=1,2$ ) is the bending stiffness of link  $i$ . Taking into account the fact that link 1 is attached to body A in a cantilevered way, and link 2 is attached to body B<sub>2</sub> in a cantilevered way also, it is seen that



$$\begin{aligned}
\phi_i(0) = \phi'_i(0) = 0 & \quad i = 1, \dots, n \\
\psi_j(0) = \psi'_j(0) = 0 & \quad j = 1, \dots, m
\end{aligned} \tag{4}$$

Using these boundary conditions, and executing the required operations, equations (2) reduce to:

$$\begin{aligned}
(\tilde{F}_{\omega_3})_I &= 0 \\
(\tilde{F}_{\Omega_3})_I &= 0 \\
(\tilde{F}_{\dot{q}_j})_I &= -\sum_{i=1}^n H_{ij} q_i, \quad j = 1, \dots, n \\
(\tilde{F}_{\dot{p}_j})_I &= -\sum_{i=1}^m H_{ij}^* p_i, \quad j = 1, \dots, m,
\end{aligned} \tag{5}$$

where

$$\begin{aligned}
H_{ij} &= \int_0^{l_1} (EI)_1 \phi''_i(x) \phi''_j(x) dx \\
H_{ij}^* &= \int_0^{l_2} (EI)_2 \psi''_i(y) \psi''_j(y) dy
\end{aligned} \tag{6}$$

and the orthogonality conditions governing these integrals have been presented in equation 2.3.8.

For the case at hand, the generalized active forces due to external forces have a particularly simple form

$$\begin{aligned}
(\tilde{F}_r)_C &= {}^N \underline{\omega}_r^A \bullet \mathbf{T}_S + {}^N \underline{\omega}_r^{B_1} \bullet (-\mathbf{T}_E) + {}^N \underline{\omega}_r^{B_2} \bullet \mathbf{T}_E \\
r &= \omega_3, \Omega_3, \dot{q}_i, \dot{p}_j \quad (i = 1, \dots, n; j = 1, \dots, m)
\end{aligned} \tag{7}$$

where the control forces are couples of torque  $\mathbf{T}_S$  and  $\mathbf{T}_E$  applied at the shoulder body, A, and the elbow body, B<sub>2</sub>, respectively:

$$\mathbf{T}_S = T_1 \hat{\mathbf{a}}_3, \quad \mathbf{T}_E = T_2 \hat{\mathbf{a}}_3$$

Again effecting the required dot products, and making use of Table 2.1, equations (7) simplify to

$$\begin{aligned}
 (\tilde{F}_{\omega_3})_C &= T_1 \\
 (\tilde{F}_{\Omega_3})_C &= T_2 \\
 (\tilde{F}_{\dot{q}_j})_C &= 0, \quad j = 1, \dots, n \\
 (\tilde{F}_{\dot{p}_j})_C &= 0, \quad j = 1, \dots, m.
 \end{aligned} \tag{8}$$

From equations (5) and (8) the linearized generalized active forces result

$$\begin{aligned}
 \tilde{F}_{\omega_3} &= T_1 \\
 \tilde{F}_{\Omega_3} &= T_2 \\
 \tilde{F}_{\dot{q}_j} &= -\sum_{i=1}^n H_{ij} q_i, \quad j = 1, \dots, n \\
 \tilde{F}_{\dot{p}_j} &= -\sum_{i=1}^m H_{ij}^* p_i, \quad j = 1, \dots, m.
 \end{aligned} \tag{9}$$

### 2.4.3 Equations of Motion

Finally, the 2+n+m ordinary differential equations of motion are obtained from

$$\tilde{F}_r^* + \tilde{F}_r = 0, \quad r = \omega_3, \Omega_3, \dot{q}_i, \dot{p}_j \quad (i = 1, \dots, n; j = 1, \dots, m) \tag{1}$$

Let  $\mathbf{x}$  be a state vector such that

$$\mathbf{x} = \begin{bmatrix} \mathbf{x}_R \\ \mathbf{x}_E \end{bmatrix} = [\theta, \beta, q_1, \dots, q_n, p_1, \dots, p_m]^T$$

and  $\mathbf{T}$  be the control input vector

$$\mathbf{T} = \begin{bmatrix} T_1 \\ T_2 \end{bmatrix}$$

Then equation (1) can be written in the matrix form:

$$\begin{bmatrix} M_{RR}(\mathbf{x}) & M_{RE}(\mathbf{x}) \\ M_{ER}(\mathbf{x}) & M_{EE}(\mathbf{x}) \end{bmatrix} \ddot{\mathbf{x}} + \begin{bmatrix} 0 & 0 \\ 0 & K_{EE} \end{bmatrix} \dot{\mathbf{x}} = \begin{bmatrix} I \\ 0 \end{bmatrix} \mathbf{T} + \mathbf{F}(\mathbf{x}, \dot{\mathbf{x}}) \quad (2)$$

where  $\mathbf{F}(\mathbf{x}, d\mathbf{x}/dt)$  is a  $2+n+m$  vector of gyroscopic (centripetal and coriolis) forces;

$$(K_{EE})_{ij} = H_{ij}, \quad i, j = 1, \dots, n$$

$$(K_{EE})_{n+i, n+j} = H_{ij}^*, \quad i, j = 1, \dots, m$$

and  $M(\mathbf{x})$  is the configuration dependent mass matrix.

Setting

$$\mathbf{y} = \begin{bmatrix} \mathbf{x} \\ \dot{\mathbf{x}} \end{bmatrix}$$

the matrix equation (2) can be written in the form

$$\dot{\mathbf{y}} = \begin{bmatrix} 0 & I \\ -M^{-1}K & 0 \end{bmatrix} \mathbf{y} + \begin{bmatrix} 0 \\ M^{-1} \end{bmatrix} \mathbf{T} + \begin{bmatrix} 0 \\ M^{-1}\mathbf{F} \end{bmatrix} \quad (3)$$

in which form it can be integrated straightforwardly using a Runge-Kutta fourth-order integration scheme (see chapter 4).

The full equations of motion that result from the above development are quite extensive. For this reason, they are presented in Appendix C in the matrix form of equation (2).

# CHAPTER 3: DYNAMIC ANALYSIS

## INTRODUCTION

In the previous chapter, the motion equations for the two link arm, correct to first order in small elastic deflections and speeds, and exact in rigid body motions, were obtained. It is now desired to investigate the relative significance of nonlinear terms which involve the elastic coordinates and speeds. For this purpose, this chapter begins with a brief general presentation of the equations of motion for open chains of elastic bodies, linearized in small elastic deflections and rates. After considering possible simplifications to these equations, three models are proposed for purposes of investigating the effects of these simplifications on the systems under consideration.

Using these three models as a guide, the simple one link example of section A.2 is analyzed. By virtue of its simplicity, this model serves to clearly identify the issues of importance, and to highlight the complexity introduced by inertial coupling between multiple links. Predictions using this example are made as to the relative significance of elastic nonlinear terms in the equations of motion of more complex systems. These predictions are tested in the next chapter via simulation of the two link arm using the equations developed in chapter two. The chapter ends with an eigenanalysis of the two link manipulator that will be useful when the simulation results are analyzed in chapter four.

## 3.1 FORM OF THE EQUATIONS OF MOTION FOR A CHAIN OF ELASTIC BODIES

The equations of motion of an open chain of elastic bodies can be expressed quite generally as [8]:

$$\begin{bmatrix} M_{RR}(x, q) & M_{RE}(x, q) \\ M_{ER}(x, q) & M_{EE}(x, q) \end{bmatrix} \begin{bmatrix} \ddot{x} \\ \ddot{q} \end{bmatrix} = \begin{bmatrix} T_C \\ 0 \end{bmatrix} + \begin{bmatrix} T_{ext,R} \\ T_{ext,E} \end{bmatrix} + \begin{bmatrix} F_R(x, q, \dot{x}, \dot{q}) \\ F_E(x, q, \dot{x}, \dot{q}) \end{bmatrix} \quad (1)$$

where  $x$  is a vector of rigid generalized coordinates;  $q$  is a vector of the elastic generalized coordinates;  $M_{RR}$ ,  $M_{RE}$ ,  $M_{EE}$  form the configuration-dependent mass matrix;  $T_C$  is a vector

of control forces and we assume only the rigid coordinates are directly actuated (as in joint-torque actuators in a manipulator);  $T_{ext}$  is a vector of other generalized external forces;  $K_{EE}$  is a constant stiffness matrix (see equation (2) below) and  $F$  is a vector of nonlinear inertial (including coriolis and centripetal) forces.

The important class of systems for which the elastic deformations remain small, so that terms of second order in  $q$  and  $dq/dt$  can be ignored, is often considered. Strictly speaking this requires that  $\|q\|$  and  $\|dq/dt\|$  be infinitesimally small. However it is known that if, for example, a flexible body is modelled as a beam, it is sufficient that the elastic deformations do not exceed one tenth of the length of the beam in order to use linear Bernoulli-Euler beam theory. At any rate, given this assumption of small elastic deflections, the previous equation could be expanded in order to show more explicitly the form of the nonlinear terms:

$$\begin{aligned}
& \begin{bmatrix} M_{RR}(x, q) & M_{RE}(x, q) \\ M_{ER}(x, q) & M_{EE}(x, q) \end{bmatrix} \begin{bmatrix} \ddot{x} \\ \ddot{q} \end{bmatrix} = \begin{bmatrix} T_C \\ 0 \end{bmatrix} + \begin{bmatrix} T_{ext,R} \\ T_{ext,E} \end{bmatrix} - \begin{bmatrix} 0 & 0 \\ 0 & K_{EE} \end{bmatrix} \begin{bmatrix} x \\ q \end{bmatrix} \\
& + \sum_{i=1}^n f_{1ii}(x) \dot{x}_i^2 + \frac{1}{2} \sum_{i=1}^n \sum_{j \neq i}^n f_{1ij}(x) \dot{x}_i \dot{x}_j + \frac{1}{2} \sum_{i=1}^n f_{2ii}(x) q \dot{x}_i^2 \\
& + \frac{1}{2} \sum_{i=1}^n \sum_{j \neq i}^n f_{2ij}(x) q \dot{x}_i \dot{x}_j + \sum_{i=1}^n f_{3i}(x) q \dot{x}_i - \begin{bmatrix} M_{RR}^*(x, q) \\ M_{ER}^*(x, q) \end{bmatrix} \ddot{x}, \\
& (M_{RR}^*(x, q))_{ij} = m_{1ij}^T(x) q, \quad (M_{ER}^*(x, q))_{ij} = m_{2ij}^T(x) q
\end{aligned} \tag{2}$$

where  $n$  above is the number of rigid body coordinates;  $f_{1ij}$  is a column matrix, but  $f_{2ij}$  and  $f_{3i}$  are  $n+m$  by  $m$  matrices, where  $m$  is the number of elastic coordinates.

In light of the discussion in Appendix A, some of the terms in equation (2) could be written as:

$$\begin{aligned}
f_{2ij}(x) &= f_{2ij}^1(x) + f_{2ij}^2(x) \\
m_{1ij}(x) &= m_{1ij}^1(x) + m_{1ij}^2(x) \\
m_{2ij}(x) &= m_{2ij}^1(x) + m_{2ij}^2(x)
\end{aligned} \tag{3}$$

where the superscript <sup>2</sup> terms can only be obtained through the use of displacement and velocity expressions, in the development of the equations of motion, that are accurate to

second order in the elastic generalized coordinates and speeds ( $q$  and  $u$ ). This requires the use of nonlinear strain-displacement relations (as in App. A, [13]), nonlinear kinematic constraints [11, 24], or the use of a nonlinear "geometric stiffening" term appended to the incorrectly linearized equations of motion [27, 1].

The complexity of equations (2) and the difficulty involved in obtaining the nonlinear terms have historically prompted attempts at simplification. It is common [8] for example to assume small velocities and drop all terms nonlinear in rates. This results in rate-linear motion equations that greatly simplify the dynamicist's task. It has been pointed out [4], however, that in the case of  $n$ -link rigid manipulators in any configuration, the velocity and acceleration terms of the dynamic equations have the same relative significance at any speed of movement. The fact that the omission of these terms does not significantly affect simulation results is attributed to the fact that gravity and joint friction usually overpower inertial terms. These results have not been extended to chains of flexible bodies. One might argue that in some limit (e.g., vanishingly small  $q$ ) the equations of motion of the flexible multibody system should reduce to those of the rigid multibody system. Then it seems that a good case could be made for the inclusion of at least nonlinear terms in the rigid body rates in the rate-linear equations (i.e.,  $f_{1ij}(x)$ ), particularly considering the fact that future, fast, space manipulators with low joint frictions are part of the class of systems under consideration.

Faced with this, there are two ways in which to proceed with respect to the equations of motion: we can be consistent, or we can be selective. To be consistent requires keeping all terms of order  $\|q\|$  and  $\|u\|$  in equation (2), i.e., no simplification. There is also the problem that the superscript <sup>2</sup> terms in equations (3) are not readily available in the general case since they depend on nonlinear elastic theory or nonlinear kinematics of deformation for their derivation. We could just make do with the superscript <sup>1</sup> terms in equations (3) (standard approach) but this would not be consistent nor justifiable since there is no *a priori* reason to guarantee  $\|f_{2ij}^1\| \gg \|f_{2ij}^2\|$ , for example.

We are forced then to be selective, at least in the general case. Now we have to rely mostly on experience and simulation to determine which terms are important and which negligible under given conditions. Using a dynamic system very much like the one used in the simple example of section A.2, an empirical speed limit has been found beyond which the standard linear finite element or modal formulations of the model give erroneous results [11]. This limit is specified as follows: the magnitude of the spinning rate of the system has to be one order of magnitude less than the fundamental vibration frequency of the beam nominally stationary in Newtonian reference frame. This simulation result is used to claim

the following: unless the equations of motion exact to first order in elastic generalized coordinates and speeds are available, rigid body angular rates are limited to less than an order of magnitude lower than the lowest fundamental bending frequency of the system. In view of this, it might be possible to model the system accurately enough by just keeping the rate-linear equations together with terms  $f_{1ij}$ . In other words, it might not be detrimental to drop all nonlinear terms involving elastic coordinates and speeds. It can further be claimed that speed or acceleration limits also exist in translational rates or accelerations, arising both from those mass matrix terms that depend on  $q$  and cannot be obtained through the standard approaches and from such terms in  $f_{2ij}$ . In section 3.3 these claims are investigated analytically.

### 3.2 COMPARISON MODELS

In what follows, taking the above discussion into account, three types of models for a flexible multibody system under study shall be considered. The "consistent" model will be that which retains all terms to first order in elastic coordinates and speeds. This is the correctly, or consistently, linearized model. The equations of motion developed in chapter two for the two-link manipulator, and in Appendix A for the simple one link example, are representative of this type. This model implies no further simplification of the linearized equations and, as can be seen from Appendix C, even for the case of only two flexible links results in unwieldy expressions.

The second model to be considered is the "inconsistent" model. This is obtained through the use of linear kinematics of deformation in the determination of system velocities. It is clear from the discussion in Appendix A that this results in equations of motion that are incorrectly linearized. They lack the superscript <sup>2</sup> terms mentioned in the previous section. While this model results in equations that are as unwieldy as those of the consistent model, it yields erroneous results, as shall be seen. The advantage of this model lies in its use of linear elastic theory, and in the fact that, as it turns out, its results are valid within certain rigid body rate limits.

A "ruthlessly linearized", or simply "ruthless" model, shall be the last one considered. In this model all nonlinear terms which include elastic coordinates and speeds are ignored, including those terms in the mass matrix which depend on elastic coordinates. Referring to section 3.1, a ruthless model does not contain terms  $f_{2ij}$  and  $f_{3i}$ , or  $m_{1ij}(x)$ ,  $m_{2ij}(x)$ . Unlike the first two models, the ruthless model yields equations of motion that are greatly simplified, and since terms nonlinear in rigid body coordinates and rates are kept,

this model degrades to the correct model of a rigid multibody system as flexible deflections approach zero.

In the next section, limits of validity for all three models shall be investigated.

### 3.3 SINGLE FLEXIBLE BODY EXAMPLE

Consider the simple, slender, uniform beam cantilevered to a rigid base, of section A.2 (see Fig. A.1). The equations of motion, exact to first-order in generalized elastic coordinates and speeds were presented in eq. (A.2.1.14). All symbols have been defined in equations (A.2.1.15).

#### 3.3.1 Pure Rotation

Specializing equation (A.2.1.14) to the prescribed motion of uniform rotation of the base,

$$v_1=v_2=0, \quad v_3=\Omega=\text{constant}$$

the following is obtained,

$$\sum_{i=1}^n G_{ij} \ddot{q}_i + \sum_{i=1}^n [H_{ij} + \Omega^2(b\mu_{ij} + \eta_{ij} - G_{ij})] q_i = 0$$

$$(j = 1, \dots, n) \tag{1}$$

We recall that the terms  $\mu_{ij}$  and  $\eta_{ij}$  cannot be obtained using linear kinematics of deformation but were obtained in section A.2.1 through the use of nonlinear strain-displacement relations. Equation (1) represents the consistent model. The term

$$\Omega^2(b\mu_{ij} + \eta_{ij})$$

is known as the geometric stiffness matrix for this specialized rigid body motion (rotation). Laskin et al. [13] point out that this matrix provides coupling among the transverse vibrational modes of the beam and this coupling leads to the phenomenon of geometric stiffening. They further mention that this stiffening mainly raises the value of the bending vibrational frequencies.

Indeed, noting that equation (2.3.8) is true for a variety of simple beam mode shapes, and using the relations of Appendix B, equation (1) becomes



$$\begin{bmatrix} \ddots & 0 & 0 \\ 0 & m_B & 0 \\ 0 & 0 & \ddots \end{bmatrix} \begin{bmatrix} \vdots \\ \tilde{q}_i \\ \vdots \end{bmatrix} + \left\{ \begin{bmatrix} \ddots & 0 & 0 \\ 0 & m_B \omega_i^2 & 0 \\ 0 & 0 & \ddots \end{bmatrix} + \Omega^2 \begin{bmatrix} \ddots & & \vdots & \ddots \\ \dots & b\mu_{ij} + \eta_{ij} - m_B \delta_{ij} & \dots & \dots \\ \vdots & & \vdots & \ddots \end{bmatrix} \right\} \begin{bmatrix} \vdots \\ q_i \\ \vdots \end{bmatrix} = 0 \quad (2)$$

where the following equation has been used

$$\lambda_i^2 = \omega_i l^2 \sqrt{\frac{\rho}{EI}},$$

and the Kronecker delta is given by

$$\delta_{ij} = \begin{cases} 1, & i = j \\ 0, & i \neq j \end{cases}.$$

As it turns out in the case of cantilever mode shapes, the geometric stiffness matrix is positive definite (see section B.2.2), and dominates over the modal mass matrix  $G_{ij}$ . Consequently, equation (2) yields the correct spin-stiffening result as the angular rate  $\Omega$  is increased.

The inconsistent model is obtained using linear kinematics of deformation, so that the geometric stiffness matrix is absent. In this case, equation (2) reduces to

$$\begin{bmatrix} \ddots & 0 & 0 \\ 0 & m_B & 0 \\ 0 & 0 & \ddots \end{bmatrix} \begin{bmatrix} \vdots \\ \tilde{q}_i \\ \vdots \end{bmatrix} + m_B \begin{bmatrix} \ddots & 0 & 0 \\ 0 & \omega_i^2 - \Omega^2 & 0 \\ 0 & 0 & \ddots \end{bmatrix} \begin{bmatrix} \vdots \\ q_i \\ \vdots \end{bmatrix} = 0 \quad (3)$$

It is clear from the above equation that when  $\Omega$  reaches the value of the first fundamental bending frequency of the beam, the stiffness matrix will be singular. This amounts to the model predicting divergence under large enough spin, which is incorrect. On the other hand, if  $\Omega$  is much less than the first fundamental bending frequency, say about one order of magnitude less, then the discrepancy between equations (2) and (3) may be less noticeable and results using equation (3) might be qualitatively "correct."

From this it is apparent that a limit on the rigid body spin rate exists, below which the inconsistent model is "valid." This limit has been pointed out experimentally in the

literature in recent years [11,24,27]. Its analytical confirmation here serves as a check on the equations.

Ignoring all nonlinear terms that involve the elastic coordinates and speeds in equations (A.2.1.14), the ruthless model for uniform rotation of the base results in the equations

$$\begin{bmatrix} \ddots & 0 & 0 \\ 0 & m_B & 0 \\ 0 & 0 & \ddots \end{bmatrix} \begin{bmatrix} \vdots \\ \tilde{q}_i \\ \vdots \end{bmatrix} + m_B \begin{bmatrix} \ddots & 0 & 0 \\ 0 & \omega_i^2 & 0 \\ 0 & 0 & \ddots \end{bmatrix} \begin{bmatrix} \vdots \\ q_i \\ \vdots \end{bmatrix} = 0 \quad (4)$$

While equation (4) does not exhibit the correct spin-stiffening of equation (2), it also does not show the incorrect destiffening of equation (3). Clearly, if the angular rate  $\Omega$  is small enough, equation (4) will be as "valid" as equations (3) or (2), with the added advantage of yielding results that are more conservative than those of equations (3). In other words, even for large  $\Omega$ , the ruthless model yields qualitatively similar results to those of the consistent one, while the inconsistent model fails.

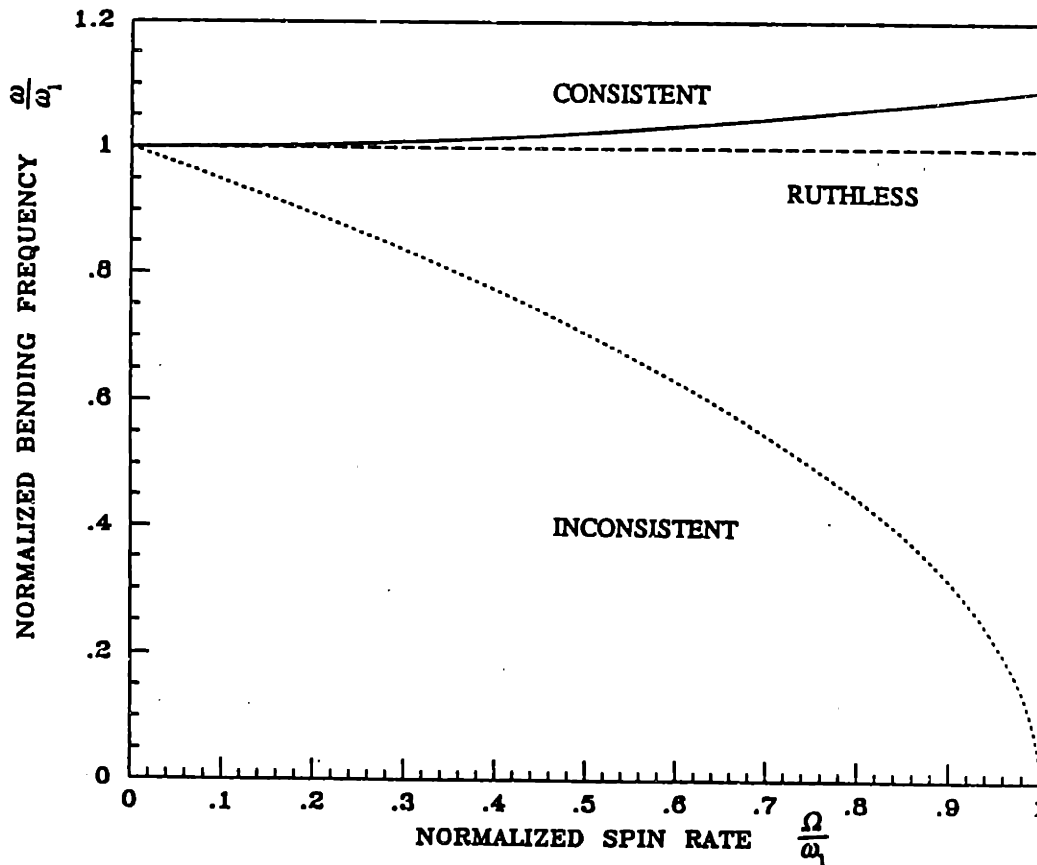


Fig. 3.1: Fundamental Bending Frequency of Spinning Beam v.s. Spin Rate

The above results are succinctly summarized in Fig. 3.1, where the first fundamental bending frequency of the spinning beam is plotted versus spin rate for all three models (for the case of only one assumed mode).

### 3.3.2 Pure Linear Acceleration

Specializing to the prescribed motion of constant translational acceleration along the neutral axis of the beam

$$\dot{v}_1 = g = \text{constant}, \quad v_2 = v_3 = 0$$

equation (A.2.1.14) turns into

$$\sum_{i=1}^n G_{ij} \ddot{q}_i + \sum_{i=1}^n (H_{ij} - g\mu_{ij}) q_i = 0$$

(j = 1, \dots, n)

(1)

which are the consistent model equations. Making use of relations (2.3.8), equation (1) becomes

$$\begin{bmatrix} \ddots & 0 & 0 \\ 0 & m_B & 0 \\ 0 & 0 & \ddots \end{bmatrix} \begin{bmatrix} \vdots \\ \ddot{q}_i \\ \vdots \end{bmatrix} + \left\{ \begin{bmatrix} \ddots & 0 & 0 \\ 0 & m_B \omega_i^2 & 0 \\ 0 & 0 & \ddots \end{bmatrix} - g \begin{bmatrix} \ddots & \vdots & \ddots \\ \cdots & \mu_{ij} & \cdots \\ \ddots & \vdots & \ddots \end{bmatrix} \right\} \begin{bmatrix} \vdots \\ q_i \\ \vdots \end{bmatrix} = 0$$
(2)

Since  $\mu_{ij}$  is positive definite in this case, for large enough  $g$  destiffening is again predicted. For  $g$  large enough, the stiffness matrix becomes non-positive definite which implies that the beam buckles due to its own weight. The predicted buckling is correct, and is lost with the inconsistently or ruthlessly linearized models, as shall be seen. This suggests that a translational acceleration limit also exists beyond which our model is again grossly incorrect if we do not use equations exact to first order.

Reducing the model to a single assumed mode, it is easy to obtain a first approximation to this translational acceleration limit:

$$g = \frac{l\omega_1^2}{\xi_1} = \frac{EI\lambda_1^4}{m_B l^2 \xi_1}$$
(3)

$\xi_1$  and  $\lambda_1$  are constants that depend on the mode shapes chosen (see section B.2.2). For the parameters used for the outboard link of the manipulator, this limit is approximately  $g \sim 45g$ 's.

The inconsistent and the ruthless models have the same equations for this case, mainly

$$\begin{bmatrix} \ddots & 0 & 0 \\ 0 & m_B & 0 \\ 0 & 0 & \ddots \end{bmatrix} \begin{bmatrix} \vdots \\ \bar{q}_i \\ \vdots \end{bmatrix} + \begin{bmatrix} \ddots & 0 & 0 \\ 0 & m_B \omega_i^2 & 0 \\ 0 & 0 & \ddots \end{bmatrix} \begin{bmatrix} \vdots \\ q_i \\ \vdots \end{bmatrix} = 0 \quad (4)$$

Once again it might be expected that for small enough axial accelerations,  $g$ , equation (4) will yield results qualitatively similar to those of the consistent model, equation (2). It is significant that the ruthless model is as good as the inconsistent model.

### 3.3.3 General Stability Boundary of the Consistent Model

In general, from equations (A.2.1.14), an effective stiffness matrix can be written as

$$(K)_{ij} = H_{ij} + v_2 v_3 \mu_{ij} + v_3^2 [b \mu_{ij} + \eta_{ij} - G_{ij}] - \dot{v}_1 \mu_{ij} \quad (1)$$

whence it can be seen that besides being affected by axial acceleration and centripetal terms, the "dynamic" stiffness contains a coriolis term. Again using only one assumed mode, it is possible to obtain a three-dimensional stability boundary depending on the values, all functions of time, of  $dv_1/dt$ ,  $v_2$ , and  $v_3$ . The boundary is given by the equation

$$y = - \left\{ \frac{\frac{1}{\xi_1} - z}{x} + \left[ \frac{b}{l} + \frac{1}{\xi_1} (\gamma_1 - 1) \right] x \right\} \quad (2)$$

where  $x$ ,  $y$ , and  $z$  are nondimensional variables given by

$$x = \frac{v_3}{\omega_1}, \quad y = \frac{v_2}{l\omega_1}, \quad z = \frac{\dot{v}_1}{l\omega_1^2}$$

and  $\xi_1$  and  $\gamma_1$  are constants that arise from the foreshortening matrices  $\eta_{ij}$  and  $\mu_{ij}$ , and that depend on the mode shapes (see section B.2.2). Equation (2) is obtained by requiring the "dynamic" stiffness to equal zero.

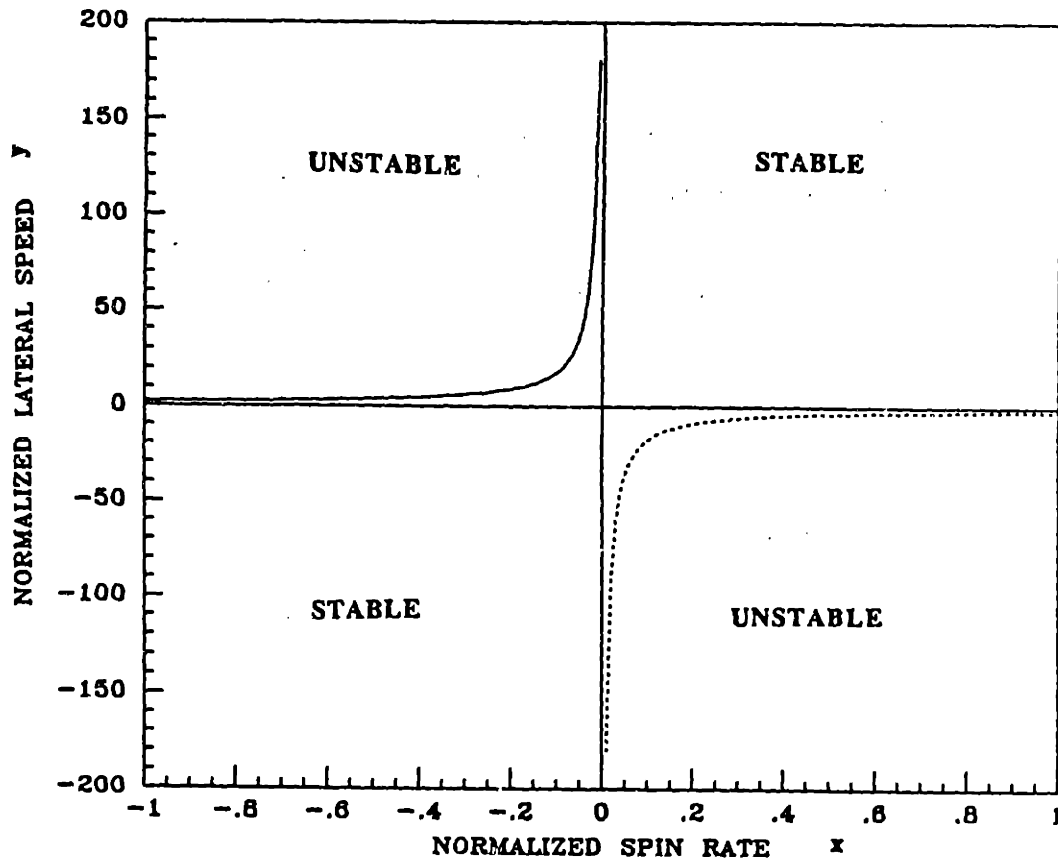


Fig. 3.2: Stability Boundary for Axial Acceleration Below Critical

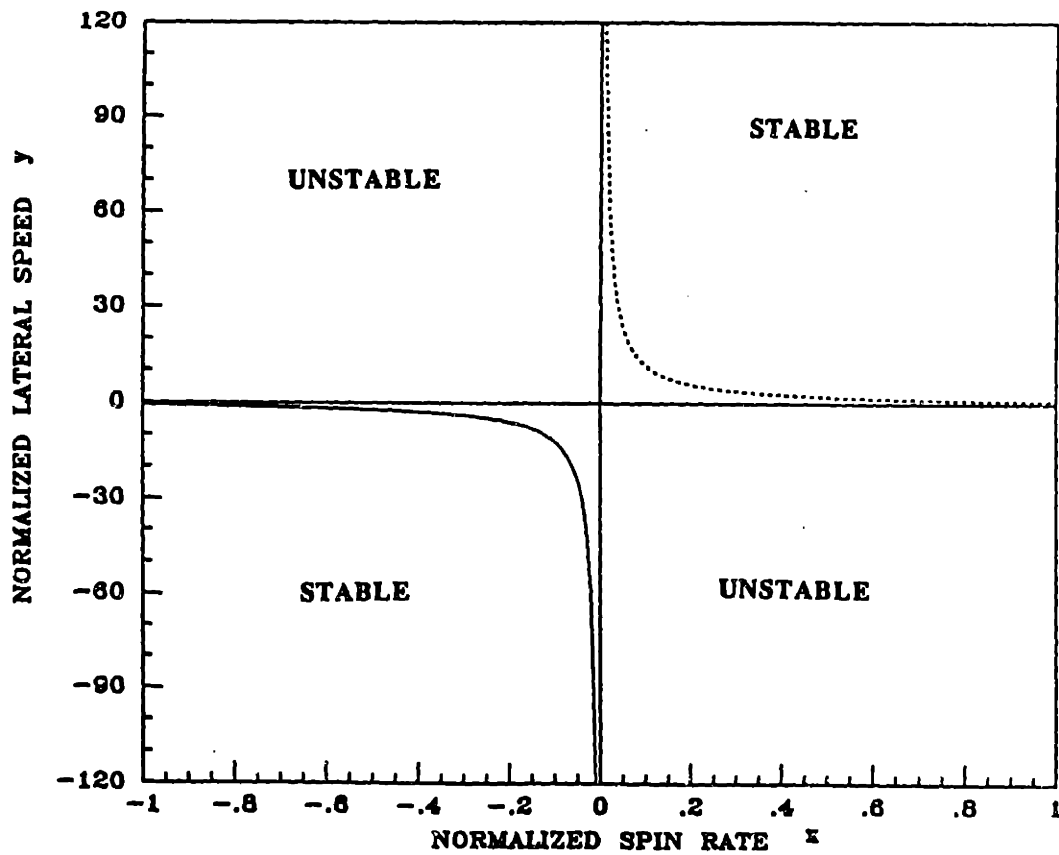


Fig. 3.3: Stability Boundary for Axial Acceleration Above Critical

Figs. 3.2 and 3.3 show two-dimensional projections onto the  $x$ - $y$  plane for two non-dimensionalized values of axial acceleration. Not surprisingly, taking into consideration the previous results, the larger  $z$  is, the larger the region in the  $x$ - $y$  plane where divergence is predicted. Also note there are two qualitatively different  $x$ - $y$  boundaries, corresponding to values of  $z$  above and below the "critical" value which is the limit predicted in the previous section for the case of axial acceleration only.

This stability boundary is used in the simulation of the two-link manipulator (see section 4.3.3), to determine when (and if) divergence of the outboard link is predicted by the consistent equations for the tried maneuvers. This helped distinguish between correct results and numerical ill-behavior.

### **3.4 PREDICTIONS**

From an examination of the analytical results presented above, the following predictions are ventured in what concerns the relative significance of nonlinear terms found in more complex systems.

For the values of the beam properties selected (see Table 4.1), and for maneuvers typical of a manipulator, it seems that the more restrictive limit on the validity of other than the correctly linearized equations is by far the one imposed on the rotational rigid body rates. Therefore, for rotational rigid body rates of less than an order of magnitude of the first fundamental bending frequency of a system of the type under consideration, no significant difference might be expected among the three models studied above. For rates larger than this limit, the inconsistent model will degrade, eventually predicting divergence; while the ruthless model will become increasingly more inaccurate with increasing rates, when compared to the consistent model.

### **3.5 EIGENANALYSIS OF THE TWO-LINK MANIPULATOR**

An examination of the equations of motion for the two-link, flexible manipulator (see App. C) makes it clear that the complexity of the mass matrix and nonlinear inertial terms could be diminished immensely by dropping terms involving the generalized elastic coordinates and speeds (i.e., the "ruthless" case). It would be advantageous to know, then, if these terms have a significant effect on the dynamics of a chain of elastic bodies if we are limited to the low rotational speeds and translational accelerations encountered during slew maneuvers with joint torques limited by the requirement that flexible

deflections remain small. In order to investigate this, we propose to examine the three models presented in section 3.2, to note, consistent, inconsistent, and ruthless, as applied to the two-link arm. The complexity of the motion equations precludes an analytical study akin to the one presented in section 3.3. It is therefore necessary to rely on numerical simulation and compare the performance of the three "models" of the arm when it is subjected to several possibly typical maneuvers.

In order to examine the above predictions on the manipulator, it is desirable to obtain a measure of the fundamental vibration frequency of the system, since this quantity dominates the first approximation of the limit on the validity of the simplified models. The two-link manipulator, however, is a nonlinear dynamical system with configuration dependent mass matrix, as presented in section 3.1 (see also App. C). In this case, the standard eigenanalysis does not strictly apply. To obtain a first order linear approximation of the system frequencies and mode shapes, a configuration dependent eigenanalysis is performed on the manipulator.

An examination of the equations for the system presented in Appendix C reveals that the mass matrix depends on the relative angle between the links ( $\beta$ ), as well as on the elastic generalized coordinates of both links. Choosing the nominal configurations to be the undeformed links, all the generalized elastic coordinates are zero, and the system frequencies and mode shapes are determined for several values of  $\beta$ . For each configuration, the eigenanalysis is performed for both free and locked joints. The values of the parameters used in this analysis correspond to those presented in chapter four for the numerical simulation (see Table 4.1).

(deg)	Free joints				(rad/sec)	Locked joints			
$\beta$	i= 1	2	3	4	i= 1	2	3	4	
0	42.9	68.1	153.7	224.3	3.03	7.36	62.2	120.7	
45	42.8	68.0	153.6	224.3	3.15	6.82	62.0	120.7	
90	42.7	68.0	153.5	224.3	3.53	5.90	61.6	120.7	
135	42.8	68.0	153.6	224.3	4.08	5.32	61.6	120.7	
180	42.9	68.1	153.7	224.3	4.35	5.19	61.8	120.8	

**Table 3.1: Configuration Dependent Manipulator Frequencies**

As might be expected, the free joints results are almost identical for all values of  $\beta$  considered (see Table 3.1). Fig. 3.5 shows these results for  $\beta$  equal to zero. For fixed joints, on the other hand, the lowest two frequencies move closer together on the  $j\omega$  axis as  $\beta$  is increased from 0 to 180 degrees (see Fig. 3.4 and Table 3.1). The higher frequencies are less affected by changes in  $\beta$ . Figs. 3.6 to 3.10 show the first four fixed joints mode shapes for the different values of relative angle. Since only eight assumed modes (four per link) were used (as a maximum) in implementing the simulation, it is to be expected that only the first four frequencies of the system presented herein are accurate, while perhaps even fewer mode shapes.

(deg)	Link 2 rigid				(rad/sec)	Link 1 rigid			
$\beta$	i=1	2	3	4	i=1	2	3	4	
0	3.52	29.2	320.5	907.0	4.67	63.6	202.0	479.2	
90	4.04	23.9	318.6	905.6	-	-	-	-	

Table 3.2: Frequencies for Each Link when Other is Rigid and Joints are Locked

For comparison purposes, and for reference, Table 3.2 lists the eigenfrequencies for each link, when the other is considered rigid and both joints are locked. In the following pages, the system mode shapes have been normalized so that the largest deflection of either link be approximately ten percent of the link lengths, which have been normalized to one.

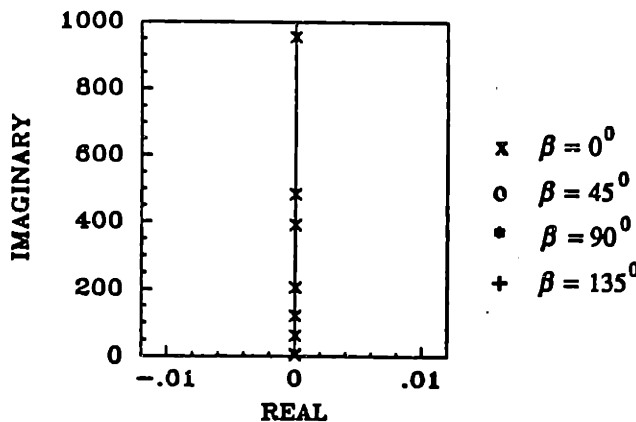


Fig. 3.4a: s-plane Plot of Manipulator Frequencies with Locked Joints for Elbow Angle equal to 0 deg.

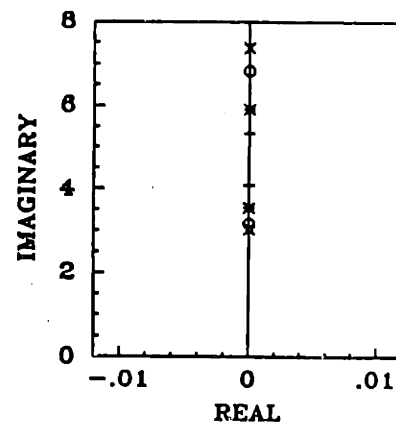
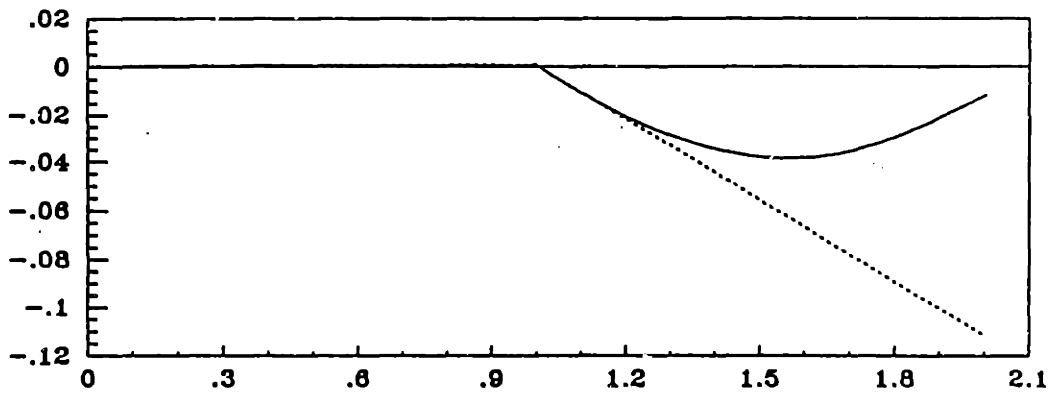
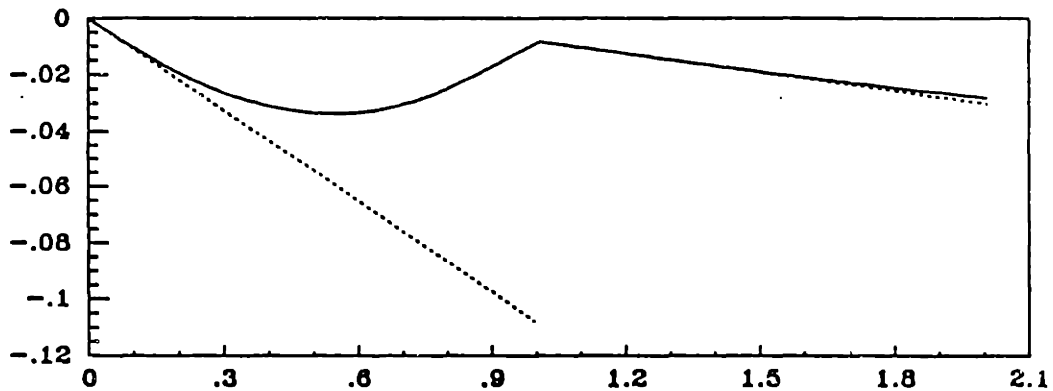


Fig. 3.4b: Close-up of Lower Frequency Range for Different Values of the Elbow Angle

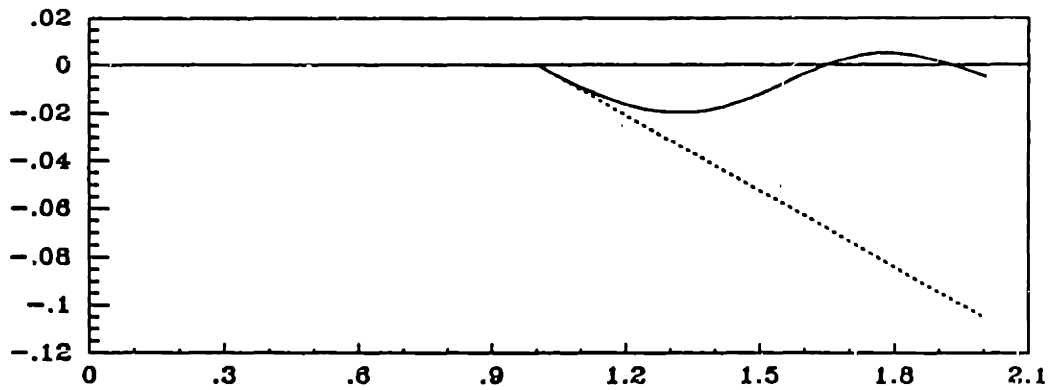




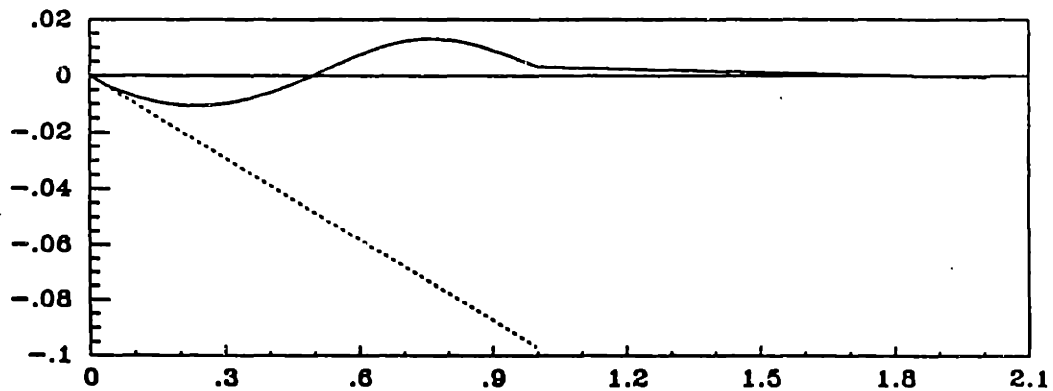
FIRST MODE



SECOND MODE



THIRD MODE



FOURTH MODE

Fig. 3.5 First Four Manipulator Mode Shapes with Joints Free

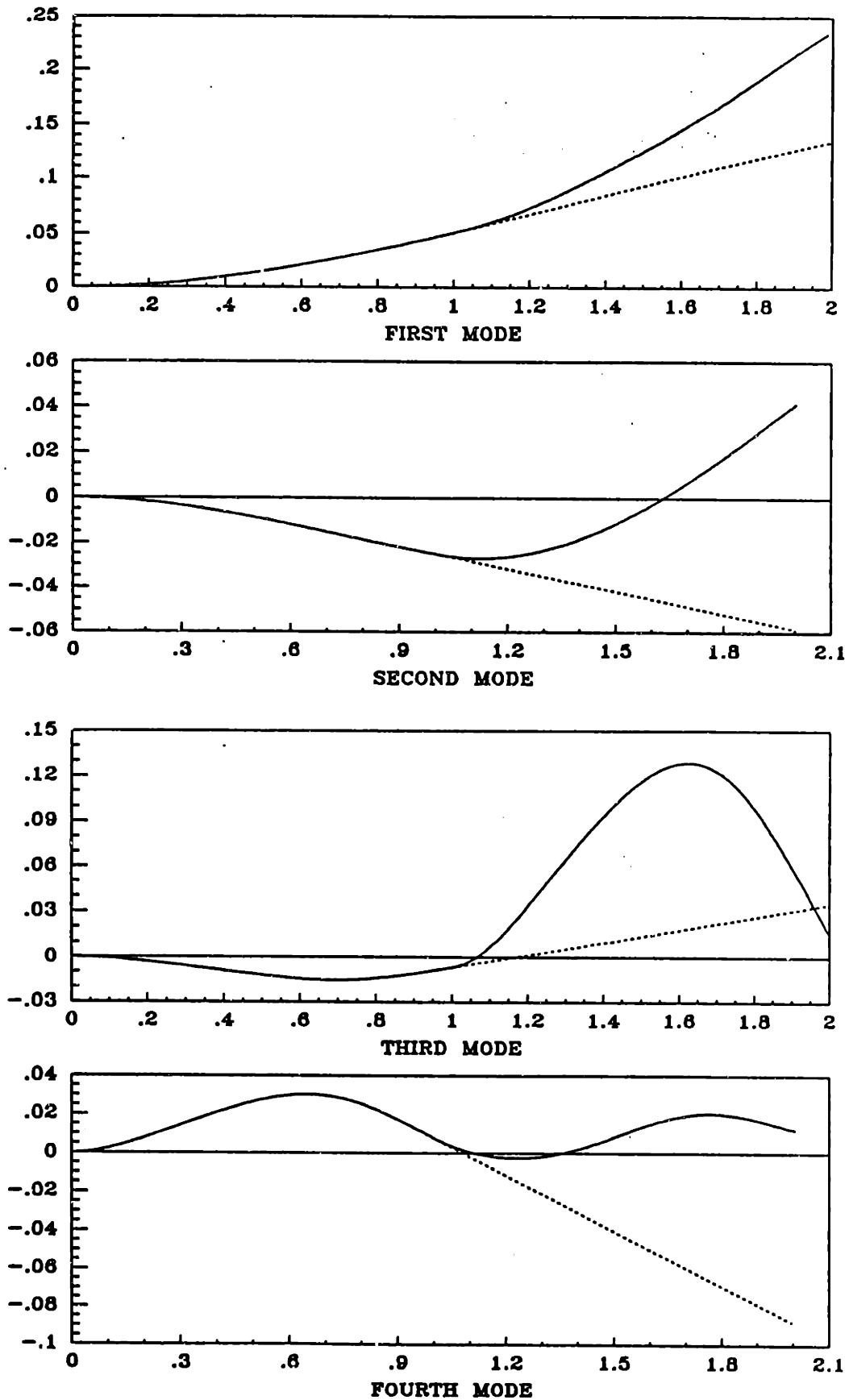


Fig. 3.6: First Four Manipulator Mode Shapes with Joints Locked ( $\beta=0$  deg)

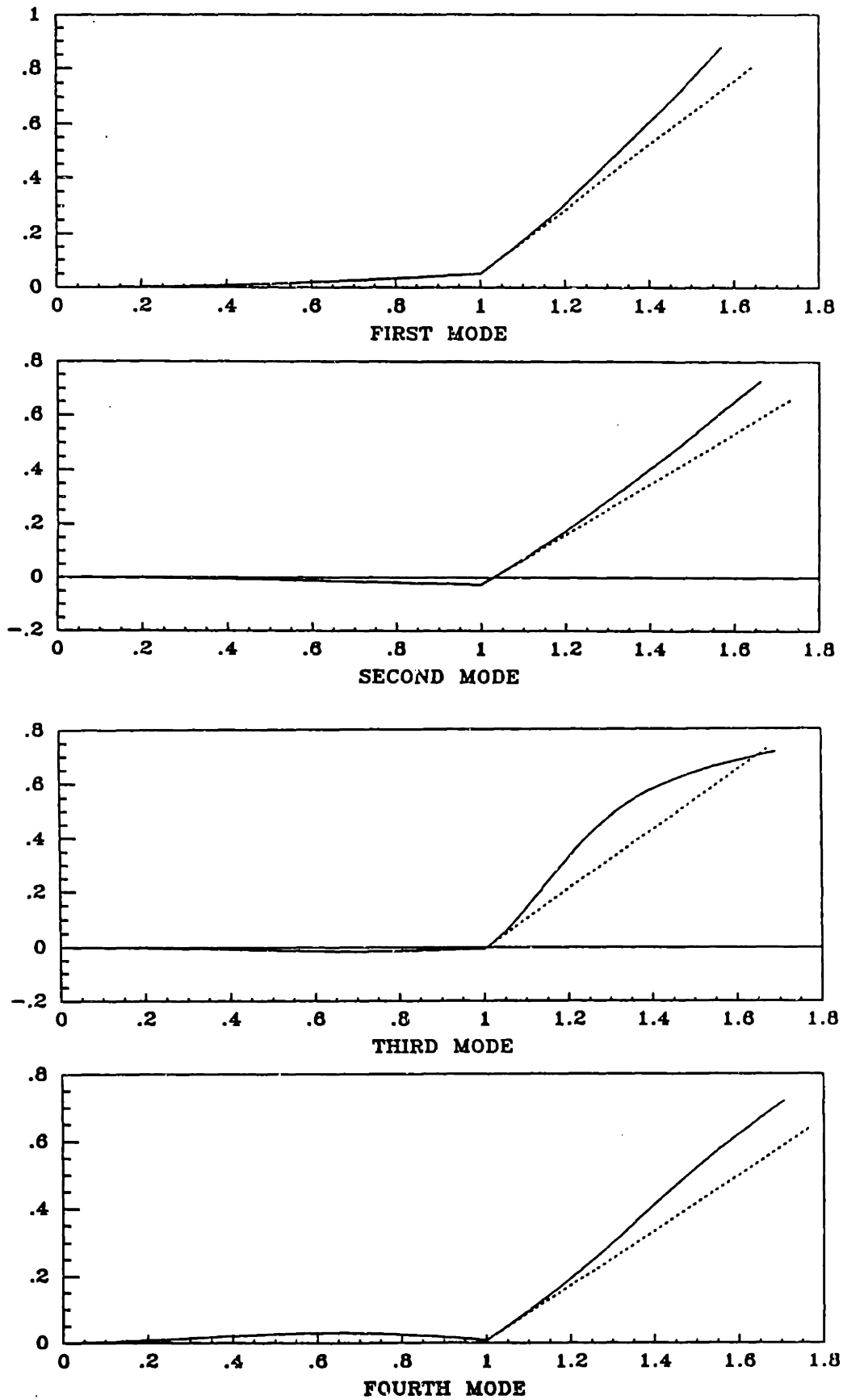


Fig. 3.7: First Four Manipulator Mode Shapes with Joints Locked ( $\beta=45$  deg)

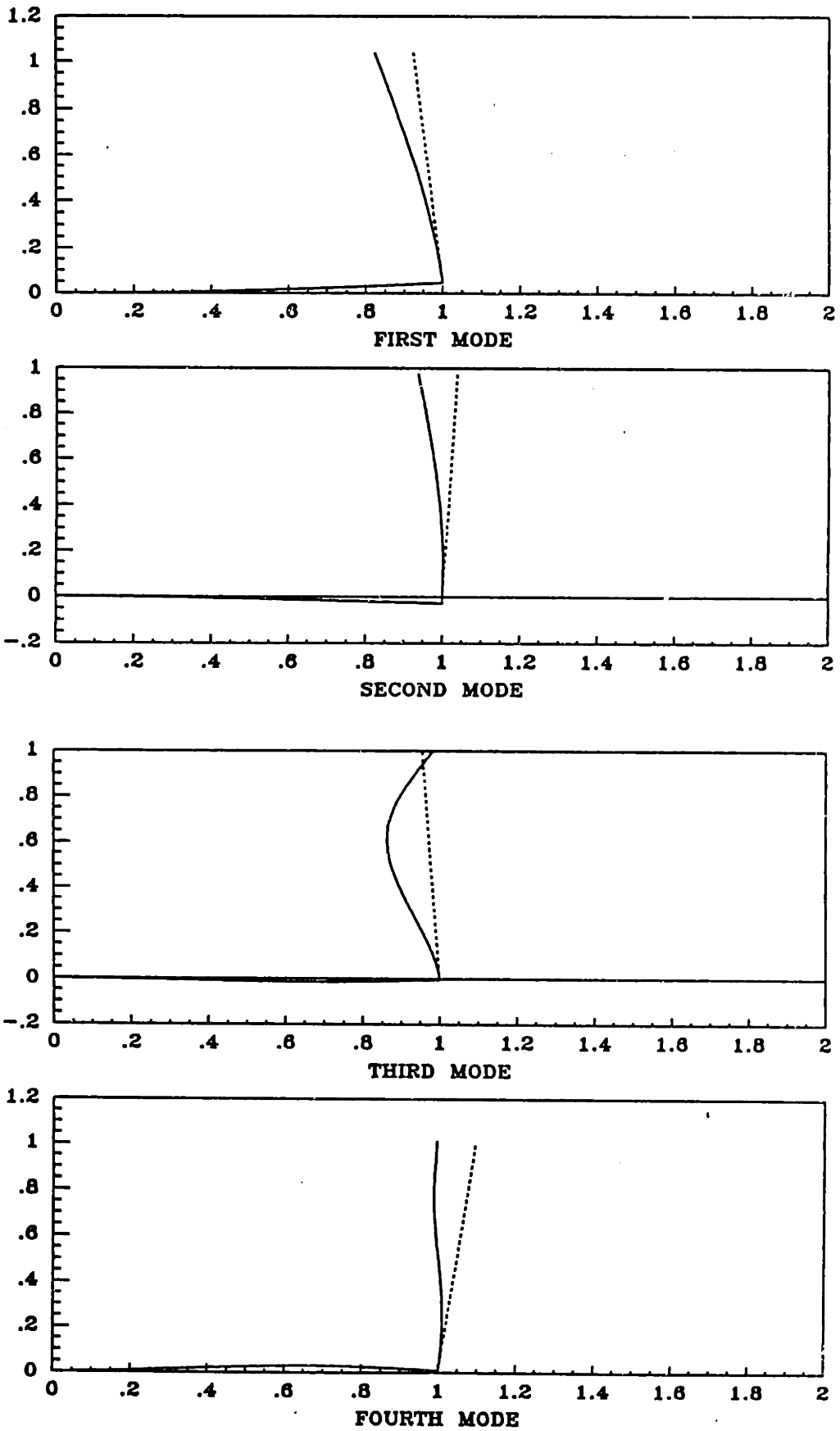


Fig. 3.8: First Four Manipulator Mode Shapes with Joints Locked ( $\beta=90$  deg)

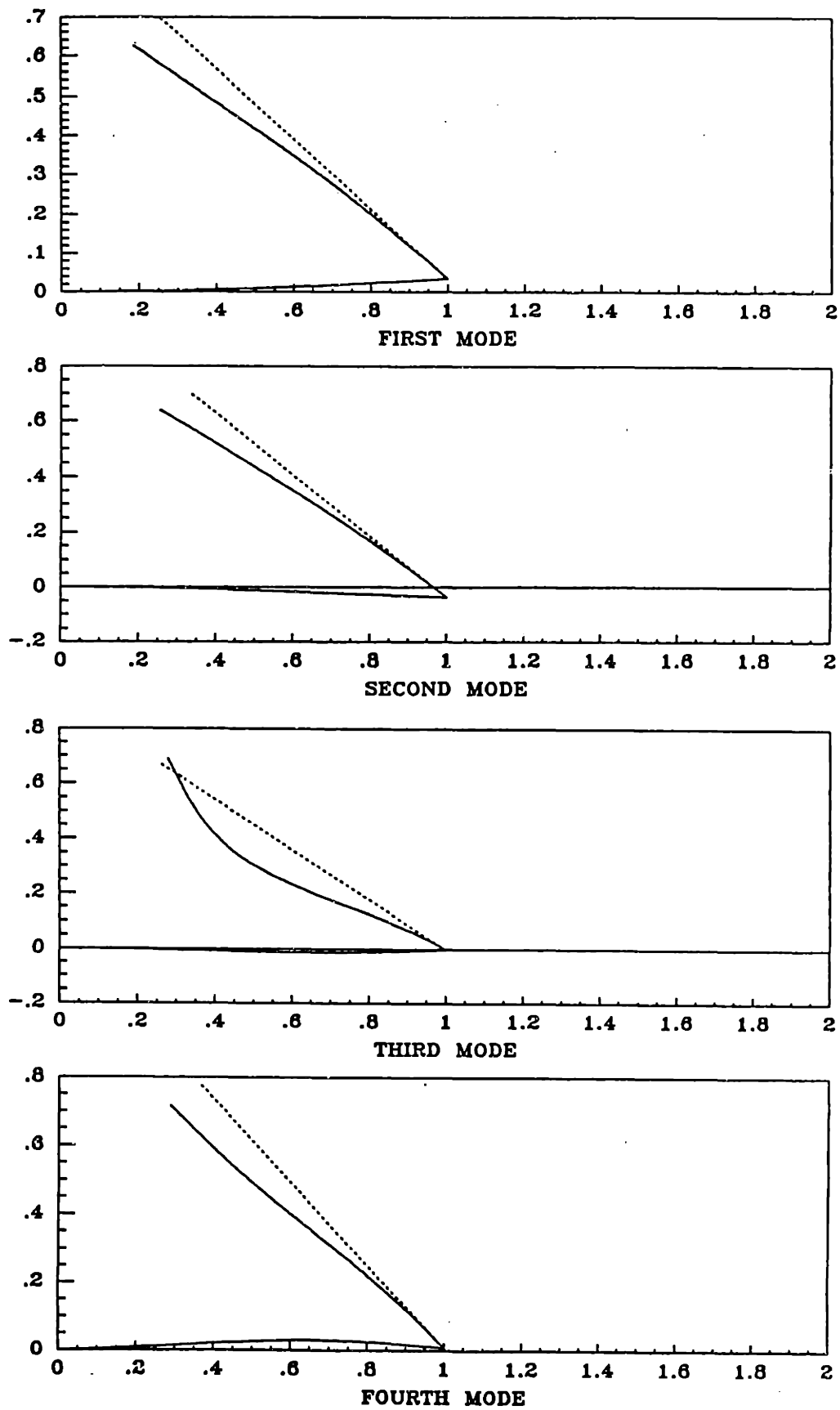


Fig. 3.9: First Four Manipulator Mode Shapes with Joints Locked ( $\beta=135$  deg)

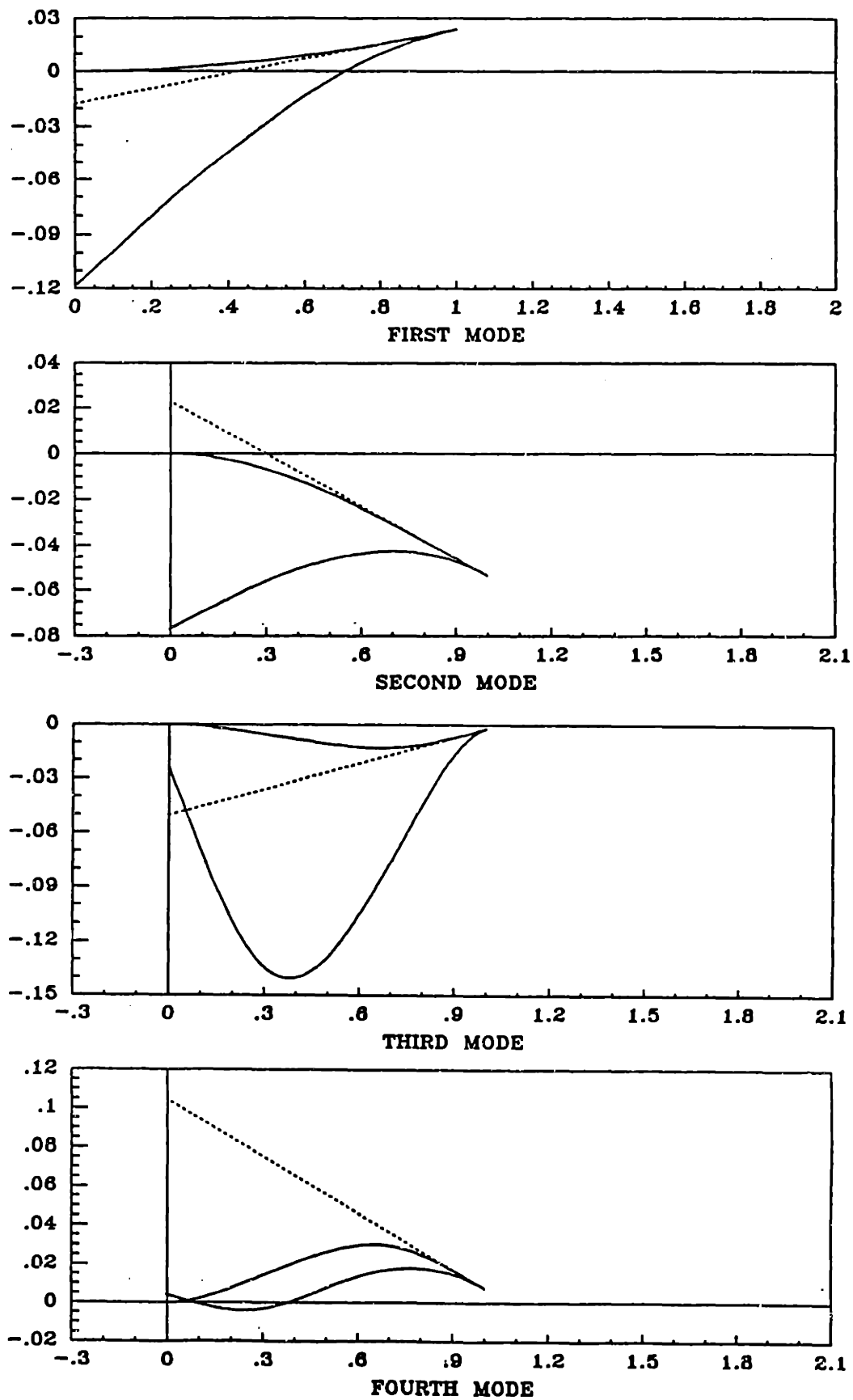


Fig. 3.10: First Four Mode Shapes with Joints Locked ( $\beta=180$  deg)

# CHAPTER 4: SIMULATION RESULTS

## INTRODUCTION

In the previous chapter, three levels of increasing simplification of the correctly linearized equations of motion were proposed. Based on the results of the simple one beam example, predictions were made concerning the relative significance of elastic nonlinear terms in the equations of motion of chains of flexible bodies undergoing large rigid body motion, but small elastic deflections. Recall that elastic nonlinear terms are those nonlinear terms in the equations of motion which involve the generalized elastic coordinates and speeds.

In this chapter the same three models are used to test these predictions for the case of the manipulator with two flexible links. The chapter starts with a description of the numerical simulation capabilities. After a brief section on trajectory time-scaling, the simulation results of implementing four different trajectories for each model are presented.

## 4.1 NUMERICAL SIMULATION

The motion equations for the two-link, flexible, planar manipulator, consistently linearized in small elastic deflections and speeds, were programmed in FORTRAN and implemented in a VAXstation 2000. The code developed for this purpose allows the joint and tip bodies to have mass, moment of inertia, and planar dimensions, just as in the case of the equations developed in chapter two (see Fig. 2.1). A maximum of four cantilever modes per beam are implemented, although only two per link are used in most of the actual simulations. One percent damping ratio is assumed for each cantilever mode to approximately model material damping in the manipulator. The structure of the code is modular for ease of handling and to facilitate expansion. A short separate program handles user interface by creating the input files needed by the main program, which can then be run as time-sharing or in batch mode. This user interface has a short and a long version. The long version allows the user to input the physical manipulator parameters such as mass density, link lengths, modal damping, joint planar dimensions, etc. The short version lets

the user select initial and final times for the simulation, initial configuration of the manipulator, number of modes to be used for each link, initial time step to be tried, and the kind of model to be run, i.e., consistent, inconsistent, or ruthless (see section 3.2).

Actuation is assumed in the form of joint torques, as in chapter two. Torque time histories, which can be open or closed-loop, are created by a subroutine which is linked to the main program. This subroutine has access to the state vector and to the simulation time, to allow for feedback and time-varying forcing schemes. It can also generate computed torques time histories, given desired trajectories. It is in this last capacity that it was used for all of the cases presented below, with the notable exception of the time-optimal bang-bang controller (section 4.3.4).

As can be seen from Appendix C, the configuration dependent mass matrix is non-symmetric due to the linearization. For this reason, the mass matrix inversion needed to obtain the form of equation (2.4.3.3) for the equations of motion is executed using LU decomposition [6] instead of the computationally cheaper Cholesky decomposition. The latter requires symmetric, positive definite matrices. Once the equations are in the form of equation (2.4.3.3), they are integrated in time using a Runge-Kutta fourth-order scheme with adaptive time step [22].

The constants that depend on modal integrals are evaluated by subroutines that use the physical parameters' input file. These subroutines are mode shape dependent and need to be rewritten if other than cantilever mode shapes are desired (see App. B and D). Two routines, ENERGY and AMOMENTUM, provide energy and angular momentum checks. They determine the instantaneous energy and angular momentum of the system and compare it to the change in the corresponding quantity due to forcing and/or damping.

The output of the simulation is of two kinds. "Raw" data is output to the file DATFILE.DAT in a format which can be used by other FORTRAN programs. Data in MATRIXx [16] format is output to MATPLOT.DAT. The latter is used to obtain the plots presented in this chapter using MATRIXx. The "raw" data file is used by another FORTRAN program, POST\_PROCESS, which processes it and puts it into the proper form to be used by ANIMATE\_ARM, which does a graphics animation in a Vax Workstation screen. The FORTRAN code for the simulation, and ancillary programs and subroutines are included in Appendix D.

The values of the physical parameters utilized for the manipulator simulation were chosen to mimic an actual experimental testbed presently under construction at Martin



Marietta by Dr. Eric Schmitz. Table 4.1 shows the assumed properties for the manipulator (see also Fig. 2.1).

Physical Properties of Planar Manipulator with Two Flexible Links			
Mass of shoulder body (kg)	20.0	Length of link 1 (m)	0.9144
Mass density of link 1 (kg/m)	1.33937	Length of link 2 (m)	0.9144
Mass of elbow body (kg)	14.0		
Mass density of link 2 (kg/m)	0.669685	Other lengths (see Fig. 2.1):	
Mass of tip body (kg)	2.0	b <sub>1</sub> (m)	0.0762
		b <sub>21</sub> (m)	0.0762
Moments of Inertia (about axis perpendicular to plane):		b <sub>22</sub> (m)	0.0127
Shoulder body (kgm <sup>2</sup> )	0.01	b <sub>t</sub> (m)	0.0508
Elbow body (kgm <sup>2</sup> )	0.03		
Tip body (kgm <sup>2</sup> )	0.01		

Table 4.1: Physical Properties of the Two-link Manipulator

## 4.2 TIME SCALING OF TRAJECTORIES

In the following sections, reference is made to time-scaled trajectories. Time-scaling of nominal trajectories [7] is achieved by replacing time as the independent variable by the new variable

$$r = \alpha t, \quad \alpha > 0$$

where  $\alpha$  is a constant. When  $\alpha$  is greater than one, the trajectory is sped up, while if  $\alpha$  is less than one it is slowed down. Notice that with this substitution, the time derivatives of the trajectories become

$$\begin{aligned} \frac{d}{dt}\theta(r) &= \alpha\dot{\theta}(\alpha t) \\ \frac{d^2}{dt^2}\theta(r) &= \alpha^2\ddot{\theta}(\alpha t) \end{aligned} \tag{1}$$

From this it is apparent that rates scale like  $\alpha$ , while accelerations, and thus torques, scale like the square of  $\alpha$ . These relations are used in the following sections to select a scaling factor that yields a desired maximum value of angular rate, or a given maximum value of torque to obtain desired maximum link tip deflections.

## 4.3 RESULTS

All the trajectories presented below were run in open loop after the torques had been computed from the inverse dynamics problem (given the desired angular trajectories) assuming rigid links for the manipulator. The exception to this is the minimum-time trajectory of section 4.3.4. Although it was run open loop like the rest, maximum torque bang-bang control was implemented instead of computed torques. For all simulation runs, only two assumed modes per link were used, since this gave adequate results and was computationally much cheaper than running the full four modes per link. With two modes per link, the first two system vibration frequencies were obtained to within three percent of the value obtained using four modes per link.

### 4.3.1 Spinning of the Outboard Link

The first maneuver tried on the two-link manipulator is the smooth spin-up maneuver of the outboard link. This is done for purposes of comparison with recent published results [11,27], and thus as a form of validation of the correctly linearized equations of motion. For this reason, the same smooth spin-up as [27] is selected

$$\dot{\beta} = \frac{\Omega}{t_f} \left( t - \frac{2\pi}{t_f} \sin \left( \frac{2\pi}{t_f} t \right) \right) \quad (1)$$

where

$$\begin{aligned} t_f &= 15 \text{ sec} \\ \Omega &= 6 \text{ rad / sec} \end{aligned}$$

and  $d\beta/dt$  is the elbow angular rate.

The above trajectory results in a constant angular rate at the elbow of 6 rad/sec at the end of 15 seconds. To implement this on the two-link manipulator simulation, the shoulder angle ( $\theta$ ) was clamped, and the inboard link was assumed rigid. Note that the first fundamental bending frequency of the second (outboard) link, with the first (inboard) link rigid and the shoulder angle locked, is 4.67 rad/sec (see Table 3.2). Accordingly, from the discussion in chapter three, summarized in the predictions of section 3.4, it can be surmised that the inconsistent model will fail, while the ruthless model will yield results that are not correct, but more conservative. This is indeed the case as can be observed in the results presented in Fig. 4.1.

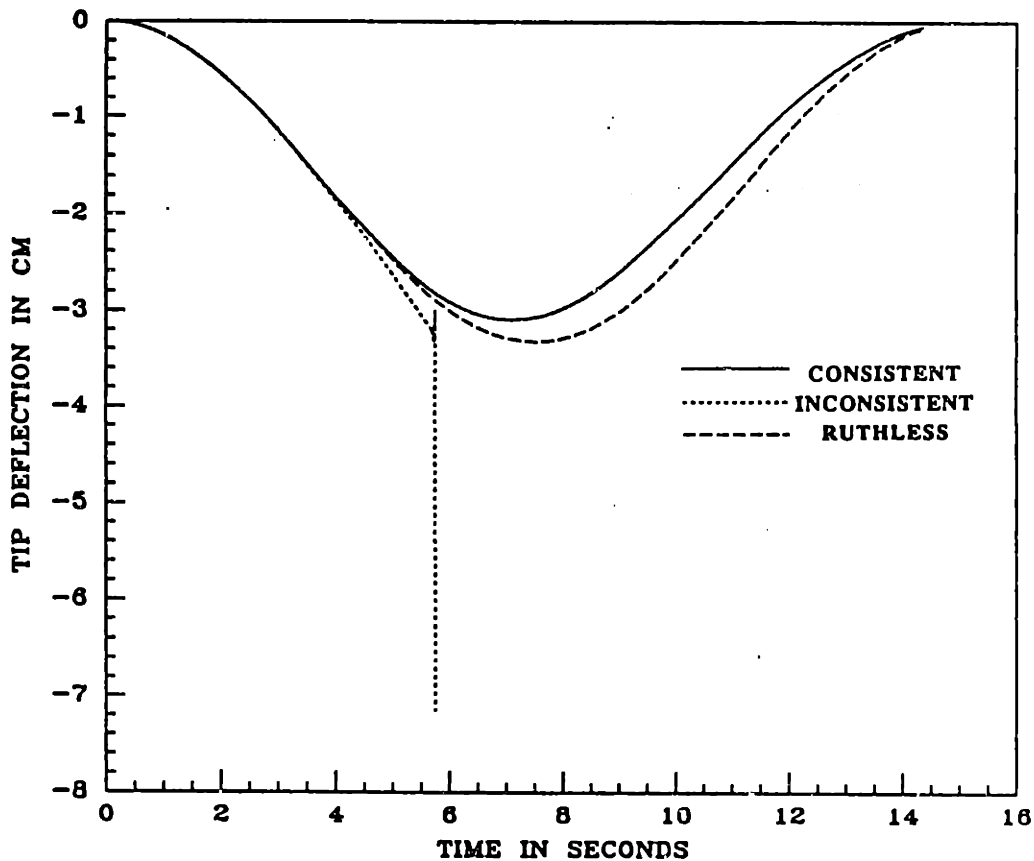


Fig. 4.1: Smooth Spin-up Maneuver for the Outboard Link

It can be seen from the figure that the consistent model yields results that are stiffer than those for the ruthless model. This agrees with the analysis presented in section 3.3.1. The two models yield otherwise qualitatively similar results. The inconsistent model, on the other hand, predicts divergence under the smooth spin-up.

### 4.3.2 First Smooth Trajectory

In section 3.4 it was predicted that the more severe limit on the validity of other than consistently linearized equations would be the limit on rigid body angular rates. In the case of chains of flexible bodies, as exemplified by the two-link manipulator in this simulation, the nonlinearity arising from dependence on configuration makes it difficult to select a "characteristic" angular rate in the general case. This suggests a case by case approach. With this in mind, the first trajectory tried on the full two-link manipulator is a smooth maneuver intended to mimic as much as possible a single slewing beam. This implies little motion of the relative elbow angle  $\beta$ , and thus small elbow angular rates. In this manner the shoulder angular rate dominates and becomes the "characteristic" angular rate of importance. This provides possibly the simplest way to test the rigid body angular rate limit in the two-link manipulator.

The smooth trajectory is obtained by assuming a form of the angular time histories that is quintic in time. This allows the specification of angle, angular rate and angular acceleration at the initial and final times of the trajectories [5]. Selecting

$$\begin{aligned}\theta_i &= 0 & \beta_i &= 0.0873 \text{ rad} \\ \theta_f &= \pi \text{ rad} & \beta_f &= 0 \\ \dot{\theta}_i &= \dot{\theta}_i = \dot{\beta}_i = \dot{\beta}_i = \dot{\theta}_f = \dot{\theta}_f = \dot{\beta}_f = \dot{\beta}_f = 0 \\ t_f &= 8.0 \text{ sec}\end{aligned}$$

the coefficients for the quintic polynomial in time are obtained from the relations

$$\begin{aligned}a_1 &= \dot{\theta}_i \\ a_2 &= \frac{\ddot{\theta}_i}{2} \\ a_3 &= \frac{20\theta_f - 20\theta_i - (8\dot{\theta}_f + 12\dot{\theta}_i)t_f - (3\ddot{\theta}_i - \ddot{\theta}_f)t_f^2}{2t_f^3} \\ a_4 &= \frac{30\theta_f - 30\theta_i + (14\dot{\theta}_f + 16\dot{\theta}_i)t_f + (3\ddot{\theta}_i - 2\ddot{\theta}_f)t_f^2}{2t_f^4} \\ a_5 &= \frac{12\theta_f - 12\theta_i - (6\dot{\theta}_f + 6\dot{\theta}_i)t_f - (\ddot{\theta}_i - \ddot{\theta}_f)t_f^2}{2t_f^5}\end{aligned}\tag{1}$$

with analogous relations for the relative elbow angle ( $\beta$ ). The desired trajectory results

$$\begin{aligned}\theta(t) &= a_0 + a_1t + a_2t^2 + a_3t^3 + a_4t^4 + a_5t^5 \\ \beta(t) &= b_0 + b_1t + b_2t^2 + b_3t^3 + b_4t^4 + b_5t^5\end{aligned}\tag{2}$$

Fig. 4.2 shows the computed torques for the nominal trajectory scaled by a factor of two ( $\alpha=2.0$ ).

Figs. 4.3 to 4.5 show the results of the three time-scaled trajectories tried. The maneuvers were scaled to vary the maximum value of the characteristic rigid body rate, i.e., the shoulder angular rate. The first fundamental bending frequency of the arm, in extended configuration and with joints locked ( $\beta=0$ ) is approximately three radians per second (see section 3.5). The first case shown exhibits low shoulder angular rate relative

to the fundamental ( $d\theta/dt$  about 0.2 rad/sec at maximum). As expected, the elbow rate is very small. For this case, all three models exhibit excellent agreement, as expected from the discussion in chapter three.

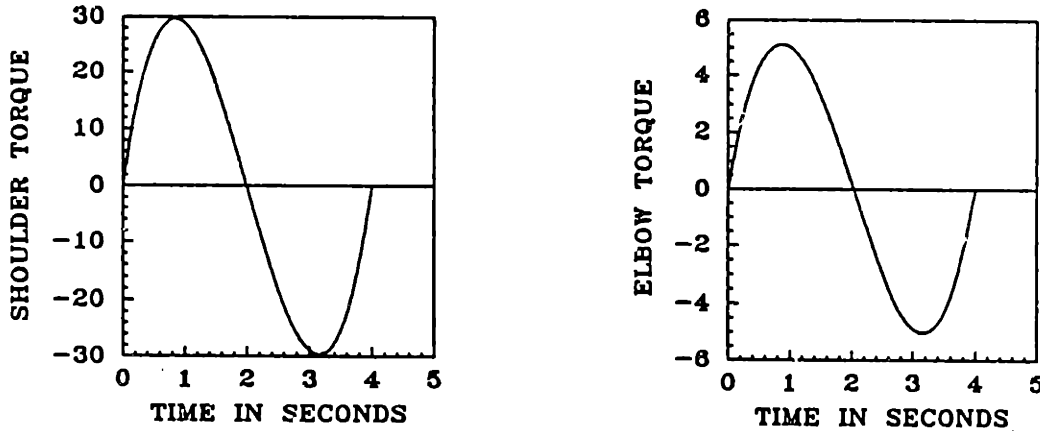


Fig. 4.2: Computed Torques for First Smooth Trajectory (Nm)

In the second case, the nominal trajectory was scaled down by a factor of 0.4297. In this case the shoulder angular rate is about 0.3 rad/sec at maximum, or ten percent of the first fundamental bending frequency of the system. This is the limit of accuracy of the inconsistent model, if the predictions of section 3.4 are correct. From Fig. 4.4 it is clear that while ruthless and consistent models still agree very well, the inconsistent model exhibits a high frequency "chattering." This was deemed a sort of onset of ill-conditioning, since the chattering seems to be numerical in nature. As shall be seen for the last case tried, for shoulder rates higher than this limit (ten percent of the fundamental), the inconsistent model fails altogether.

Figure 4.5 shows the last time-scaled trajectory, where the nominal trajectory was sped up ( $\alpha=2.0$ ). For this case, the shoulder angular rate is high, about half of the first fundamental vibration frequency of the manipulator. In this case, the plots show only the ruthless and consistent models, since the inconsistent model has failed. While good agreement is still evident between the two remaining models, a notable discrepancy is apparent in the elbow angle and elbow angular rates. This is to be expected since the "characteristic" rate is a significant fraction of the fundamental, and from the discussion in chapter three, it would be expected that the ruthless be valid accurately only for very low rigid angular rates compared to the fundamental. Note that the nominal trajectory cannot be sped up anymore without violating the small elastic deflection assumption, since for this case deflections of ten percent of the length of the second link are already in evidence.

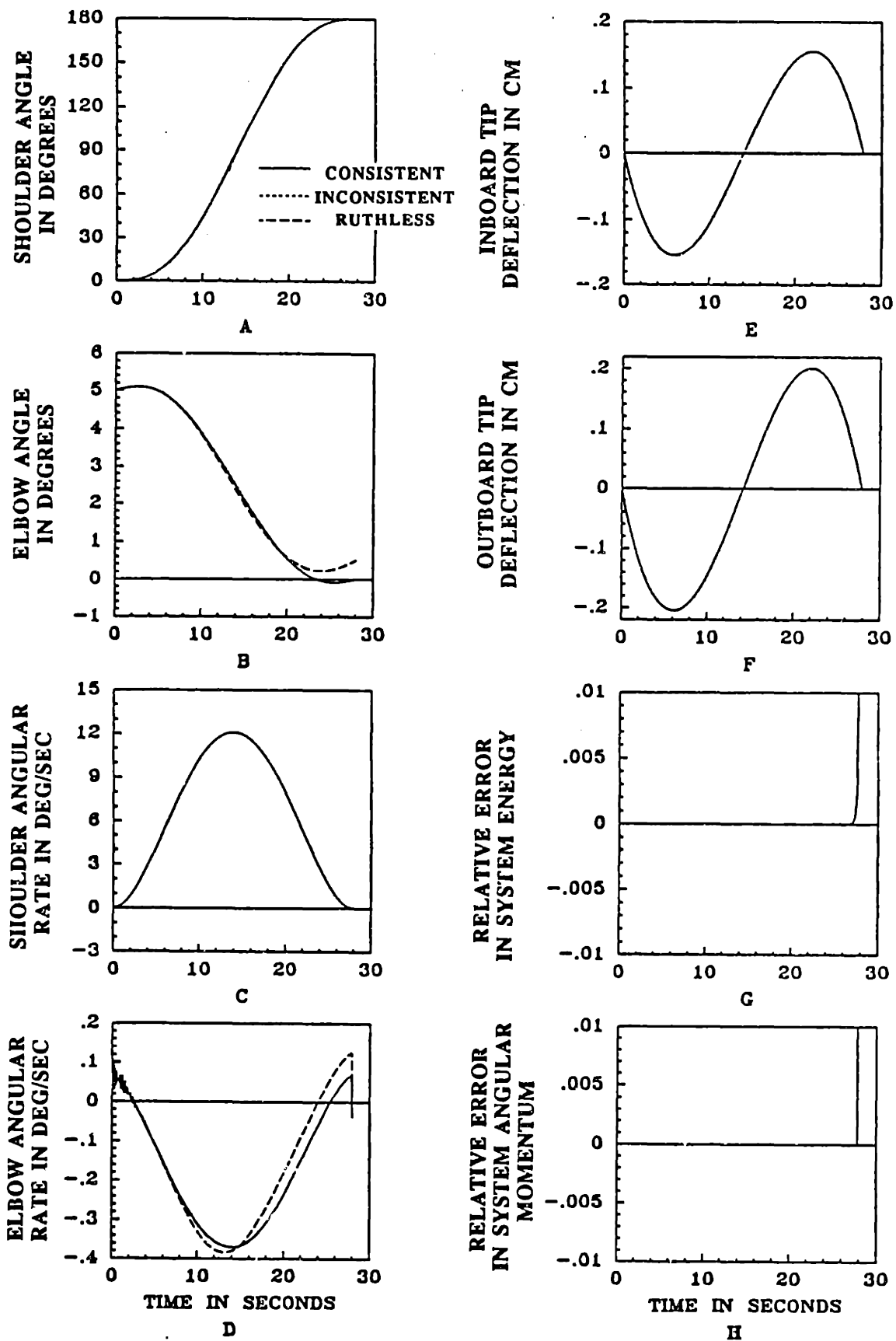


Fig. 4.3: First Smooth Trajectory with  $\alpha=0.2865$

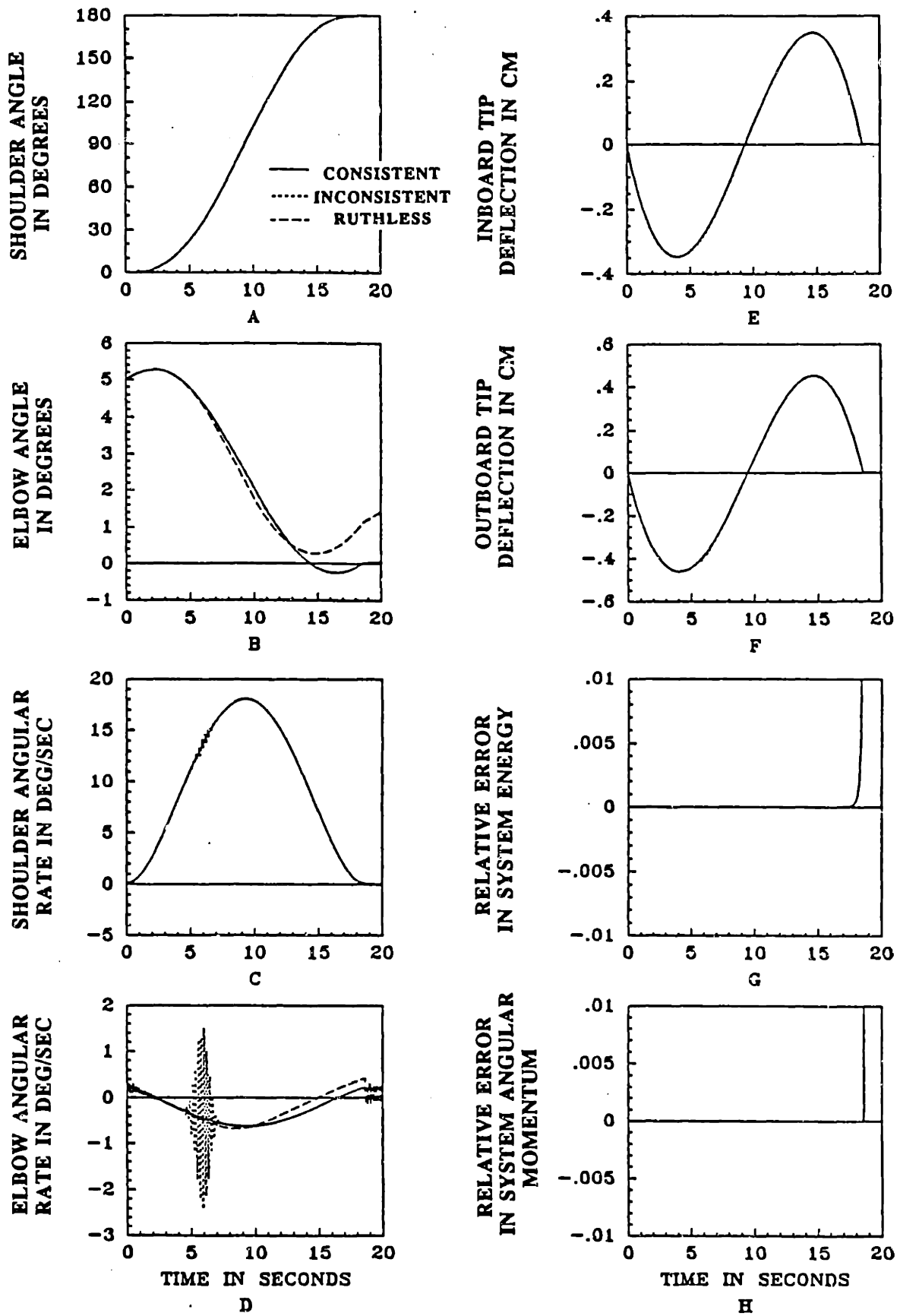


Fig. 4.4: First Smooth Trajectory with  $\alpha=0.4197$

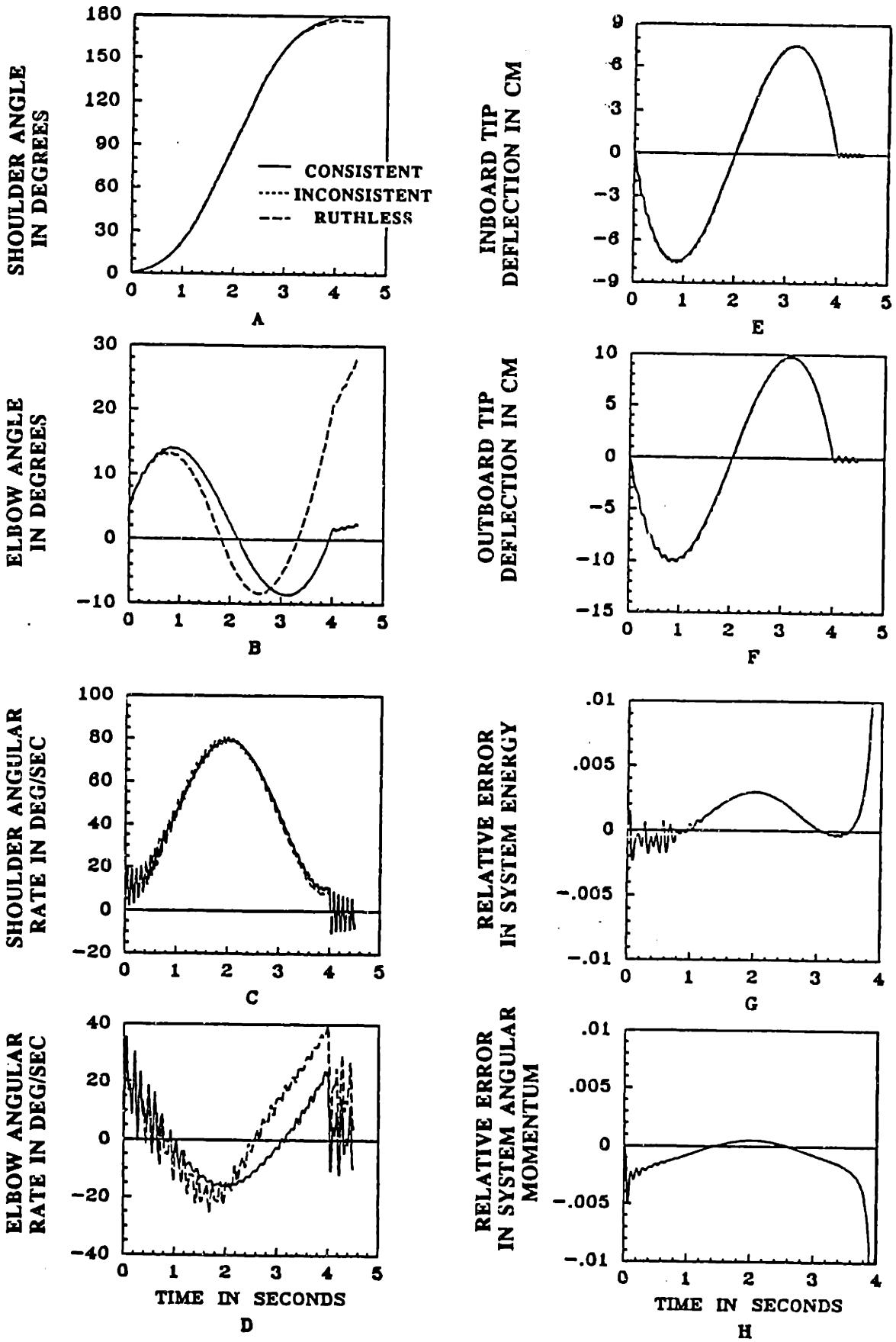


Fig. 4.5 First Smooth Trajectory with  $\alpha=2.0$



It is interesting to note that the inconsistent model fails whenever the shoulder angular rate is higher than ten percent of the fundamental, much earlier than predicted by the single beam example of chapter three. This could be due to the exacerbation of an ill-conditioning of the mass matrix due to the lack of the foreshortening terms. This situation could be the result of nonlinear interactions between the links that are absent in the one link example. For a more complete discussion of ill-conditioning in the simulation, see the discussion in section 4.4.

Finally, it is worth pointing out the excellent agreement in the tip deflections for both links, in all three cases. This is probably due to the fact that the equations of motion (see App. C) are elastically decoupled, and, while inertially coupled, the elastic degrees of freedom mass matrix ( $M_{EE}$  of section 3.1) does not depend on elastic nonlinear terms due to linearization. Also, the agreement in shoulder angle and angular rates is remarkable. This indicates that, depending on what state variable is of interest in a given trajectory, the ruthless model will be as good as the more cumbersome consistent model. In all cases, the ruthless is more conservative and better conditioned than the inconsistent model.

### 4.3.3 Second Smooth Trajectory

The second trajectory tried on the two-link manipulator is intended to examine the relative significance of the nonlinear elastic terms in the equations of motion of a chain of elastic bodies as a function of trajectory. In the previous section, the shoulder-rate dominant slew maneuver confirmed the predictions of section 3.4. It is now desired to see how these results are affected by a change in trajectory. For this purpose, a typical "deployment" maneuver of the two link manipulator is commanded.

As in the previous section, the smooth trajectory is obtained by assuming a form of the angular time histories that is quintic in time. Selecting

$$\begin{aligned} \theta_i &= -1.570796 & \beta_i &= 2.96706 \text{ rad} \\ \theta_f &= 0.2617994 \text{ rad} & \beta_f &= 0.8726646 \text{ rad} \\ \dot{\theta}_i &= \ddot{\theta}_i = \dot{\beta}_i = \ddot{\beta}_i = \dot{\theta}_f = \ddot{\theta}_f = \dot{\beta}_f = \ddot{\beta}_f = 0 \\ t_f &= 4.0 \text{ sec} \end{aligned}$$

and solving for the coefficients of the polynomial in time as in the previous section, the trajectory results in

$$\theta(t) = a_0 + a_1t + a_2t^2 + a_3t^3 + a_4t^4 + a_5t^5$$

$$\beta(t) = b_0 + b_1t + b_2t^2 + b_3t^3 + b_4t^4 + b_5t^5 \quad (1)$$

Figure 4.6 shows the computed torques for the nominal trajectory.

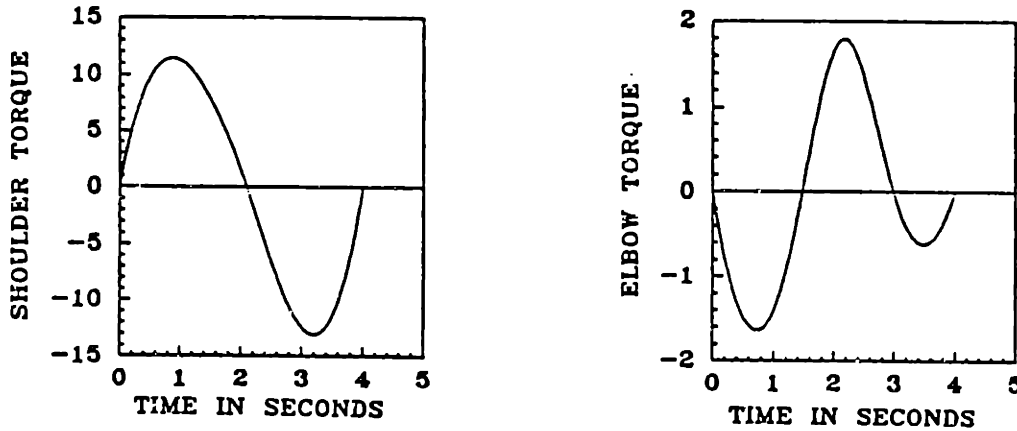


Fig. 4.6: Computed Torques for Second Smooth Trajectory (Nm)

Figure 4.7 shows the nominal trajectory. In this figure, plots for both the ruthless and the consistent models have been overlaid. The inconsistent model fails for this case. This is not surprising after examining the results of the previous section and noting that the angular rates for the nominal maneuver are as large as thirty percent of the "fundamental vibration frequency." From table 3.1 in section 3.5, the system frequencies for the manipulator with locked joints are seen to fluctuate from 3 rad/sec to 4 rad/sec for corresponding elbow relative angles of zero to 135 degrees. For this reason, in the case at hand reference is made to "one" fundamental frequency, and it is assumed that it lies in the range specified above and is about 3.5 rad/sec. For the two models shown, the agreement is again excellent for the shoulder angle and tip deflections, with the elbow angular position being off by only a maximum of ten percent relative error.

In the second case considered, the nominal maneuver is slowed down until the inconsistent model does not fail ( $\alpha=0.1685$ ). Figure 4.8 shows that for this case, all three models yield identical results. This confirms the predictions in section 3.4, and further suggests that within the limit of validity of the inconsistent model, the ruthless is as good as the inconsistent, and actually better since it is much easier to obtain. Note that the angular rates are well within the ten percent of the fundamental mark.

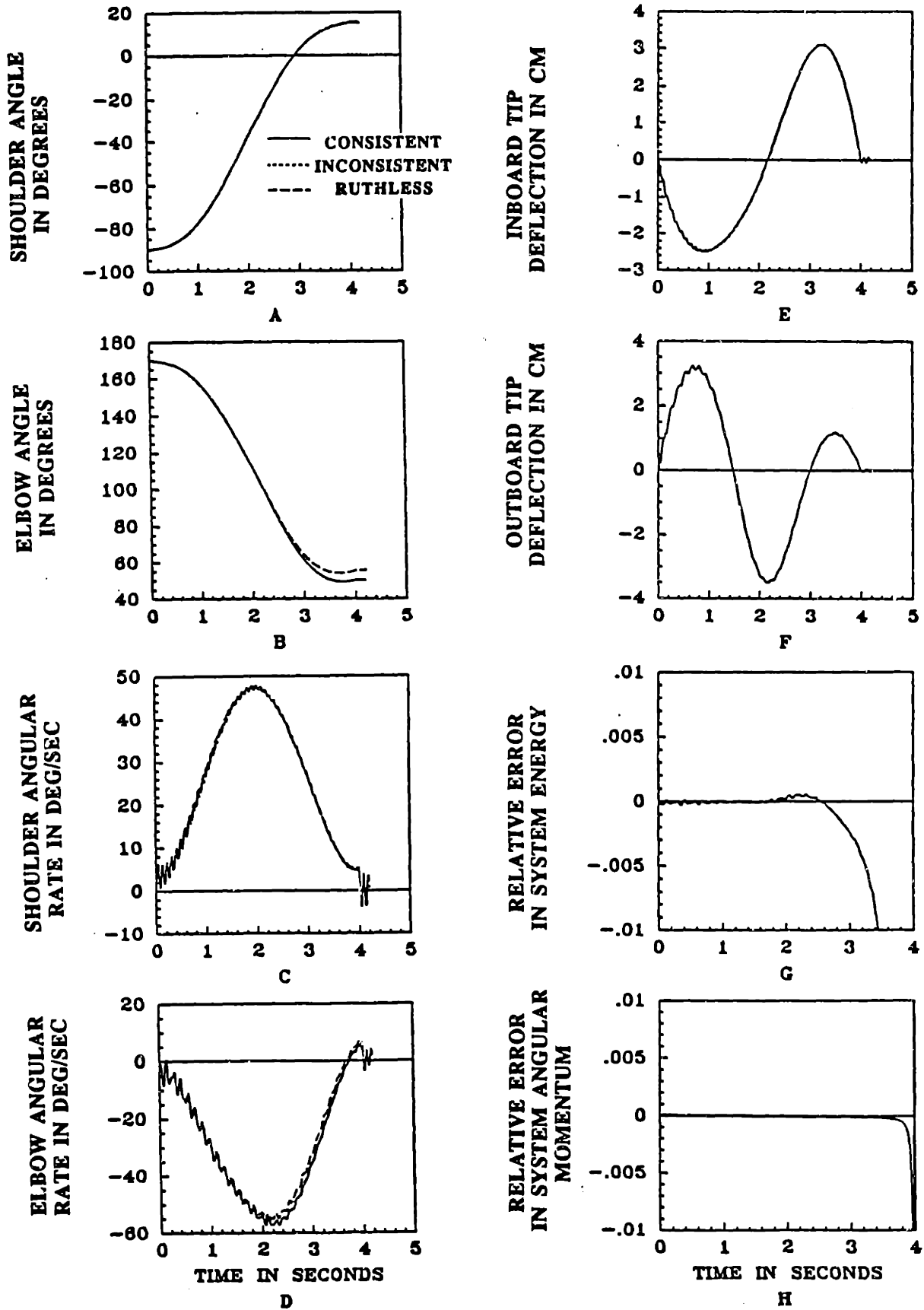


Fig. 4.7: Second Smooth Trajectory with  $\alpha=1.0$

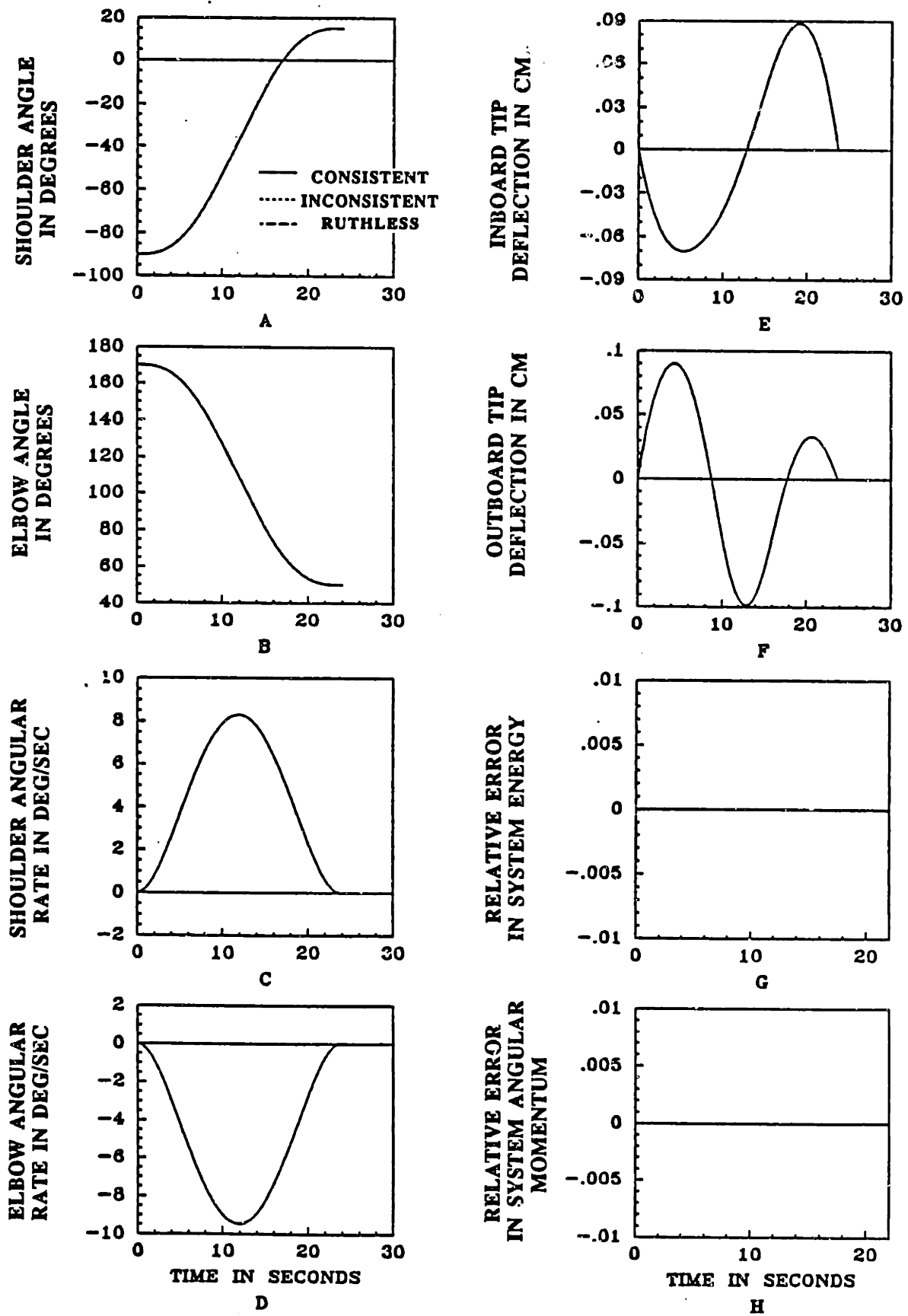


Fig. 4.8: Second Smooth Trajectory with  $\alpha=0.1685$

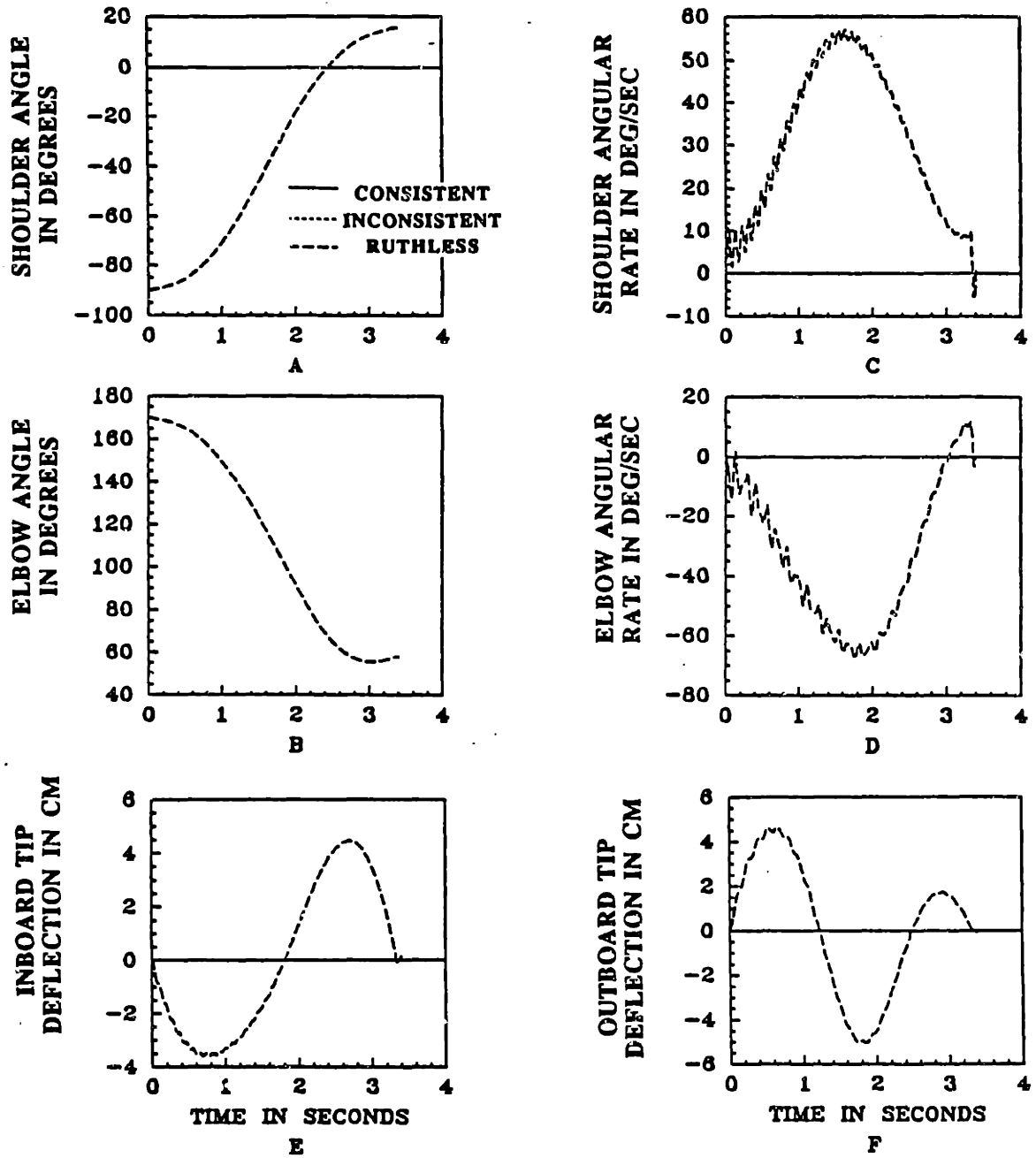


Fig. 4.9: Second Smooth Trajectory with  $\alpha=1.2$

The last case considered consists of the nominal trajectory scaled upwards in time ( $\alpha=1.2$ ). As in the previous section, it was desired to reach the "hard" simulation limit of link tip deflections of about ten percent of the link lengths. As Figure 4.9 shows, only the ruthless model did not fail under the given speed-up of the trajectory, even though tip deflections should only be about four percent of link lengths. To investigate these results, the stability boundary of section 3.3.3 was implemented in the simulation and checked at every time step to determine whether the simulation failure of the consistent model was due to the correct prediction of divergence, or due to some numerical or other phenomenon. For the case of two assumed modes per link, the lowest eigenvalue of the effective stiffness matrix (see section 3.3.3) was actually checked, with the conclusion that no divergence was predicted by the analytical consistent equations. Section 4.4 offers further comments on this problem.

In summary, the above results again show a strong correlation between the limit of validity of the inconsistent model and the maximum values of angular rates. Contrary to the case in section 4.3.2, however, for the present maneuver no "characteristic" rigid body rate is apparent. The limit at which the inconsistent model fails seems to be even before any of the two angular rates (shoulder or elbow) reach ten percent of the fundamental vibration frequency. A strong point can still be made, nevertheless, in that the ruthless model is as good as the inconsistent whenever the inconsistent is valid, and more conservative since the ruthless model does not fail. Even at high angular rates the ruthless model yields results that are quantitatively very close to the consistent model results.

#### **4.3.4 Minimum-Time Trajectory**

The last trajectory attempted on the two-link manipulator is a minimum time trajectory executed via bang-bang controls [17]. The idea behind implementing this maneuver is to get a feel for how the results of the previous two sections change when a "typical" fast maneuver is commanded with abrupt forcing. For comparison purposes, the torque bounds for the minimum-time problem are set to the maximum values of the torques obtained for the nominal first smooth trajectory (section 4.3.2) scaled by a factor of  $\alpha=0.4297$  (see Fig. 4.4). The actual forcing time history for the manipulator simulation is adapted from that presented by Meier and Bryson [17], to fit the chosen arm parameters and configuration.

The maneuver chosen was that referenced in [17] as one  $D/L=3.9$ , where  $L$  is the link length, assumed the same for both links, and  $D$  is the distance traveled by the manipulator end effector. The switching times for shoulder and elbow torques, and the final time are given as

$$\begin{aligned} t_{s1} &= 1.13 & t_{e1} &= 1.46 \\ t_{s2} &= 1.44 & t_f &= 2.91 \\ t_{s3} &= 1.77 \end{aligned}$$

with initial angular values of

$$\theta_i = 0 \quad \beta_i = -0.21 \text{ rad}$$

where it has been assumed that the normalized torque bounds are

$$\frac{T_e}{mL^2} = \frac{T_s}{mL^2} = \pm 1$$

where  $m$  is the link mass, also assumed the same for both links and the same for the tip load. Elbow mass and the moments of inertia of shoulder, elbow and tip effectors are ignored. For the case at hand, the switch times were scaled to obtain the proper trajectory taking into account elbow and tip masses, moments of inertia of all bodies, and different link masses. The resulting trajectory is shown in Fig. 4.10 for the case of both links rigid.

The results are presented in Fig. 4.11. As in the previous two sections, the inconsistent model fails for angular rates larger than about ten percent of the fundamental vibration frequency of the system (in this case about one third of the fundamental at maximum). For this reason, only the consistent and ruthless models are compared. As in section 4.3.2, the ruthless model yields results that are within ten percent relative error of the consistent results, and this for relatively large angular rates. The interesting thing to note is the high frequency oscillation induced in the flexible links by the bang-bang controller. Recall that all the maneuvers are run open loop, and that one percent modal damping was assumed for the cantilever mode shapes.

The large discrepancy shown in the energy and angular momentum balance plots is probably due to round-off error accumulation due to the relatively large tip deflections and high frequency excitation.

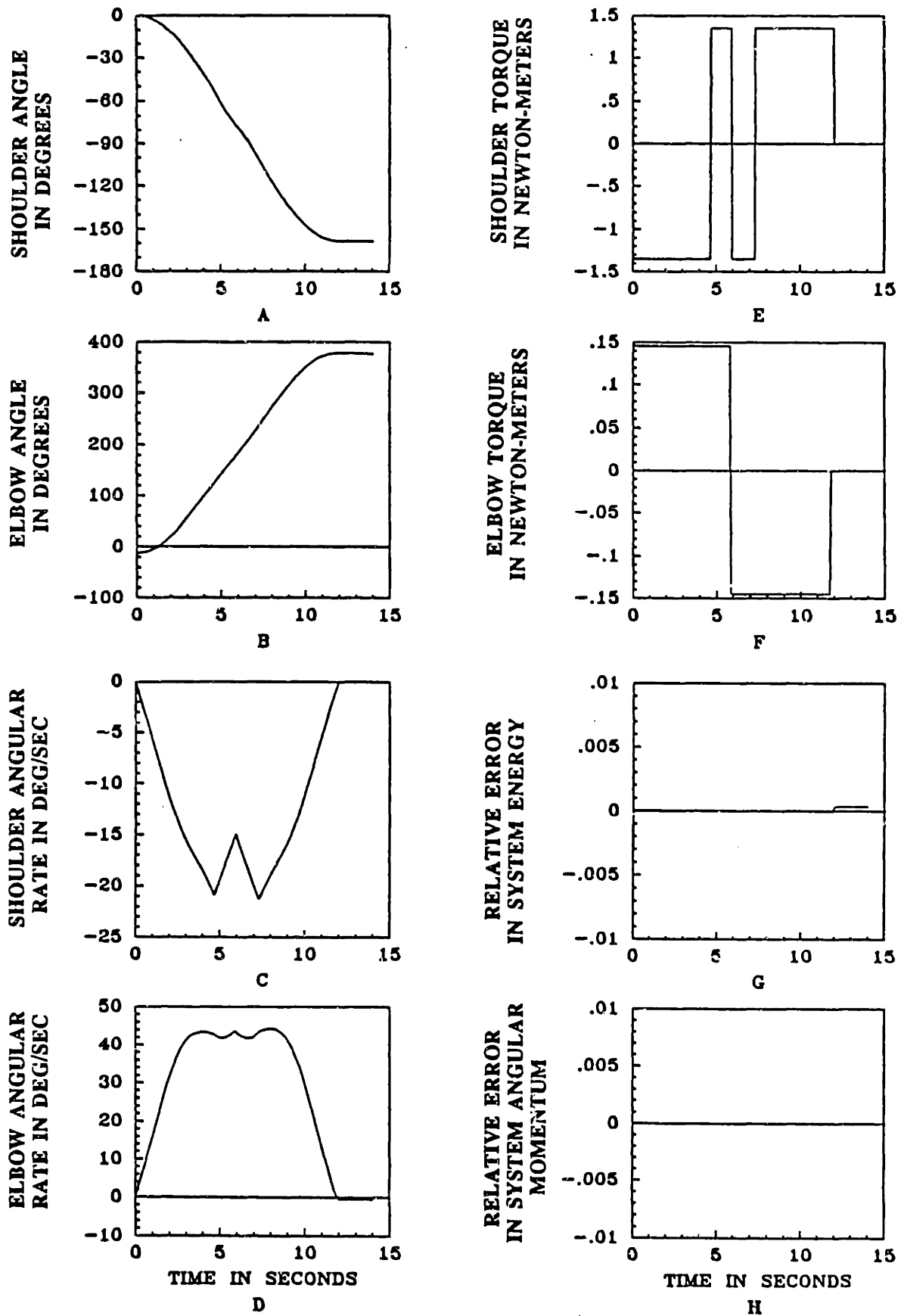


Fig. 4.10: Time-Optimal Trajectory for Two-link Rigid Manipulator



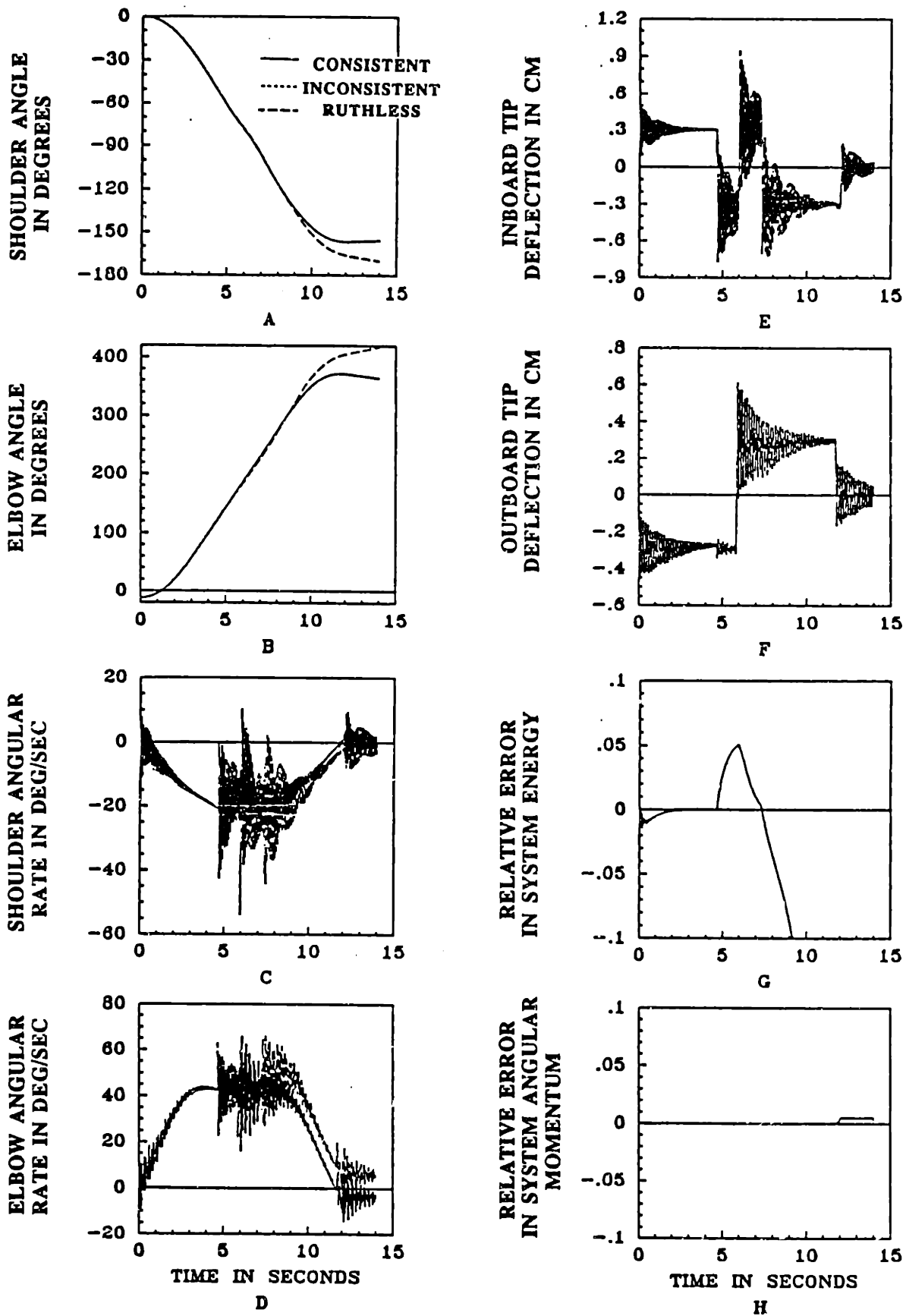


Fig. 4.11: Time-Optimal Trajectory for Two-link Flexible Manipulator

## 4.4 DISCUSSION

Having determined in section 4.3.3 that a numerical problem existed that might be responsible for some of the unexpected results in section 4.3, a more detailed examination of this problem is in order. The possibility of a programming error was ruled out to a large extent through thorough debugging and the use of energy and angular momentum checks. Numerical experiments determined that the problem was caused by ill-conditioning of the mass matrix brought about somehow by its dependence on the elastic coordinates. This suggests that this could be the reason behind the premature failing of the inconsistent model in the previous section. Numerical ill-conditioning of the mass matrix implies that at some configurations the configuration dependent mass matrix is numerically singular. A singular mass matrix indicates massless degrees of freedom being modelled. The problem therefore seems to come down to modelling error.

It appears that at least two ways of solving the problem are available. One way is to solve the problem numerically. This is most appealing at first glance since it entails keeping all the developed software. On the other hand, as shall be seen, it requires a much more computationally intensive algorithm to implement. Also, the second possible solution retains all of the derived equations of motion (and thus most of the software), while requiring changes to only a few mode shape dependent subroutines.

The first solution calls for determining at every time step, and thus for every configuration, if there are any massless degrees of freedom. This is achieved doing a singular value decomposition (SVD) of the mass matrix. If a near zero singular value is detected, a least squares projection is used to obtain the optimal (in a least squares sense) inversion of the mass matrix so that the acceleration vector thus obtained does not grow without bounds [22]. This is to some extent the equivalent of Guyan reduction performed on the mass matrix after it has been transformed into a space where the massless degrees of freedom are apparent. The problem with this solution is that it is very expensive computationally.

The other solution requires realizing that the selected assumed mode shapes are not appropriate for modelling the manipulator. In chapter two it was explained that cantilevered-free mode shapes were chosen because they simplified the equations of the two link arm. Indeed these mode shapes are easier to include in the development of the motion equations than the pinned, system or unconstrained mode shapes [25]. Unfortunately, the free end condition forces the cantilever mode shapes to have zero second

and third derivatives with respect to beam length evaluated at the tip of the link. In other words, these mode shapes do not support moment or shear at the "free" end of the link. In the manipulator, both links end in masses with moments of inertia, and are therefore not free. The problem here might be equivalent to the mode shapes selected for the system not being "complete" in the strain energy norm [28]. This then suggests that mode shapes for a cantilever beam with a tip body, with mass and moment of inertia, be used as the beam mode shapes for the determination of modal integrals in the equations of motion.

Both these possible solutions are being pursued at present and are offered as suggestions for further work.

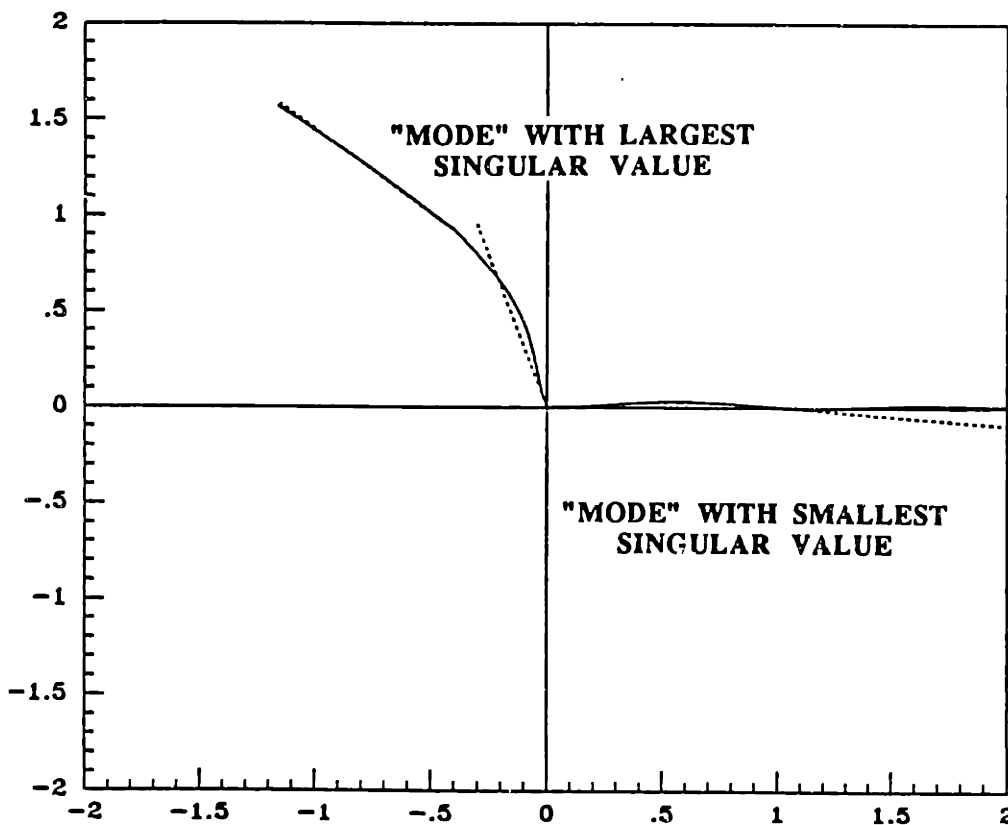


**Fig. 4.12: Comparison of Right Singular Vectors for the Mass Matrix at Failure**

It is possible that the "free play" allowed at the link tips by the cantilever mode shape assumption provides the connection between the two seemingly different approaches presented above. As a matter of fact, velocity "mode shapes" of the mass matrix at failure corresponding to near zero singular values suggest that it is the combination of positive angular rate with negative link tip velocity that yields a configuration that has little or no kinetic energy while the chosen state variable rates are nonzero. Fig. 4.12 shows these

velocity mode shapes (actually right singular vectors) for the largest and smallest singular values of the mass matrix at failure. The mode shapes have been normalized so that the largest tip deflection of either link be ten percent of the link lengths, which have been normalized to one. For the physical manipulator parameters chosen (see Table 4.1), the elbow is massive in comparison to link or tip masses. Therefore it is clear that for the mode with near zero velocity of the elbow joint the kinetic energy is near zero when compared to the kinetic energy for the largest singular value mode. Thus the mass matrix is numerically singular and this results in massless degrees of freedom being modelled.

## CHAPTER 5: CONCLUSIONS

The equations of motion for a planar, two-link, flexible manipulator, fully nonlinear in rigid body motions and rates, but linearized in small elastic coordinates and speeds, were obtained. These motion equations, developed via the Kane formalism, were correctly linearized through appropriate use of nonlinear strain-displacement relations. The links were modelled as Bernoulli-Euler beams and the elastic deflections were expanded in terms of cantilever beam modes. The resulting extensive equations were coded in FORTRAN and implemented as a simulation that allows the determination of the manipulator dynamic response to desired forcing functions in the form of joint torques. The simulation allows for a variable number of modes to be used in the modelling of the link flexibility so that effects such as spillover can be tested in control experiments. Modularity in the software developed permits the mode shapes to be changed with changes to two ancillary subroutines that determine modal constants. Further, elastic nonlinear terms in the motion equations were "flagged" in the simulation. This was done to permit running of three different models, characterized by increasing simplification of the equations, in order to test the relative significance of these nonlinear terms.

Having looked into the general form of the linearized dynamics equations for chains of flexible bodies undergoing large rigid body motions, but small elastic deflections, it was concluded that some terms cannot be obtained through the use of linear strain-displacement relations. These terms were seen to be critical in the simple rotating beam example as they provide the geometric stiffness terms necessary to obtain physical results. The absence of these terms in inconsistently linearized equations limits their validity to angular rates lower than approximately ten percent of the first fundamental vibration frequency of the system. Other terms which are unavailable through the use of linear strain-displacement relations predicted (correctly) buckling under large axial accelerations. The fact that these terms are unobtainable for the general case of an arbitrary flexible body prompted considerations of possible simplifications to the general motion equations.

The two alternative models studied, the ruthlessly linearized model and the inconsistent model, are subject to several limits in applicability. While the consistent model requires that elastic coordinates and speeds be kept small, the two alternative models will

only be accurate if low angular rates are also maintained. There also exists some translational acceleration limit that needs to be considered, although for the cases studied this limit was of no consequence. Within the domain of validity of both simplified models, it appears the ruthless model yields results as accurate as the correct consistently linearized model. This coupled to the simplification of the dynamicist's task inherent in the adoption of ruthlessly linearized models makes this option an attractive alternative.

Simulation misbehavior at certain trajectories for relatively high rigid body angular rates was tracked down to numerical ill-conditioning of the configuration dependent mass matrix. This problem was attributed to modelling error inherent in choosing cantilever (clamped-free) modes to model the flexible deflections of the manipulator links. In chapter four it was suggested that this results in effectively modelling one (or more) massless degrees of freedom. Two possible solutions were outlined. A numerical solution entails condensing out these massless degrees of freedom through the use of a singular value decomposition approximate inversion of the mass matrix. This is expected to result in a simulation that is computationally very expensive. The use of mode shapes obtained from a cantilever beam with an end mass with moment of inertia is proposed as the analytical solution. Both these concepts are under study at present and are suggested as further work.

# REFERENCES

- 1 Banerjee, A.K., Dickens, J.M., "Dynamics of an Arbitrary Flexible Body Undergoing Large Rotation and Translation with Small Vibration," Paper no. AIAA-89-1308, 30th AIAA/ASME/ASCE/AHS/ASC Structures, Structural Dynamics and Materials Conference, Mobile Alabama, April 3-5, 1989.
- 2 Blevins, R.D., *Formulas for Natural Frequency and Mode Shape*, Robert E. Krieger Publishing Company, Malabar, Florida, 1979.
- 3 Bodley, C. S., et al., "A Digital Computer Program for the Dynamic Interaction Simulation of Controls and Structure (DISCOS)," Vols. 1 & 2, NASA Technical Paper 1219, May 1978.
- 4 Brady, M., Hollerbach, J. M., et al., *Robot Motion: Planning and Control*, MIT Press, Cambridge, MA, 1982, pp 55-60.
- 5 Craig, J.J., *Introduction to Robotics Mechanics and Control*, Addison-Wesley Publishing Company, 1986, pp.191-219.
- 6 Golub, G.H., Van Loan, C.F., *Matrix Computations*, The Johns Hopkins University Press, Baltimore 1983, pp. 52-79.
- 7 Hollerbach, J.M., "Dynamic Scaling of Manipulator Trajectories," *Journal of Dynamic Systems, Measurement, and Control*, Vol. 106, March 1984, pp. 102-106.
- 8 Hughes, P. C., "Multibody Dynamics for Space Station Manipulators: Dynamics of a Chain of Elastic Bodies," DYNACON Report SS-2, DYNACON Enterprises Ltd., Feb. 1985.
- 9 Kane, T. R., Levinson, D. A., *Dynamics: Theory and Applications*, McGraw -Hill Book Company, 1985.
- 10 Kane, T. R., Likins, P. W., Levinson, D. A., *Spacecraft Dynamics*, McGraw-Hill Book Company, 1983, pp. 318-326.
- 11 Kane, T. R., Ryan, R. R., Banerjee, A. K., "Dynamics of a Cantilever Beam Attached to a Moving Base," *Journal of Guidance, Control, and Dynamics*, Vol. 10, No. 2, March-April 1987, pp. 139-151.
- 12 Kelly, F., "On the Dynamics of Flexible Multibody Systems," Ph.D. Thesis, Dept. of Engineering Science, University of Cincinnati, Cincinnati, 1982.

- 13 Laskin, R. A., Likins, P. W., Longman, R. W., "Dynamical Equations of a Free-Free Beam Subject to Large Overall Motions," AAS/AIAA Astrodynamics Conference, Lake Tahoe, NV, August 3-5, 1981
- 14 Love, A. E. H., *A Treatise on the Mathematical Theory of Elasticity*, 4th ed., Dover Publications, New York, 1944.
- 15 Man, G., Laskin, R., Editors, Proceedings of the Workshop on Multibody Simulation, JPLD-5190, Jet Propulsion Laboratory, Pasadena, California, April 15, 1988.
- 16 MATRIXx User's Guide, Version 6.0, Integrated Systems Inc., Santa Clara, California, May 1986.
- 17 Meier, E.B., Bryson, Jr., A.E., "An Efficient Algorithm for Time-Optimal Control of a Two-link Manipulator," AIAA paper no. 87-2263.
- 18 Meirovitch, L., *Analytical Methods in Vibrations*, Mcmillan Publishing Co., Inc., New York, 1967.
- 19 Meirovitch, L., *Elements of Vibration Analysis*, 2nd ed., McGraw-Hill Book Company, 1986.
- 20 Novozhilov, V. V., *Foundations of the Nonlinear Theory of Elasticity*, Graylock Press, Rochester, N.Y., 1953.
- 21 Pars, L. A., *A Treatise on Analytical Dynamics*, John Wiley & Sons, Inc., New York, N.Y., 1965.
- 22 Press, W.H., Flanner, B.P., Teukolsky, S.A., Vetterling, W.T., *Numerical Recipes: The Art of Scientific Computing*, Cambridge University Press, Cambridge, London, 1986, pp. 550-559.
- 23 Ryan, R. R., "Flexible Multibody Dynamics: Problems and Solutions," JPL D-5190, Vol. I, Proceedings of the Workshop on Multibody Simulation, April 15, 1988, pp. 103-190.
- 24 Ryan, R. R., "Flexibility Modeling Methods in Multibody Dynamics," Paper no. AAS 87-431, AAS/AIAA Astrodynamics Specialist Conference, Kalispell, Montana, August 10-13, 1987.
- 25 Schmitz, E., "Experiments on the End-Point Position Control of a Very Flexible One-link Manipulator," Ph.D. Thesis, Dept. of Aeronautics and Astronautics, Stanford University, June 1985.



- 26 Simo, J. C., "Nonlinear Dynamics of Flexible Structures, A Geometrically Exact Approach," JPL D-5190, Vol. I, Proceedings of the Workshop on Multibody Simulation, April 15, 1988, pp. 235-297.
- 27 Spanos, J., Laskin, R. A., "Geometric Nonlinear Effects in Simple Rotating Systems," JPL D-5190, Vol. I, Proceedings of the Workshop on Multibody Simulation, April 15, 1988, pp. 191-218.
- 28 Storch, J., Strang, G., "Paradox Lost: Natural Boundary Conditions in the Ritz-Galerkin Method," Numerical Analysis Report 87-7, Dept. of Mathematics, M.I.T.
- 29 Sunada, W.H., Dubowsky, S., "On the Dynamic Analysis and Behavior of Industrial Robotic Manipulators with Elastic Members," ASME paper no. 82-DET-45, ASME Design and Production Engineering Technical Conference, Washington D.C., Sept. 12-15, 1982.
- 30 Timoshenko, S. P., Young, D. H., Weaver, W., *Vibration Problems in Engineering*, 4th ed., Wiley and Sons, 1974.
- 31 User's Manual for TREETOPS, "A Control System Simulation for Structures with a Tree Topology," Singh, Likins, et al., NASA contract no. NAS8-34588, Rev. B, November 1984.
- 32 von Flotow, A. H., Lecture Notes, MIT Aeronautics and Astronautics Dept., April 1988, pp. 850-858.

# APPENDIX A: NONLINEAR STRAIN-DISPLACEMENT AND LINEARIZATION

This appendix first presents a general discussion on the proper linearization of the equations of motion of a flexible multibody system undergoing motion with large rigid body rates (not just angular velocities) and rigid body configuration changes, but with infinitesimal elastic deformations. Some of the terms in these motion equations cannot be obtained with linear kinematics of elastic deformation (i.e., the traditional linear finite element or modal formulation). It has been suggested [26] that this is not due to a fundamental flaw of the linear theories, but rather to the inability of these theories to account for nonlinear geometric effects. The role of nonlinear strain-displacement relations in the proper linearization is then investigated using the simple example of a Bernoulli-Euler beam cantilevered to a rigid base free to move in the plane.

## A.1 GENERAL DISCUSSION

The problem that concerns us is that of obtaining the correctly linearized equations of motion for an important class of systems which exhibit large rigid body motions but small elastic deflections. Needless to say this class of systems is of vital interest in many fields, particularly in aerospace. By far the most common practice to date is to handle the flexibility through discretization of the desired continuous system. This is achieved by representing the solution as a finite series of time-dependent generalized elastic coordinates multiplied by space-dependent functions, as in an assumed modes approach, or in a finite element formulation [19]. Whichever formulation one uses, in light of the class of systems under study, the next step is to require that these elastic coordinates, together with the generalized elastic speeds, be infinitesimally small. In other words, we want these coordinates and speeds to be small enough so that only terms linear in them are kept in the equations of motion, as terms of second order or higher are negligible.

Now that our goal is clearly stated, it should be an easy matter to obtain the linearized equations of motion as long as we consistently drop all terms nonlinear in the elastic coordinates and the corresponding generalized elastic speeds. Of course, the word "consistently" is the catch. When do we linearize? That is to say: Does it matter at what step in our derivation of the equations of motion we start to linearize? To answer this question we have to consider the process by which we derive these equations.

Let us consider two of the more widely known methods to derive motion equations for complex systems: Lagrange's equations of motion [21] and Kane's dynamical equations [9]. Lagrange's equations for a holonomic system with  $n$  generalized coordinates  $q_k$ :

$$\frac{d}{dt} \left( \frac{\partial L}{\partial \dot{q}_k} \right) - \frac{\partial L}{\partial q_k} = Q_k, \quad (k = 1, \dots, n) \quad (1)$$

$$L = T - V$$

where the Lagrangian  $L$  is a function of the system kinetic and potential energies ( $T$  and  $V$  respectively).  $Q_k$  are  $n$  generalized non-potential forces. The important thing to note is that using this method to derive motion equations requires differentiating both the potential and kinetic energies of the system with respect to the generalized coordinates and speeds. If these  $q_i$  and  $u_i$  ( $=dq_i/dt$ ) were to represent our generalized elastic coordinates, we see that the above differentiations imply that some terms linear in  $q_i$  and  $u_i$  in the energy expressions become terms of zeroth order in the elastic coordinates and speeds. More importantly, we see that terms of second order in the generalized coordinates and speeds in the energy expressions become terms of first order in the resulting equations of motion. Clearly then in order to obtain equations of motion correct to first order in  $q_i$  and  $u_i$  we need to have energy expressions for our system that are correct to second order in these same elastic generalized coordinates and speeds. More specifically the requirement demands in general that the expressions for displacements and velocities used in determining potential and kinetic energies be correct to second order in the elastic coordinates and speeds. Only by doing this can we ensure consistent linearization.

Kane's dynamical equations for a holonomic system of  $n$  particles with  $n$  generalized speeds  $u_i$ :

$$\begin{aligned} F_r + F_r^* &= 0 & (r = 1, \dots, n) \\ F_r^* &= \sum_{i=1}^n \mathbf{v}_r^{P_i} \bullet \mathbf{R}_i^* & , \quad \mathbf{R}_i^* = -m_i \mathbf{a}_i \\ \mathbf{v}_r^{P_i} &= \sum_{i=1}^n \mathbf{v}_r^{P_i} u_i + \mathbf{v}_i & , \quad u_i = \dot{q}_i \end{aligned} \quad (2)$$

where  $F_r$  is the generalized active force,  $F_r^*$  is the generalized inertia force,  $\mathbf{R}_i^*$  is the inertia force for particle  $P_i$  in an inertial reference frame, and  $\mathbf{v}^{P_i}$  is the velocity of this particle in the same frame.  $\mathbf{v}_r^{P_i}$  is the  $r$ -th partial velocity of particle  $P_i$  in the inertial frame. Using a

similar argument as above, it is easy to see that since the partial velocity has to be correct to first order in the generalized coordinates and speeds, and again this term is obtained through differentiation of the velocity with respect to the generalized speeds, the velocity has to be correct to second order in  $q_i$  and  $u_i$  until we form the partial velocities. This is necessary if we want our equations of motion to be consistently linear in the generalized coordinates and speeds.

## A.2 A SIMPLE EXAMPLE

We now present a simple yet very important example which will help to point out the practical consequences of the above discussion. This example could equally well represent either link of the manipulator which is the center piece of this thesis. Consider a simple uniform beam cantilevered to a solid body free to move in the plane with mass center at  $A^*$  (see Fig. A.1). The frame  $N$ , defined by the unit vectors  $\mathbf{n}_1, \mathbf{n}_2, \mathbf{n}_3$ , is inertial, and we introduce the rotating frame  $A$  defined by the unit vectors  $\mathbf{a}_1, \mathbf{a}_2, \mathbf{a}_3$ , attached to body  $A$  and whose  $\mathbf{a}_1$  axis lies along the undeformed neutral axis of the beam  $B$  initially. Let us derive the consistently linearized equations of motion using both Kane's and Lagrange's methods. We will ignore shear and rotary inertia effects (i.e., slender beam assumption). For simplicity, we assume no external forces act on the system.

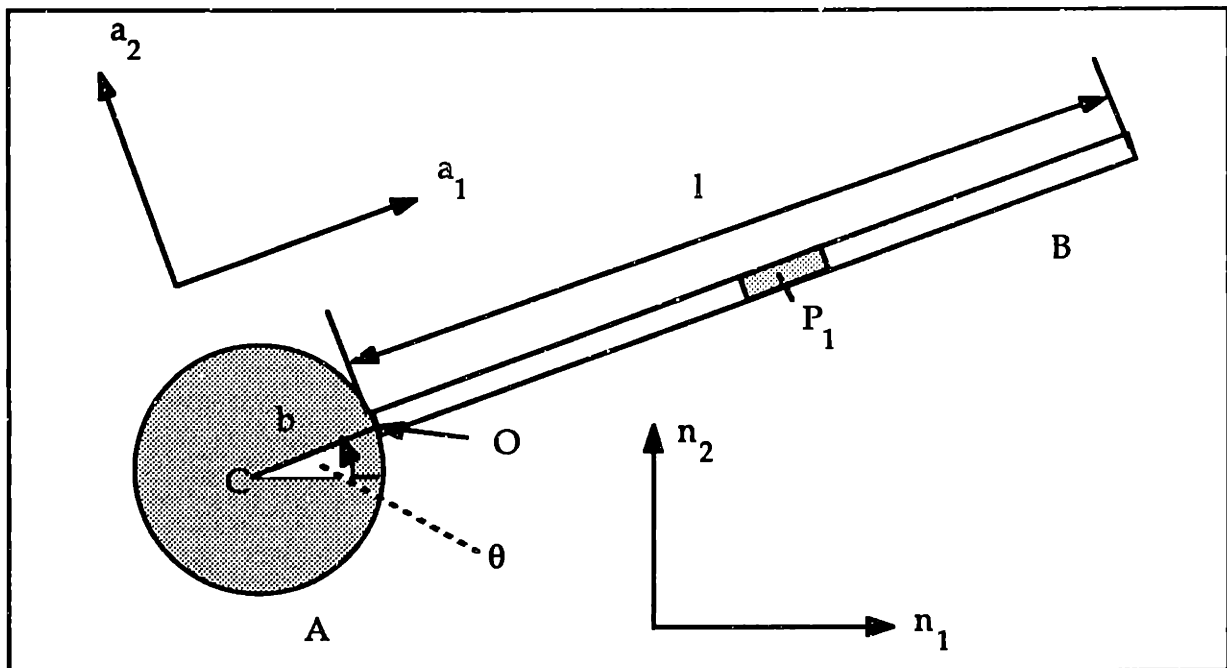


Figure A.1: Single Beam Attached to a Moving Base

## A.2.1 Lagrange's Equations of Motion

First we form the kinetic and potential energies of our system:

$$T = \frac{1}{2}I_A \dot{\theta}^2 + \frac{1}{2}m_A {}^N \mathbf{v}^{A^*} \cdot {}^N \mathbf{v}^{A^*} + \frac{1}{2} \int_0^L {}^{\mathbf{v}^{P_1}} \cdot {}^{\mathbf{v}^{P_1}} \rho dx$$

$$V = \frac{1}{2} \int_0^L EI \left( \frac{\partial^2 u_2}{\partial x^2} \right)^2 dx \quad (1)$$

where  $m_A$  is the mass of the rigid body A;  $I_A$  is the moment of inertia of the rigid body A about its mass center;  ${}^N \mathbf{v}^{A^*}$  is the velocity with respect to the inertial frame of  $A^*$ ;  ${}^{\mathbf{v}^{P_1}}$  is the velocity with respect to the inertial frame of the centroid of a rigid differential element  $P_1$  of the beam;  $\rho$  and  $EI$  are the mass per unit length and bending stiffness of the beam respectively; and,  $u_1(x,t)$  and  $u_2(x,t)$  are respectively the axial and transverse displacements in frame A of the element  $P_1$  a distance  $x$  along  $\hat{\mathbf{a}}_1$  from point O. Now we form  ${}^{\mathbf{v}^{P_1}}$  from the kinematics of the system:

$$\begin{aligned} {}^{\mathbf{v}^{P_1}} &= \mathbf{v}^{A^*} + \boldsymbol{\omega}^A \times \mathbf{p}^{A^*P_1} + {}^A \mathbf{v}^{P_1} \\ \mathbf{p}^{A^*P_1} &= (b + x + u_1)\hat{\mathbf{a}}_1 + u_2\hat{\mathbf{a}}_2 \\ \boldsymbol{\omega}^A &= v_3\hat{\mathbf{a}}_3, \quad v_3 = \dot{\theta} \\ \mathbf{v}^{A^*} &= {}^N \mathbf{v}^{A^*} = v_1\hat{\mathbf{a}}_1 + v_2\hat{\mathbf{a}}_2 \\ {}^A \mathbf{v}^{P_1} &= \dot{u}_1\hat{\mathbf{a}}_1 + \dot{u}_2\hat{\mathbf{a}}_2 \end{aligned} \quad (2)$$

where  $\boldsymbol{\omega}^A$  is the angular velocity of frame A ;  $\mathbf{p}^{A^*P_1}$  is the position vector between  $A^*$  and  $P_1$  and  ${}^A \mathbf{v}^{P_1}$  is the velocity of  $P_1$  in A. At this point it is customary to discretize the continuous variables  $u_1(x,t)$  and  $u_2(x,t)$ . To this end we use an assumed modes approach and state

$$u_1(x,t) = \sum_{i=1}^n \phi_{1i}(x) p_i(t)$$

$$u_2(x,t) = \sum_{i=1}^n \phi_{2i}(x) q_i(t) \quad (3)$$

where we choose  $\phi_{1i}$  and  $\phi_{2i}$  to be cantilevered beam mode shapes [18], and  $n$  is the number of generalized elastic coordinates. Further recognizing that under the present assumptions the axial displacements are at least an order of magnitude smaller than the transverse displacements, it is tempting to neglect  $u_1(x,t)$  entirely setting  $u_1=0$ .

Both these approaches, however, are only correct to first order in the elastic coordinates, as we will see. To obtain the correct relationships to second order, we need to turn to the nonlinear theory of elasticity as applied to beams, where we make use of nonlinear strain-displacement relations. For our case, a slender beam in pure bending, the strain-displacement relations become [20]:

$$\begin{aligned} \varepsilon_{xy} = \varepsilon_{yz} = \varepsilon_{yy} = \varepsilon_{zz} = \varepsilon_{xz} &= 0 \\ \varepsilon_{xx} = \hat{\varepsilon}_{xx} + y\chi_{xx} \quad \chi_{xx} = -\frac{d\theta}{dx}, \quad \frac{d\hat{\theta}_2}{dx} = \sin \theta \cong \theta \\ \hat{\varepsilon}_{xx} = \frac{d\hat{\theta}_1}{dx} + \frac{1}{2} \left[ \left( \frac{d\hat{\theta}_1}{dx} \right)^2 + \left( \frac{d\hat{\theta}_2}{dx} \right)^2 \right] \end{aligned} \quad (4)$$

where the  $\hat{\phantom{x}}$  indicates a quantity measured at the middle plane of the beam, i.e., the plane containing the neutral axis in this case. Note we are able to set  $\sin(\theta)=\theta$  due to our assumption of small elastic deflections. Now we consider the simpler case in which we want to neglect independent axial displacements. The correct condition for this is to require

$$\hat{\varepsilon}_{xx} = 0 \quad (5)$$

and this yields the familiar expression for axial strain under pure bending:

$$\varepsilon_{xx} = -y \frac{d^2 \hat{\theta}_2}{dx^2} \quad (6)$$

Given the above nonlinear strain-displacement relations, we see that equation (5) implies

$$\frac{d\hat{\theta}_1}{dx} + \frac{1}{2} \left[ \left( \frac{d\hat{\theta}_1}{dx} \right)^2 + \left( \frac{d\hat{\theta}_2}{dx} \right)^2 \right] = 0 \quad (7)$$

therefore to second order in the generalized elastic coordinates ( $q_i$ ):

$$u_1(x, t) = \hat{u}_1(x, t) = -\int_0^x \frac{1}{2} \left( \frac{d\hat{u}_2}{d\sigma} \right)^2 d\sigma = -\frac{1}{2} \int_0^x \sum_{i=1}^n \sum_{j=1}^n \phi_{2i}(\sigma) \phi_{2j}(\sigma) d\sigma q_i q_j \quad (8)$$

where as above:

$$u_2(x, t) = \hat{u}_2(x, t) = \sum_{i=1}^n \phi_{2i}(x) q_i(t) \quad (9)$$

So we see that if we pick  $u_2(x,t)$  to be the independent transverse displacement,  $u_1(x,t)$  depends on  $u_2$  to second order in the elastic coordinates. Now we can form the kinetic energy correct to second order. For completeness we note:

$$\dot{u}_1(x, t) = -\int_0^x \sum_{i=1}^n \sum_{j=1}^n \phi_{2i}(\sigma) \phi_{2j}(\sigma) d\sigma q_i \dot{q}_j \quad (10)$$

In view of the previous discussion we might wonder if our potential energy as given is correct to second order. To check this, we form the strain energy [14]:

$$S = \frac{1}{2} \int_V \tau_{xx} \epsilon_{xx} dV = \frac{1}{2} \int_V E \epsilon_{xx}^2 dV \quad (11)$$

where we ignore Poisson effects as customary for beam problems [30] and using equation (6):

$$S = \frac{1}{2} \int_V E y^2 \left( \frac{d^2 u_2}{dx^2} \right)^2 dx dy dz = \frac{1}{2} \int_0^L EI \left( \frac{d^2 u_2}{dx^2} \right)^2 dx \quad (12)$$

Now we proceed to obtain the equations of motion correct to first order in  $q_i$  and  $\dot{u}_i$  ( $=dq_i/dt$ ):

$$\begin{aligned} \frac{d}{dt} \left( \frac{\partial L}{\partial \dot{\theta}} \right) - \frac{\partial L}{\partial \theta} &= 0, \\ \frac{d}{dt} \left( \frac{\partial L}{\partial \dot{q}_r} \right) - \frac{\partial L}{\partial q_r} &= 0, \quad (r = 1, \dots, n) \end{aligned} \quad (13)$$

This yields:

$$\begin{bmatrix}
m_A + m_B & 0 & -\sum_{i=1}^n E_i q_i & \dots & 0 & \dots \\
0 & m_A + m_B & bm_B + e & \dots & E_i & \dots \\
-\sum_{i=1}^n E_i q_i & bm_B + e & b^2 m_B + 2eb + I_B + I_A & \dots & bE_i + F_i & \dots \\
\vdots & \vdots & \vdots & \ddots & \vdots & \ddots \\
-\sum_{i=1}^n \mu_{ij} q_i & E_j & bE_j + F_j & \dots & G_{ij} & \dots \\
\vdots & \vdots & \vdots & \ddots & \vdots & \ddots
\end{bmatrix}
\begin{bmatrix}
v_1 \\
v_2 \\
v_3 \\
\vdots \\
\tilde{q}_i \\
\vdots
\end{bmatrix}
=
\begin{bmatrix}
(m_A + m_B)v_2 v_3 + v_3^2 (bm_B + e) + 2v_3 \sum_{i=1}^n E_i q_i \\
-(m_A + m_B)v_3 v_1 + v_3^2 \sum_{i=1}^n E_i q_i \\
-v_2 v_3 \sum_{i=1}^n E_i q_i - v_3 v_1 (bm_B + e) \\
\vdots \\
-v_3 v_1 E_j + v_3^2 \sum_{i=1}^n G_{ij} q_i - v_3^2 \sum_{i=1}^n (b\mu_{ij} + \eta_{ij}) q_i - v_2 v_3 \sum_{i=1}^n \mu_{ij} q_i \\
\vdots
\end{bmatrix}
+
\begin{bmatrix}
\dots & 0 & \dots \\
\dots & 0 & \dots \\
\dots & 0 & \dots \\
\ddots & \vdots & \ddots \\
\dots & -H_{ij} & \dots \\
\ddots & \vdots & \ddots
\end{bmatrix}
\begin{bmatrix}
\vdots \\
q_i \\
\vdots
\end{bmatrix}
\tag{14}$$

where following Kane et al. [10] we have defined:

$$\begin{aligned}
m_B &\equiv \int_0^L \rho dx, & e &\equiv \int_0^L x \rho dx, & I_B &\equiv \int_0^L x^2 \rho dx \\
H_{ij} &\equiv \int_0^L EI \phi_{2i}''(x) \phi_{2j}''(x) dx, & E_i &\equiv \int_0^L \phi_{2i}(x) \rho dx \\
F_i &\equiv \int_0^L x \phi_{2i}(x) \rho dx, & G_{ij} &\equiv \int_0^L \phi_{2i}(x) \phi_{2j}(x) \rho dx \\
&&& (i, j = 1, \dots, n)
\end{aligned}
\tag{15}$$



and we have further defined:

$$\begin{aligned}\mu_{ij} &\equiv \int_0^L \rho \int_0^x \phi'_{2i}(\sigma) \phi'_{2j}(\sigma) d\sigma dx, \\ \eta_{ij} &\equiv \int_0^L x \rho \int_0^x \phi'_{2i}(\sigma) \phi'_{2j}(\sigma) d\sigma dx\end{aligned}\quad (16)$$

The above equations are equivalent to those derived in [11] through the use of geometric nonlinear constraints. The centripetal term in equation (14) exhibits the "geometric stiffening" terms ( $\mu_{ij}, \eta_{ij}$ ) which are not obtained through the standard finite element or assumed modes approach. We note that equation (14), correctly linearized in the small elastic generalized coordinates and speeds, has been obtained from a totally consistent approach to linearization. We mention in passing that the method presented above to obtain the proper second order (in  $q_i$  and  $u_i$ ) expressions for the elastic deflections and speeds can be naturally extended to accommodate the case in which we are interested in independent axial displacements. In this case, we discretize the axial strain at the neutral axis and thus obtain the following expression for the axial displacement (at the neutral axis):

$$\begin{aligned}\hat{\epsilon}_{xx} &= \sum_{i=1}^n \phi_{\epsilon i}(x) p_i \\ u_1(x, t) &= \sum_{i=1}^n \int_0^x \phi_{\epsilon i}(\sigma) d\sigma p_i - \frac{1}{2} \int_0^x \sum_{i=1}^n \sum_{j=1}^n \phi'_{2i}(\sigma) \phi'_{2j}(\sigma) d\sigma q_i q_j \\ \phi_{1i}(x) &= \int_0^x \phi_{\epsilon i}(\sigma) d\sigma\end{aligned}\quad (17)$$

## A.2.2 Kane's Dynamical Equations

In our case:

$$F_r^* = -I_B \omega_r^A \bullet \alpha^A - m_A v_r^{A*} \bullet a^{A*} - \int_0^l \rho v_r^{P1} \bullet a^{P1} dx,$$

$$(F_r)_{Ext} = 0, \quad \underline{\omega}^A = \frac{d}{dt}(\underline{\omega}^A), \quad \mathbf{a}^{A*} = \frac{d}{dt}(N \mathbf{v}^{A*})$$

$$\mathbf{a}^{P_1} = \frac{d}{dt}(\mathbf{v}^{P_1}), \quad (r = \dot{\theta}, \dot{q}_i; i = 1, \dots, n) \quad (1)$$

$(F_r)_{Ext}$  are generalized active forces due to external forces, and the time derivatives are with respect to the inertial frame. We need now to form the partial velocities and partial angular velocities correct to first order in  $q_i$  and  $u_i$ . This is simple enough using the second-order expression for  $\mathbf{v}^{P_1}$  derived in the previous example. The results are given in Table A.1:

$r$	$\underline{\omega}_r^A$	$N \mathbf{v}_r^{A*}$	$\mathbf{v}_r^{P_1}$
$\dot{\theta}$	$\hat{\mathbf{a}}_3$	0	$-u_2 \hat{\mathbf{a}}_1 + (b+x) \hat{\mathbf{a}}_2$
$v_1$	0	$\hat{\mathbf{a}}_1$	$\hat{\mathbf{a}}_1$
$v_2$	0	$\hat{\mathbf{a}}_2$	$\hat{\mathbf{a}}_2$
$\dot{q}_j$	0	0	$-\sum_{i=1}^n \int_0^x \phi'_{2i}(\sigma) \phi'_{2j}(\sigma) d\sigma q_i \hat{\mathbf{a}}_1 + \phi_{2j}(x) \hat{\mathbf{a}}_2$

**Table A.1: Linearized Partial Velocities and Angular Velocities**

We have again ignored independent axial extensions. Table 1 agrees with the linearized partial velocities obtained in [11]. And the equations of motion given by

$$F_r + F_r^* = 0, \quad (r = \dot{\theta}, \dot{q}_1, \dots, \dot{q}_n) \quad (2)$$

are the same as in equation A.2.1.14 as expected.

# APPENDIX B: CALCULATION OF MODAL INTEGRALS AND CONSTANTS

In this Appendix, modal integrals and constants that appear in the equations of motion of Appendix C are defined and evaluated. For convenience, these will be divided into three groups: 1) constants that are independent of mode shapes; 2) mode shape dependent constants that can be obtained with linear strain-displacement relations (see discussion in Appendix A); and, 3) mode shape dependent constants that result from proper linearization (and would be missing from the motion equations otherwise). These constants are evaluated by three separate subroutines in the simulation code (see Appendix D): CONSTANT, CONMOD, and FOREST respectively.

The constants below are evaluated for the physical manipulator parameters presented in Table 4.1.

## B.1 CONSTANTS INDEPENDENT OF MODE SHAPE

$$L_1 = b_1 + l_1 + b_{21} \qquad L_2 = b_{22} + l_2 + b_t$$

$$L_1 = 1.0668 \qquad L_2 = 0.9779$$

$$m_1 = \rho_1 l_1 \qquad m_2 = \rho_2 l_2$$

$$m_1 = 1.22472 \qquad m_2 = 0.61236$$

$$a_1 = \int_0^{l_1} x \rho_1 dx = \frac{1}{2} m_1 l_1 \qquad a_2 = \int_0^{l_2} y \rho_2 dy = \frac{1}{2} m_2 l_2$$

$$a_1 = 0.559942 \qquad a_2 = 0.279971$$

$$I_1 = \int_0^{l_1} x^2 \rho_1 dx = \frac{1}{3} m_1 l_1^2 \qquad I_2 = \int_0^{l_2} y^2 \rho_2 dy = \frac{1}{3} m_2 l_2^2$$

$$I_1 = 0.341341 \qquad I_2 = 0.170670$$

## B.2 MODE SHAPE DEPENDENT CONSTANTS

Cantilever (clamped-free) mode shapes are assumed in the evaluation of the modal integrals presented below. The mode shapes are given by [2]

$$\tilde{y}_i(s) = \cosh\left(\frac{\lambda_i s}{l_j}\right) - \cos\left(\frac{\lambda_i s}{l_j}\right) - \sigma_i \left( \sinh\left(\frac{\lambda_i s}{l_j}\right) - \sin\left(\frac{\lambda_i s}{l_j}\right) \right)$$

$$\tilde{y}_i = \begin{cases} \phi_i \\ \psi_i \end{cases}, \quad s = \begin{cases} x \\ y \end{cases}, \quad i = \begin{cases} 1, \dots, n & , j = 1 \\ 1, \dots, m & , j = 2 \end{cases}$$

where

$$\sigma_i = \frac{\sinh \lambda_i - \sin \lambda_i}{\cosh \lambda_i + \cos \lambda_i}$$

and  $\lambda_i$  are the solutions in increasing order of the transcendental equation

$$\cos \lambda \cosh \lambda + 1 = 0.$$

$$\lambda_i = \begin{bmatrix} 1.87510407 \\ 4.69409113 \\ 7.85475744 \\ 10.99554073 \end{bmatrix} \quad \sigma_i = \begin{bmatrix} 0.734095514 \\ 1.018467319 \\ 0.999224497 \\ 1.000033553 \end{bmatrix}$$

The following orthogonality relations hold:

$$\int_0^l \tilde{y}_i(s) \tilde{y}_j(s) ds = \int_0^l \tilde{y}_i''(s) \tilde{y}_j''(s) ds = \begin{cases} 0, & i \neq j \\ l, & i = j \end{cases}$$

with

$$\tilde{y}_i''(s) = \left(\frac{l}{\lambda_i}\right)^2 \frac{d^2 \tilde{y}_i}{ds^2}$$

$$\frac{d^n}{d\left(\frac{\lambda_i s}{l}\right)^n} \tilde{y}_i = \frac{d^{n+4}}{d\left(\frac{\lambda_i s}{l}\right)^{n+4}} \tilde{y}_i.$$

In all cases, the constants are evaluated for the first four mode shapes.

## B.2.1 Constants obtained using linear strain-displacement relations

$$A_i(l_1) = \phi_i(l_1) + b_{21}\phi'_i(l_1)$$

$$B_i(l_2) = \psi_i(l_2) + b_i\psi'_i(l_2)$$

$$A_i(l_1) = \begin{bmatrix} 2.229417 \\ -2.796795 \\ 3.308112 \\ -3.832654 \end{bmatrix} \quad B_i(l_2) = \begin{bmatrix} 2.152944 \\ -2.531196 \\ 2.872074 \\ -3.221770 \end{bmatrix}$$

$$A_{ij}(l_1) = A_i(l_1)A_j(l_1)$$

$$A_{ij}(l_1) = \begin{bmatrix} 4.970302 & -6.235223 & 7.375162 & -8.544586 \\ & 7.822060 & -9.252109 & 10.719147 \\ & & 10.943603 & -12.678848 \\ \text{symmetric} & & & 14.689239 \end{bmatrix}$$

$$B_{ij}(l_2) = B_i(l_2)B_j(l_2)$$

$$B_{ij}(l_2) = \begin{bmatrix} 4.635172 & -5.449527 & 6.183418 & -6.936292 \\ & 6.406955 & -7.269785 & 8.154931 \\ & & 3.248812 & -9.253162 \\ \text{symmetric} & & & 10.379799 \end{bmatrix}$$

$$E_i = \int_0^{l_1} \phi_i(x) \rho_1 dx$$

$$E_i^* = \int_0^{l_2} \psi_i(y) \rho_2 dy$$

$$E_i = \begin{bmatrix} 0.958946 \\ 0.531450 \\ 0.311600 \\ 0.222774 \end{bmatrix}$$

$$E_i^* = \begin{bmatrix} 0.479473 \\ 0.265725 \\ 0.155800 \\ 0.111387 \end{bmatrix}$$

$$F_i = \int_0^{l_1} x \phi_i(x) \rho_1 dx$$

$$F_i^* = \int_0^{l_2} y \psi_i(y) \rho_2 dy$$

$$F_i = \begin{bmatrix} 0.637019 \\ 0.101648 \\ 0.036303 \\ 0.018525 \end{bmatrix}$$

$$F_i^* = \begin{bmatrix} 0.318509 \\ 0.050824 \\ 0.018151 \\ 0.009263 \end{bmatrix}$$

$$G_{ij} = \int_0^{l_1} \phi_i(x) \phi_j(x) \rho_1 dx$$

$$G_{ij} = \begin{bmatrix} 1.22472 & 0 & 0 & 0 \\ 0 & 1.22472 & 0 & 0 \\ 0 & 0 & 1.22472 & 0 \\ 0 & 0 & 0 & 1.22472 \end{bmatrix}$$

$$G_{ij}^* = \int_0^{l_2} \psi_i(y) \psi_j(y) \rho_2 dy$$

$$G_{ij}^* = \begin{bmatrix} 0.61236 & 0 & 0 & 0 \\ 0 & 0.61236 & 0 & 0 \\ 0 & 0 & 0.61236 & 0 \\ 0 & 0 & 0 & 0.61236 \end{bmatrix}$$

$$H_{ij} = \int_0^{l_1} (EI)_1 \phi_i''(x) \phi_j''(x) dx$$

$$H_{ij} = \begin{bmatrix} 1843.30 & 0 & 0 & 0 \\ 0 & 72393.95 & 0 & 0 \\ 0 & 0 & 567580.3 & 0 \\ 0 & 0 & 0 & 2179528.6 \end{bmatrix}$$

$$H_{ij}^* = \int_0^{l_2} (EI)_2 \psi''_i(y) \psi''_j(y) dy$$

$$H_{ij}^* = \begin{bmatrix} 226.37 & 0 & 0 & 0 \\ 0 & 8890.5 & 0 & 0 \\ 0 & 0 & 69702.8 & 0 \\ 0 & 0 & 0 & 267661.4 \end{bmatrix}$$

## B.2.2 Constants obtained through proper linearization

$$\beta_{ij}(x) = \int_0^x \phi'_i(\sigma) \phi'_j(\sigma) d\sigma \quad \beta_{ij}^*(y) = \int_0^y \psi'_i(\sigma) \psi'_j(\sigma) d\sigma$$

$$C_{ij}(l_1) = \beta_{ij}(l_1) + b_{21} \phi'_i(l_1) \phi'_j(l_1)$$

$$C_{ij}(l_1) = \begin{bmatrix} 5.773586 & -10.469668 & 8.248862 & -12.728235 \\ & 43.783916 & -38.123383 & 34.017360 \\ & & 106.991190 & -70.446206 \\ \text{symmetric} & & & 200.355635 \end{bmatrix}$$

$$C_{ij}^*(l_2) = \beta_{ij}^*(l_2) + b_1 \psi'_i(l_2) \psi'_j(l_2)$$

$$C_{ij}^*(l_2) = \begin{bmatrix} 5.543348 & -9.670022 & 6.936073 & -10.889029 \\ & 41.006644 & -33.563899 & 27.629564 \\ & & 99.505825 & -59.959278 \\ \text{symmetric} & & & 185.663544 \end{bmatrix}$$

$$\mu_{ij} = \int_0^{l_1} \rho_1 \beta_{ij}(x) dx$$

$$\mu_{ij} = \begin{bmatrix} 0.742933 & -0.565643 & -1.435918 & -1.169454 \\ & 8.510827 & 2.532483 & -4.879840 \\ & & 28.808327 & 11.168055 \\ \text{symmetric} & & & 62.730250 \end{bmatrix}$$

$$\mu_{ij}^* = \int_0^{l_2} \rho_2 \beta_{ij}^*(y) dy$$

$$\mu_{ij}^* = \begin{bmatrix} 0.371467 & -0.282822 & -0.717959 & -0.584727 \\ & 4.255413 & 1.265741 & -2.439920 \\ & & 14.404163 & 5.584028 \\ \text{symmetric} & & & 31.365125 \end{bmatrix}$$

$$\eta_{ij} = \int_0^{l_1} \rho_1 x \beta_{ij}(x) dx$$

$$\eta_{ij} = \begin{bmatrix} 1.461503 & -0.839981 & -0.970443 & -0.669203 \\ & 7.934011 & 0.207477 & -3.566202 \\ & & 21.872910 & 4.010066 \\ \text{symmetric} & & & 44.157753 \end{bmatrix}$$

$$\eta_{ij}^* = \int_0^{l_2} \rho_2 y \beta_{ij}^*(y) dy$$

$$\eta_{ij}^* = \begin{bmatrix} 0.730751 & -0.419990 & -0.485221 & -0.334602 \\ & 3.967006 & 0.103739 & -1.783101 \\ & & 10.936455 & 2.005033 \\ \text{symmetric} & & & 22.078876 \end{bmatrix}$$

The following constants are used in sections 3.3.2 and 3.3.3:

$$\xi_1 = \frac{\mu_{11}}{\rho_1} = 0.554689$$

$$\gamma_1 = \frac{\eta_{11}}{m_1} = 1.193336.$$



# APPENDIX C: EQUATIONS OF MOTION

The  $2+n+m$  ordinary differential equations of motion for the two-link, planar, flexible manipulator are given below (refer to section 2.4.3). The motion equations are given in the form of equation (2.4.3.2):

$$\begin{bmatrix} M_{RR}(\mathbf{x}) & M_{RE}(\mathbf{x}) \\ M_{ER}(\mathbf{x}) & M_{EE}(\mathbf{x}) \end{bmatrix} \ddot{\mathbf{x}} + \begin{bmatrix} 0 & 0 \\ 0 & K_{EE} \end{bmatrix} \mathbf{x} = \begin{bmatrix} I \\ 0 \end{bmatrix} \mathbf{T} + \mathbf{F}(\mathbf{x}, \dot{\mathbf{x}}) \quad (1)$$

where as in section 2.4.3 the following definitions have been made

$$\mathbf{x} = \begin{bmatrix} \mathbf{x}_R \\ \mathbf{x}_E \end{bmatrix} = [\theta, \beta, q_1, \dots, q_n, p_1, \dots, p_m]^T$$

$$\mathbf{T} = \begin{bmatrix} T_1 \\ T_2 \end{bmatrix} \quad (2)$$

In the rest of this Appendix, the individual entries in the mass matrix, the stiffness matrix, and the vector of nonlinear forces are presented for the system defined in chapter 2. The definitions of Appendix B and equation (2.3.10) are used together with the following definitions to simplify the form of the entries.

$$I_{Tot} = J_A + I_1 + J_{B_1} + J_{B_2} + I_2 + J_C$$

$$I_{out} = J_{B_2} + I_2 + J_C$$

$$m_{Tot} = m_2 + m_{B_1} + m_{B_2} + m_C$$

$$c_\beta = \cos \beta, \quad s_\beta = \sin \beta$$

$$co_1 = a_2 + b_{22}m_2 + m_{B_2}e_2 \cos \gamma_2 + m_C L_2$$

$$\begin{aligned}
co_2 &= m_{B_2} e_2 \sin \gamma_2 \\
co_{3j} &= A_j(l_1) + L_1 \phi_j'(l_1) \\
co_{4j} &= E_j^* + m_C B_j(l_2) \\
co_{5ij} &= \phi_j'(l_1) A_i(l_1) + \phi_i'(l_1) A_j(l_1) \\
co_{6j} &= A_j(l_1) - L_1 \phi_j'(l_1)
\end{aligned} \tag{3}$$

### C.1 ENTRIES IN THE STIFFNESS MATRIX

$$\begin{aligned}
(K_{EE})_{ij} &= H_{ij}' & i, j &= 1, \dots, n \\
(K_{EE})_{n+i, n+j} &= H_{ij}^* & i, j &= 1, \dots, m \\
(K_{EE})_{i, n+j} &= (K_{EE})_{n+j, i} = 0, & i &= 1, \dots, n; \quad j = 1, \dots, m
\end{aligned} \tag{1}$$

### C.2 ENTRIES IN THE MASS MATRIX

$$\begin{aligned}
(M_{RR})_{1,1} &= \\
&L_{Tot} + 2a_1 b_1 + m_1 b_1^2 + 2a_2 b_{22} + m_2 b_{22}^2 + m_{Tot} L_1^2 + m_{B_1} (e_1^2 + 2L_1 e_1 \cos \gamma_1) \\
&+ m_{B_2} e_2^2 + m_C L_2^2 + 2(co_1 s_\beta + co_2 c_\beta + m_{B_1} e_1 \sin \gamma_1) \sum_{i=1}^n A_i(l_1) q_i \\
&- 2m_{B_1} L_1 e_1 \sin \gamma_1 \alpha_1 - 2L_1 s_\beta \sum_{i=1}^m E_i^* p_i - 2m_C L_1 s_\beta \sum_{i=1}^m B_i(l_2) p_i \\
&+ 2L_1 (co_1 \tilde{c}_\beta - co_2 \tilde{s}_\beta)
\end{aligned} \tag{1}$$

$$\begin{aligned}
(M_{RR})_{2,1} &= (M_{RR})_{1,2} = \\
& I_{out} + 2a_2 b_{22} + m_2 b_{22}^2 + m_{B_2} e_2^2 + m_C L_2^2 + (co_1 s_\beta + co_2 c_\beta) \sum_{i=1}^n A_i(l_1) q_i \\
& - L_1 s_\beta \sum_{i=1}^m E_i^* p_i - m_C L_1 s_\beta \sum_{i=1}^m B_i(l_2) p_i + co_1 \tilde{c}_\beta - co_2 \tilde{s}_\beta
\end{aligned} \tag{2}$$

$$\begin{aligned}
(M_{RR})_{2,2} &= \\
& I_{out} + 2a_2 b_{22} + m_2 b_{22}^2 + m_{B_2} e_2^2 + m_C L_2^2
\end{aligned} \tag{3}$$

$$\begin{aligned}
(M_{ER})_{j,1} &= \quad (j = 1, \dots, n) \\
& F_j + b_1 E_j + \phi_j(l_1) [J_{B_1} + I_{out} + 2a_2 b_{22} + m_2 b_{22}^2 + m_{B_1} (e_1^2 + L_1 e_1 \cos \gamma_1) \\
& + m_{B_2} e_2^2 + m_C L_2^2] + A_j(l_1) [m_{Tot} L_1 + m_{B_1} e_1 \cos \gamma_1] + \phi_j(l_1) [co_1 s_\beta + co_2 c_\beta \\
& + m_{B_1} e_1 \sin \gamma_1] \sum_{i=1}^n A_i(l_1) q_i - co_{3j} m_{B_1} e_1 \sin \gamma_1 \alpha_1 - co_{3j} s_\beta \sum_{i=1}^m E_i^* p_i \\
& - co_{3j} m_C s_\beta \sum_{i=1}^m B_i(l_2) p_i + [co_1 s_\beta + co_2 c_\beta + m_{B_1} e_1 \sin \gamma_1] \sum_{i=1}^n C_{ij}(l_1) q_i \\
& + co_{3j} (co_1 \tilde{c}_\beta - co_2 \tilde{s}_\beta)
\end{aligned} \tag{4}$$

$$\begin{aligned}
(M_{ER})_{n+j,1} &= \quad (j = 1, \dots, m) \\
& F_j^* + b_{22} E_j^* + \psi_j(l_2) J_C + m_C B_j(l_2) L_2 + co_{4j} s_\beta \sum_{i=1}^n A_i(l_1) q_i - L_1 s_\beta \sum_{i=1}^m \mu_{ij}^* p_i \\
& - m_C L_1 s_\beta \sum_{i=1}^m C_{ij}^*(l_2) p_i + co_{4j} L_1 \tilde{c}_\beta
\end{aligned} \tag{5}$$

$$(M_{ER})_{j,2} = \quad (j = 1, \dots, n)$$

$$\begin{aligned} & \phi'_j(l_1)[I_{out} + 2a_2b_{22} + m_2b_{22}^2 + m_{B_2}e_2^2 + m_C L_2^2] - A_j(l_1)s_\beta \sum_{i=1}^m E_i^* p_i \\ & - m_C A_j(l_1)s_\beta \sum_{i=1}^m B_i(l_2)p_i + (co_1s_\beta + co_2c_\beta) \sum_{i=1}^n C_{ij}(l_1)q_i \\ & + A_j(l_1)(co_1\tilde{c}_\beta - co_2\tilde{s}_\beta) \end{aligned} \quad (6)$$

$$(M_{ER})_{n+j,2} = \quad (j = 1, \dots, m)$$

$$F_j^* + b_{22}E_j^* + \psi'_j(l_2)J_C + m_C B_j(l_2)L_2 \quad (7)$$

$$(M_{RE})_{1,j} = \quad (j = 1, \dots, n)$$

$$\begin{aligned} & F_j + b_1E_j + \phi'_j(l_1)[J_{B_1} + I_{out} + 2a_2b_{22} + m_2b_{22}^2 + m_{B_1}(e_1^2 + L_1e_1 \cos \gamma_1) \\ & + m_{B_2}e_2^2 + m_C L_2^2] + A_j(l_1)[m_{Tot}L_1 + m_{B_1}e_1 \cos \gamma_1] + co_{3j}(co_1c_\beta - co_2s_\beta) \end{aligned} \quad (8)$$

$$(M_{RE})_{1,n+j} = \quad (j = 1, \dots, m)$$

$$F_j^* + b_{22}E_j^* + \psi'_j(l_2)J_C + m_C B_j(l_2)L_2 + co_{4j}L_1c_\beta \quad (9)$$

$$(M_{RE})_{2,j} = \quad (j = 1, \dots, n)$$

$$\phi'_j(l_1)[I_{out} + 2a_2b_{22} + m_2b_{22}^2 + m_{B_2}e_2^2 + m_C L_2^2] + A_j(l_1)(co_1c_\beta - co_2s_\beta) \quad (10)$$

$$(M_{RE})_{2,n+j} = \quad (j = 1, \dots, m)$$

$$F_j^* + b_{22}E_j^* + \psi'_j(l_2)J_C + m_C B_j(l_2)L_2 \quad (11)$$

$$(M_{EE})_{i,j} = \quad (i = 1, \dots, n; j = 1, \dots, n)$$

$$\begin{aligned} & \phi'_j(l_1)\phi'_i(l_1)[J_{B_1} + I_{out} + 2a_2b_{22} + m_2b_{22}^2 + m_{B_1}e_1^2 + m_{B_2}e_2^2 + m_C L_2^2] \\ & + A_{ij}(l_1)m_{Tot} + G_{ij} + co_{sij} m_{B_1} e_1 \cos \gamma_1 + co_{sij}(co_1 c_\beta - co_2 s_\beta) \end{aligned} \quad (12)$$

$$(M_{EE})_{n+j,i} = (M_{EE})_{i,n+j} \quad (i = 1, \dots, n; j = 1, \dots, m)$$

$$\phi'_i(l_1)[F_j^* + b_{22}E_j^* + \psi'_j(l_2)J_C + B_j(l_2)m_C L_2] + A_i(l_1)co_{4j}c_\beta \quad (13)$$

$$(M_{EE})_{n+i,n+j} = \quad (i = 1, \dots, m; j = 1, \dots, m)$$

$$\psi'_j(l_2)\psi'_i(l_2)J_C + G_{ij}^* + m_C B_{ij}(l_2) \quad (14)$$

### C.3 ENTRIES IN THE VECTOR OF NONLINEAR FORCES

$$F_1 =$$

$$\begin{aligned} & [({}^N \omega^B)^2 - \omega_3^2] \{ (-co_1 c_\beta + co_2 s_\beta) \sum_{i=1}^n A_i(l_1) q_i + L_1 c_\beta \sum_{i=1}^m E_i^* p_i \\ & + m_C L_1 c_\beta \sum_{i=1}^m B_i(l_2) p_i + L_1 (co_1 \tilde{s}_\beta + co_2 \tilde{c}_\beta) \} \\ & - 2\omega_3 \{ (co_1 s_\beta + co_2 c_\beta + m_{B_1} e_1 \sin \gamma_1) \sum_{i=1}^n A_i(l_1) \dot{q}_i - m_{B_1} e_1 \sin \gamma_1 L_1 \dot{\alpha}_1 \} \\ & + 2 {}^N \omega^B \{ L_1 s_\beta \sum_{i=1}^m E_i^* \dot{p}_i + m_C L_1 s_\beta \sum_{i=1}^m B_i(l_2) \dot{p}_i \} \end{aligned} \quad (1)$$

$$\begin{aligned}
F_2 = & \\
& - \omega^3 \{ (-\cos \alpha_1 \cos \beta + \cos \alpha_2 \sin \beta) \sum_{i=1}^n A_i(l_1) q_i + L_1 c_\beta \sum_{i=1}^m E_i^* p_i + m_C L_1 c_\beta \sum_{i=1}^m B_i(l_2) p_i \\
& + L_1 (\cos \alpha_1 \tilde{s}_\beta + \cos \alpha_2 \tilde{c}_\beta) \} \\
& - 2\omega_3 (\cos \alpha_1 \sin \beta + \cos \alpha_2 \cos \beta) \sum_{i=1}^n A_i(l_1) \dot{q}_i
\end{aligned} \tag{2}$$

$$\begin{aligned}
F_{2+j} = & \quad (j = 1, \dots, n) \\
& \omega_3^2 \{ \sum_{i=1}^n [G_{ij} - (\eta_{ij} + b_1 \mu_{ij})] q_i + m_{Tot} \sum_{i=1}^n [A_{ij}(l_1) - L_1 C_{ij}(l_1)] q_i \\
& + \phi_j(l_1) (\cos \alpha_1 \cos \beta - \cos \alpha_2 \sin \beta + m_{B_1} e_1 \cos \gamma_1) \phi_j(l_1) \sum_{i=1}^n A_i(l_1) q_i \\
& + \cos \alpha_6 m_{B_1} e_1 \cos \gamma_1 \alpha_1 - \phi_j(l_1) L_1 c_\beta \sum_{i=1}^m E_i^* p_i - \phi_j(l_1) m_C L_1 c_\beta \sum_{i=1}^m B_i(l_2) p_i \\
& - m_{B_1} e_1 \cos \gamma_1 \sum_{i=1}^n C_{ij}(l_1) q_i - \phi_j(l_1) L_1 (\cos \alpha_1 \tilde{s}_\beta + \cos \alpha_2 \tilde{c}_\beta) + \cos \alpha_6 m_{B_1} e_1 \sin \gamma_1 \} \\
& + ({}^N \omega^B)^2 \{ A_j(l_1) c_\beta \sum_{i=1}^m E_i^* p_i + m_C A_j(l_1) c_\beta \sum_{i=1}^m B_i(l_2) p_i \\
& + (-\cos \alpha_1 \cos \beta + \cos \alpha_2 \sin \beta) \sum_{i=1}^n C_{ij}(l_1) q_i + A_j(l_1) (\cos \alpha_1 \tilde{s}_\beta + \cos \alpha_2 \tilde{c}_\beta) \} \\
& - 2\omega_3 \{ \phi_j(l_1) (\cos \alpha_1 \sin \beta + \cos \alpha_2 \cos \beta + m_{B_1} e_1 \sin \gamma_1) \sum_{i=1}^n A_i(l_1) \dot{q}_i \\
& - A_j(l_1) m_{B_1} e_1 \sin \gamma_1 \dot{\alpha}_1 \} \\
& + 2({}^N \omega^B)^2 \{ A_j(l_1) s_\beta \sum_{i=1}^m E_i^* \dot{p}_i + m_C A_j(l_1) s_\beta \sum_{i=1}^m B_i(l_2) \dot{p}_i \}
\end{aligned} \tag{3}$$

$$\begin{aligned}
F_{2+n+j} &= & (j = 1, \dots, m) \\
& - \omega_3^2 \left\{ -c\omega_{4j}c_\beta \sum_{i=1}^n A_i(l_1)q_i + m_C L_1 c_\beta \sum_{i=1}^m C_{ij}^*(l_2)p_i + L_1 c_\beta \sum_{i=1}^m \mu_{ij}^* p_i \right. \\
& \quad \left. + L_1 c\omega_{4j}\tilde{s}_\beta \right\} \\
& + ({}^N\omega^B)^2 \left\{ \sum_{i=1}^m [G_{ij}^* - (\eta_{ij}^* + b_{22}\mu_{ij}^*)] p_i + m_C \sum_{i=1}^m [B_{ij}(l_2) - L_2 C_{ij}^*(l_2)] p_i \right\} \\
& - 2\omega_3 \left\{ c\omega_{4j}s_\beta \sum_{i=1}^n A_i(l_1)\dot{q}_i \right\}
\end{aligned} \tag{4}$$

**APPENDIX D:**  
**FORTRAN SIMULATION CODE**



```

C*****
C*****
C      This is the main program for the two-link flex. arm
C      simulation developed by Carlos E. Padilla for his M.S. thesis.
C      DOUBLE PRECISION version.
C*****
C*****
C      INCLUDE '[USER.AVF.CARLOS.FORTRAN]DCONSTANTS.FOR'
C      INCLUDE '[USER.AVF.CARLOS.FORTRAN]DTORQUES.FOR'
C      INCLUDE '[USER.AVF.CARLOS.FORTRAN]DINVERSE.FOR'
C      INCLUDE '[USER.AVF.CARLOS.FORTRAN]DARMAIN.FOR'
C      INCLUDE '[USER.AVF.CARLOS.FORTRAN]DARMNEW.FOR'
C
C      In order to run the simulation, it is also necessary to
C      link the following files:
C      MATSAV.OBJ,DODEINT.OBJ,DRKQC.OBJ,DRK4.OBJ -for variable step
C      MATSAV.OBJ,DRKDUMB.OBJ,DRK4.OBJ          -for plain RK
C
PROGRAM ARM_SIMULATION
IMPLICIT REAL*8 (A-Z)
INTEGER N,M,NR,NOK,NBAD,KMAX,KOUNT,NSAV,MCOUNT,PMAX,NMAX
INTEGER NSTEP
PARAMETER (ZERO=0.0,NMAX=4,EPS=1.0D-6,TITLE=1.0D-3)
CHARACTER*9 DAT,TIM
REAL TINIT,TODE,TOUT
COMMON /PROP/ N,M
COMMON /INPU/ T1,T2,H1,PMAX,YSTART(8+4*NMAX)
COMMON /PATH/ KMAX,KOUNT,DXSAV
COMMON /DIAG/ HSAV,TSAV
COMMON /DIAG/ NOK,NBAD,H1SAV,DAT,TIM,TINIT,TODE,TOUT
COMMON /BUG/ HMIN,INTERVAL,FAVPT,TRA,TIM2,BETA,NSAV,CPS,THET
COMMON /BUG/ MCOUNT
C
C      This is the main program of the two-link flexible arm
C      simulation.
C
CALL DATE(DAT)
CALL TIME(TIM)
C
C      Input the arm constants from the input files ARMDAT.DAT
C      and INIDAT.DAT (both in the THESIS sub-directory) created
C      by ARMINP.FOR.
C
CALL INPUT
C
C      Using these constants, initialize the mass matrix and
C      the updating coefficients.
C
TINIT=SECNDS(0.0)
CALL INITIALIZE
TINIT=SECNDS(TINIT)
C
C      Determine number of points to be saved (KMAX) and the
C      save interval (DXSAV).
C
KMAX=PMAX
DXSAV=(T2-T1)/PMAX
INTERVAL=DXSAV
FAVPT=SAVPTS
TIM2=T2

```

```

THET=YSTART(3+H+M)
BETA=YSTART(4+H+M)
NSAV=N
CPS=EPS
MOUNT=0

C
C      Determine the trial initial time step if not provided.
C
IF (H1 .EQ. ZERO) THEN
  CALL INITIME(H1)
ENDIF
H1SAV=H1
HMIN=TTLE*H1

C
C      Solve the differential equations for the given time interval
C      with the given initial conditions.
C
NR=2+H+M

C
C      Initial conditions for "integration checks."
C
YSTART(1+2*NR)=ZERO
YSTART(2+2*NR)=ZERO
YSTART(3+2*NR)=ZERO
YSTART(4+2*NR)=ZERO
TODE=SECNDS(0.0)
CALL ODEINT(YSTART,4+2*NR,T1,T2,EPS,H1,HMIN,NOK,NBAD)

C
C      The following lines implement the RKDUMB R.-K. integration.
C
c      NSTEP=INT((T2-T1)/H1*10.0)
c      PRINT *, 'NSTEP=',NSTEP
c      CALL RKDUMB(YSTART,4+2*NR,T1,T2,NSTEP)
c      TODE=SECNDS(TODE)

C
C      Output data from simulation to MATPLOT.DAT and DATFILE.DAT
C      and diagnostics to ARMDIAG.DAT.
C
TOUT=SECNDS(0.0)
CALL OUTPUT
TOUT=SECNDS(TOUT)
CALL OUT_DIAGNOSTICS
END

```

```

C*****
C*****
C      This short program is used to interface with the user and
C      create appropriate input data files for the arm simulation.
C      It is written by Carlos E. Padilla as part of his M.S. thesis.
C      DOUBLE PRECISION version.
C*****
C*****

```

```

PROGRAM CREATE_INPUT
IMPLICIT REAL*8 (A-Z)
INTEGER N,M,FORE,I,CHOICE,BRANCH,PMAX,ANGMO,NMAX,RLINE,MDAMP
INTEGER FOOL
PARAMETER (ZERO=0.0,NMAX=4)
DIMENSION BM(8),RL(4),LA(NMAX),EI(4),MM(4),JM(4),Y(8+4*NMAX)
DIMENSION KSI(2*NMAX)
OPEN (3,FILE='[USER.AVF.CARLOS.THESIS]INIDAT',STATUS='NEW',
&      FORM='FORMATTED')
PRINT *,'Short or long version of input? (0-short,1-long)'
READ *,CHOICE
PRINT *,'Enter initial and final times for simulation:'
READ *,T1,T2
PRINT *,'Enter # of pts. to be saved (0-defaults to 200; max. 500):'
READ *,PMAX
IF (PMAX .EQ. 0) PMAX=200
PRINT *,'Ignore foreshortening? (0-No,1-Yes)'
READ *,FORE
PRINT *,'Include angular momentum and energy checks? (0-No,1-Yes)'
READ *,ANGMO
PRINT *,'Use ruthless equations? (0-No,1-Yes)'
READ *,RLINE
IF (RLINE.EQ.1) THEN
    PRINT *,'Use foolish linearization? (0-No,1-Yes)'
    READ *,FOOL
ENDIF
PRINT *,'Enter # of modes for links 1 and 2 (separated by spaces):'
READ *,N,M
PRINT *,'Enter displacement initial conditions for joint angles(rad):'
READ *,Y(1),Y(2)
PRINT *,'Enter velocity initial conditions for joint angles(rad/sec):'
READ *,Y(3+N+M),Y(4+N+M)
PRINT *,'Use default(all zero)initial cond. for links?(0-N,1-Y)'
READ *,BRANCH
IF (BRANCH .EQ. 1) THEN
    DO 50 I=1,N
        Y(2+I)=ZERO
        Y(4+N+M+I)=ZERO
50    CONTINUE
    DO 60 I=1,M
        Y(2+N+I)=ZERO
        Y(4+2*N+M+I)=ZERO
60    CONTINUE
ELSE
    DO 100 I=1,N
        PRINT *,'Enter displ. initial cond. for link 1 mode',I,':'
        READ *,Y(2+I)
100    CONTINUE
    DO 200 I=1,M
        PRINT *,'Enter displ. initial cond. for link 2 mode',I,':'
        READ *,Y(2+N+I)
200    CONTINUE

```

```

DO 300 I=1,N
  PRINT *, 'Enter vel. initial cond. for link 1 mode', I, ':'
  READ *, Y(4+N*M+I)
300  CONTINUE
DO 400 I=1,M
  PRINT *, 'Enter vel. initial cond. for link 2 mode', I, ':'
  READ *, Y(4+2*N*M+I)
400  CONTINUE
ENDIF
PRINT *, 'Enter initial time step (0.0 will yield default):'
READ *, H1
IF (CHOICE .NE. 1) GOTO 1000
OPEN (1, FILE='[USER.AVF.CARLOS.THESIS]ARMDAT', STATUS='NEW',
&     FORM='FORMATTED')
PRINT *, 'Enter lengths b1, b21, b22, bt, b, b':
READ *, BM(1), BM(2), BM(3), BM(4), BM(5), BM(6)
PRINT *, 'Enter angles beta12 and beta21':
READ *, BM(7), BM(8)
PRINT *, 'Enter rho1, rho2, l1, l2:'
READ *, RL(1), RL(2), RL(3), RL(4)
PRINT *, 'Enter lambda(1):'
READ *, LA(1), LA(2), LA(3), LA(4)
PRINT *, 'Enter E and I of link 1 and then of link 2:'
READ *, EI(1), EI(2), EI(3), EI(4)
PRINT *, 'Include modal damping?(0-N, 1-Y)'
READ *, MDAMP
IF (MDAMP.EQ.1) THEN
  PRINT *, 'Same damping for all modes (link 1)?(0-N, 1-Y)'
  READ *, CHOICE
  IF (CHOICE.NE.0) THEN
    PRINT *, 'Enter damping coefficient (ksi):'
    READ *, TA
    DO 700 I=1, NMAX
      KSI(I)=TA
700  CONTINUE
  ELSE
    DO 800 I=1, NMAX
      PRINT *, 'Enter damping coeff. (ksi) for link 1 mode', I, ':'
      READ *, KSI(I)
800  CONTINUE
  ENDIF
  PRINT *, 'Same damping for all modes (link 2)?(0-N, 1-Y)'
  READ *, CHOICE
  IF (CHOICE.NE.0) THEN
    PRINT *, 'Enter damping coefficient (ksi):'
    READ *, TA
    DO 900 I=1, NMAX
      KSI(NMAX+I)=TA
900  CONTINUE
  ELSE
    DO 1100 I=1, NMAX
      PRINT *, 'Enter damping coeff. (ksi) for link 2 mode', I, ':'
      READ *, KSI(NMAX+I)
1100 CONTINUE
  ENDIF
ELSE
  DO 1200 I=1, 2*NMAX
    KSI(I)=ZERO
1200 CONTINUE
ENDIF

```

```

PRINT *, 'Enter masses ma, mb1, mb2, mc1:'
READ *, MM(1), MM(2), MM(3), MM(4)
PRINT *, 'Enter inertias ja, jb1, jb2, jc1:'
READ *, JM(1), JM(2), JM(3), JM(4)
WRITE(1, *) BM(1), BM(2), BM(3), BM(4)
WRITE(1, *) BM(5), BM(6), BM(7), BM(8)
WRITE(1, *) RL(1), RL(2), RL(3), RL(4)
WRITE(1, *) LA(1), LA(2), LA(3), LA(4)
WRITE(1, *) EI(1), EI(2), EI(3), EI(4)
WRITE(1, *) MM(1), MM(2), MM(3), MM(4)
WRITE(1, *) JM(1), JM(2), JM(3), JM(4)
WRITE(1, *) (KSI(I), I=1, NMAX)
WRITE(1, *) (KSI(NMAX+I), I=1, NMAX)
CLOSE (1)
1000 CONTINUE
WRITE(3, *) T1, T2, H1, N, M
WRITE(3, *) FORE, ANGMO, RLINE, FOOL
WRITE(3, *) Y(1), Y(2), Y(3+N*M), Y(4+N*M), PMAX
DO 500 I=1, N
    WRITE(3, *) Y(2+I), Y(4+N*M+I)
500 CONTINUE
DO 600 I=1, M
    WRITE(3, *) Y(2+N*I), Y(4+2*N*M+I)
600 CONTINUE
CLOSE (3)
END

```

```

C*****
C*****
C      This file contains the subroutines that take care of the main
C      steps of the two-link flexible arm simulation. All of the
C      following were written by Carlos E. Padilla as part of the M.S.
C      thesis work.
C      DOUBLE PRECISION version.
C*****
C*****

```

```

SUBROUTINE INPUT
IMPLICIT REAL*8 (A-Z)
INTEGER N,M,FORE,I,PMAX,ANGMO,NMAX,SING,RLINE,FOOL
PARAMETER (NMAX=4)
COMMON /CONTROL/ FORE,ANGMO,SING,RLINE,FOOL
COMMON /PROP/ N,M,BM(8),RL(4),LA(NMAX),EI(4),MM(4),JM(4)
COMMON /PROCP/ KSI(2*NMAX)
COMMON /INPU/ T1,T2,H1,PMAX,YSTART(8+4*NMAX)
COMMON /BUG/ TRA,TRE,TRI,DX2

```

```

C
C      This subroutine is in charge of obtaining the constants
C      necessary for the arm simulation from the file ARMDAT.DAT.
C      The constants are in turn placed there in the appropriate order
C      by the user-interface program ARMINP.
C

```

```

OPEN (1,FILE='[USER.AVF.CARLOS.THESIS]ARMDAT',STATUS='OLD',
&      FORM='FORMATTED')
OPEN (3,FILE='[USER.AVF.CARLOS.THESIS]INIDAT',STATUS='OLD',
&      FORM='FORMATTED')
READ(1,*)BM(1),BM(2),BM(3),BM(4)
READ(1,*)BM(5),BM(6),BM(7),BM(8)
READ(1,*)RL(1),RL(2),RL(3),RL(4)
READ(1,*)LA(1),LA(2),LA(3),LA(4)
READ(1,*)EI(1),EI(2),EI(3),EI(4)
READ(1,*)MM(1),MM(2),MM(3),MM(4)
READ(1,*)JM(1),JM(2),JM(3),JM(4)
READ(3,*)T1,T2,H1,N,M
READ(1,*) (KSI(I),I=1,NMAX)
READ(1,*) (KSI(NMAX+I),I=1,NMAX)
READ(3,*)FORE,ANGMO,RLINE,FOOL
READ(3,*)YSTART(1),YSTART(2),YSTART(3+N*M),YSTART(4+N*M),PMAX
DO 500 I=1,N
    READ(3,*)YSTART(2+I),YSTART(4+I+M+I)
500 CONTINUE
DO 600 I=1,M
    READ(3,*)YSTART(2+N+I),YSTART(4+2*N+M+I)
600 CONTINUE
DX2=SAVPTS
CLOSE (1)
CLOSE (3)
RETURN
END

```

```

C
C
C

```

```

SUBROUTINE INITIALIZE
IMPLICIT REAL*8 (A-Z)
INTEGER N,M,NR,I,J,N2,N3,M2,M3,FORE,ANGMO,NMAX
PARAMETER (ZERO=0.0,TWO=2.0,NMAX=4)
COMMON /CONTROL/ FORE,ANGMO
COMMON /PROP/ N,M,BM(8),RL(4),LA(NMAX),EI(4),MM(4),JM(4)

```

```

COMMON /PROP/ KSI(2*NMAX)
COMMON /FIX/ MF(2+2*NMAX,2+2*NMAX),CO(3*NMAX+8),COM(3*NMAX,NMAX)
COMMON /FIX/ E1(4*NMAX),G1(3*NMAX,NMAX),E2(4*NMAX),G2(3*NMAX,NMAX)
COMMON /FIX/ BIJ1(3*NMAX,NMAX),BIJ2(3*NMAX,NMAX)
COMMON /FIX/ ET1(NMAX,NMAX),ET2(NMAX,NMAX)
COMMON /ANG1/ AN(3*NMAX+4)

```

C  
C  
C  
C  
C  
C

This routine determines whether foreshortening constants are to be evaluated or not, and then it evaluates all constants needed for the simulation and initializes the mass matrix in MF and the updating constants in CO and COM.

```

DIMENSION CONL1(6),CONL2(6),PHI(NMAX,4),BI(NMAX),SI(NMAX)
DIMENSION DAIJ(2+2*NMAX,2+2*NMAX)
NR=2+N+M
N2=2*N
M2=2*M
N3=3*N
M3=3*M

```

C  
C  
C

Determine all integration constants from the input constants.

```

CALL CONSTANT(CONL1,CONL2)
CALL CONMOD(E1,G1,E2,G2)
IF (FORE .EQ. 0) THEN
  CALL FOREST(BIJ1,BIJ2)
ELSE
  CALL CMODES(N,LA,RL(3),RL(3),BI,PHI,SI)
  DO 100 I=1,N
    DO 200 J=1,N
      BIJ1(I,J)=ZERO
      BIJ1(N+I,J)=ZERO
      BIJ1(N2+I,J)=SM(2)*PHI(I,2)*PHI(J,2)
200   CONTINUE
100   CONTINUE
  CALL CMODES(M,LA,RL(4),RL(4),BI,PHI,SI)
  DO 300 I=1,M
    DO 400 J=1,M
      BIJ2(I,J)=ZERO
      BIJ2(M+I,J)=ZERO
      BIJ2(M2+I,J)=BM(4)*PHI(I,2)*PHI(J,2)
400   CONTINUE
300   CONTINUE
ENDIF

```

C  
C  
C

Determine fixed parts of the mass matrix.

```

SUM=JM(3)+JM(4)+CONL2(3)+TWO*CONL2(2)*BM(3)
SUM=SUM+CONL2(1)*BM(3)*BM(3)+MM(3)*BM(6)*BM(6)
MF(2,2)=SUM+MM(4)*CONL2(4)*CONL2(4)
BASIC=MF(2,2)
MF(2,1)=BASIC
MF(1,2)=MF(2,1)
SUM=BASIC+JM(1)+JM(2)+CONL1(3)+TWO*CONL1(2)*BM(1)
SUM=SUM+CONL1(1)*BM(1)*BM(1)
SUM=SUM+MM(2)*(BM(5)*BM(5)+TWO*CONL1(4)*CONL1(5))
MASS=CONL2(1)+MM(2)+MM(3)+MM(4)
MF(1,1)=SUM+MASS*CONL1(4)*CONL1(4)
DO 500 J=1,N
  SUM1=BASIC+JM(2)+MM(2)*(BM(5)*BM(5)+CONL1(4)*CONL1(5))
500

```

```

SUM1=E1(N3+J)*SUM1
SUM1=SUM1+E1(N2+J)*(MASS*CONL1(4)+MM(2)*CONL1(5))
MF(2+J,1)=SUM1+E1(N+J)+BM(1)*E1(J)
MF(1,2+J)=MF(2+J,1)
MF(2+J,2)=E1(N3+J)*BASIC
MF(2,2+J)=MF(2+J,2)
DO 600 I=1,J
    SUM2=BASIC+JM(2)+MM(2)*BM(5)*BM(5)
    SUM2=E1(N3+J)*E1(N3+I)*SUM2
    SUM2=SUM2+G1(N2+I,J)*MASS
    FAC=E1(N3+J)*E1(N2+I)+E1(N2+J)*E1(N3+I)
    SUM2=SUM2+MM(2)*CONL1(5)*FAC
    MF(2+J,2+I)=SUM2+G1(I,J)
    IF (I .NE. J) THEN
        MF(2+I,2+J)=MF(2+J,2+I)
    ENDIF
600    CONTINUE
500    CONTINUE
DO 700 J=1,M
    SUM=E2(M3+J)*JM(4)+E2(M+J)+BM(3)*E2(J)
    MF(2+N+J,1)=SUM+E2(M2+J)*MM(4)*CONL2(4)
    BASIC2=MF(2+N+J,1)
    MF(1,2+N+J)=MF(2+N+J,1)
    MF(2+N+J,2)=BASIC2
    MF(2,2+N+J)=MF(2+N+J,2)
    DO 800 I=1,N
        MF(2+N+J,2+I)=E1(N3+I)*BASIC2
        MF(2+I,2+N+J)=MF(2+N+J,2+I)
800    CONTINUE
DO 900 I=1,J
    SUM=E2(M3+J)*E2(M3+I)*JM(4)+G2(I,J)+MM(4)*G2(M2+I,J)
    MF(2+N+J,2+N+I)=SUM
    IF (I .NE. J) THEN
        MF(2+N+I,2+N+J)=MF(2+N+J,2+N+I)
    ENDIF
900    CONTINUE
700    CONTINUE
C
C     Determine the coefficients for updating the mass matrix
C     and the offset vector b.
C
CO(1)=CONL2(2)+BM(3)*CONL2(1)+MM(3)*CONL2(5)+MM(4)*CONL2(4)
CO(2)=MM(3)*CONL2(6)
CO(3)=CONL1(4)
CO(4)=MM(4)
CO(5)=MM(2)*CONL1(6)
CO(6)=MASS
CO(7)=MM(2)*CONL1(5)
CO(8)=CONL2(4)
DO 1000 J=1,N
    CO(8+J)=E1(N2+J)+CONL1(4)*E1(N3+J)
    CO(8+N+J)=E1(N2+J)-CONL1(4)*E1(N3+J)
    DO 1100 I=1,J
        COM(J,I)=E1(N3+I)*E1(N2+J)+E1(N3+J)*E1(N2+I)
        COM(N+J,I)=BIJ1(N+I,J)+BM(1)*BIJ1(I,J)
        IF (I .NE. J) THEN
            COM(I,J)=COM(J,I)
            COM(N+I,J)=COM(N+J,I)
        ENDIF
1100    CONTINUE

```



```

1000 CONTINUE
      DO 1200 J=1,M
        CO(8+N2+J)=E2(J)+MM(4)*E2(M2+J)
        DO 1300 I=1,J
          COM(N2+J,I)=BIJ2(M+I,J)+BM(3)*BIJ2(I,J)
          IF (I .NE. J) THEN
            COM(N2+I,J)=COM(N2+J,I)
          endif
        ENDIF
      1300 CONTINUE
1200 CONTINUE
C
C      Determine constant diagonal modal damping matrix.
C
      DO 1600 I=1,N
        ET1(I,I)=TWO*KSI(I)*SQRT(G1(N+I,I)*G1(I,I))
        DAIJ(2+I,2+I)=ET1(I,I)
        DO 1700 J=1,I-1
          ET1(I,J)=ZERO
          ET1(J,I)=ZERO
          DAIJ(2+I,2+J)=ET1(I,J)
          DAIJ(2+J,2+I)=ET1(J,I)
        1700 CONTINUE
1600 CONTINUE
      DO 1800 I=1,M
        ET2(I,I)=TWO*KSI(NMAX+I)*SQRT(G2(M+I,I)*G2(I,I))
        DAIJ(2+N+I,2+N+I)=ET2(I,I)
        DO 1900 J=1,I-1
          ET2(I,J)=ZERO
          ET2(J,I)=ZERO
          DAIJ(2+N+I,2+N+J)=ET2(I,J)
          DAIJ(2+N+J,2+N+I)=ET2(J,I)
        1900 CONTINUE
1800 CONTINUE
C
C      CALL WRMATRIX(NR,NR,DAIJ,'DAMP','CMATT0')
C
C      Determine the coefficients to update angular momentum
C      if needed.
C
      IF (ANGMO.EQ.1) THEN
        SUM=JM(1)+JM(2)+CONL1(3)+TWO*CONL1(2)*BM(1)
        SUM=SUM+CONL1(1)*BM(1)*BM(1)+CO(6)*CONL1(4)*CONL1(4)
        AN(1)=SUM+MM(2)*BM(5)*BM(5)+TWO*CO(7)*CONL1(4)
        SUM=JM(3)+JM(4)+CONL2(3)+TWO*CONL2(2)*BM(3)
        SUM=SUM+CONL2(1)*BM(3)*BM(3)+MM(3)*BM(6)*BM(6)
        AN(2)=SUM+MM(4)*CONL2(4)*CONL2(4)
        AN(3)=JM(2)+MM(2)*BM(5)*BM(5)+CONL1(4)*CO(7)
        AN(4)=JM(4)
        DO 1400 I=1,N
          AN(4+I)=E1(N+I)+BIJ(1)*E1(I)
        1400 CONTINUE
        DO 1500 I=1,M
          AN(4+N+I)=E2(M+I)+BM(3)*E2(I)
          AN(4+N+M+I)=E2(M3+I)
        1500 CONTINUE
      endif
      RETURN
      END
C
C
C

```

```

SUBROUTINE UPDATE(T,Y,TOR,MJ,BU)
IMPLICIT REAL*8 (A-Z)
INTEGER N,M,I,J,N2,N3,M2,M3,MCOUNT,NMAX,NRE
INTEGER FORE,ANGMO,SINGUL,RLINE,FNT,FOOL
PARAMETER (ZERO=0.0,TWO=2.0,NMAX=4)
COMMON /CONTROL/ FORE,ANGMO,SINGUL,RLINE,FOOL
COMMON /PROP/ N,M
COMMON /FIX/ MF(2+2*NMAX,2+2*NMAX),CO(3*NMAX+8),COM(3*NMAX,NMAX)
COMMON /FIX/ E1(4*NMAX),G1(3*NMAX,NMAX),E2(4*NMAX),G2(3*NMAX,NMAX)
COMMON /FIX/ BIJ1(3*NMAX,NMAX),BIJ2(3*NMAX,NMAX)
COMMON /FIX/ ET1(NMAX,NMAX),ET2(NMAX,NMAX)
COMMON /ANG2/ AQ,ADQ,PQ,PDQ,EP,FDP,BP,BDP,FNT
COMMON /DAMP/ DDQ(NMAX),DDP(NMAX)
COMMON /BUG/ TRA,TRE,TRI,TRO,TRU,CRA,NRE,CRI,CRO
COMMON /BUG/ MCOUNT
COMMON /OUS/ SAV(12,NMAX)

```

```

C
C      This routine is called by the DERIVS routine used by the
C      differential equation solver to determine the current value of
C      the derivatives to be integrated. UPDATE returns in MU and BU
C      the current value of the mass matrix and offset vector b, given
C      the current "state" vector Y, and the current values
C      of the command joint torques TOR.
C

```

```

DIMENSION MU(2+2*NMAX,2+2*NMAX)
DIMENSION BU(2+2*NMAX),TOR(2),Y(8+4*NMAX)
DIMENSION CQ(NMAX),GQ(NMAX),NBMQ(NMAX),AAQ(NMAX),HQ(NMAX)
DIMENSION LCQ(NMAX),UP(NMAX),CP(NMAX),GP(NMAX),NBMP(NMAX)
DIMENSION BBP(NMAX),HP(NMAX),LCP(NMAX)
C
DIMENSION DDQ(NMAX),DDP(NMAX)
N2=2*N
M2=2*M
N3=3*N
M3=3*M

```

```

C
C      Generate time dependent factors. Link 1.
C

```

```

CB=COS(Y(2))
SB=SIN(Y(2))
AQ=ZERO
PQ=ZERO
ADQ=ZERO
PDQ=ZERO

```

```

C
C      If rate-linear eqs. flag set, make mass matrix indep. of
C      elastic deflections q and p, too.
C

```

```

IF (RLINE.EQ.1) THEN
DO 110 J=1,N
CQ(J)=ZERO
GQ(J)=ZERO
NBMQ(J)=ZERO
AAQ(J)=ZERO
HQ(J)=ZERO
DDQ(J)=ZERO
DO 210 I=1,N
HQ(J)=HQ(J)+G1(N+I,J)*Y(2+I)
DDQ(J)=DDQ(J)+ET1(I,J)*Y(4+N+I)
CONTINUE
LCQ(J)=ZERO

```

```

110      CONTINUE
      ELSE
        DO 100 J=1,N
          AQ=AQ+E1(N2+J)*Y(2+J)
          PQ=PQ+E1(N3+J)*Y(2+J)
          ADQ=ADQ+E1(N2+J)*Y(4+N+M+J)
          PDQ=PDQ+E1(N3+J)*Y(4+N+M+J)
          CQ(J)=ZERO
          GQ(J)=ZERO
          NBMQ(J)=ZERO
          AAQ(J)=ZERO
          HQ(J)=ZERO
          DDQ(J)=ZERO
        DO 200 I=1,N
          CQ(J)=CQ(J)+BIJ1(N2+I,J)*Y(2+I)
          GQ(J)=GQ(J)+G1(I,J)*Y(2+I)
          NBMQ(J)=NBMQ(J)+COM(N+I,J)*Y(2+I)
          AAQ(J)=AAQ(J)+G1(N2+I,J)*Y(2+I)
          HQ(J)=HQ(J)+G1(N+I,J)*Y(2+I)
          DDQ(J)=DDQ(J)+ET1(I,J)*Y(4+N+M+I)
200      CONTINUE
          LCQ(J)=CO(3)*CQ(J)
100      CONTINUE
ENDIF
C
C      Generate time dependent factors. Link 2.
C
C      CAB=CB-SB*PQ
C      SAB=CB*PQ+SB
C      CAB=COS(Y(2)+PQ)
C      SAB=SIN(Y(2)+PQ)
      EP=ZERO
      BP=ZERO
      EDP=ZERO
      BDP=ZERO
      IF (RLINE.EQ.1) THEN
        DO 310 J=1,M
          UP(J)=ZERO
          CP(J)=ZERO
          GP(J)=ZERO
          NBMP(J)=ZERO
          BBP(J)=ZERO
          HP(J)=ZERO
          DDP(J)=ZERO
        DO 410 I=1,M
          HP(J)=HP(J)+G2(M+I,J)*Y(2+N+I)
          DDP(J)=DDP(J)+ET2(I,J)*Y(4+N2+M+I)
410      CONTINUE
          LCP(J)=ZERO
310      CONTINUE
      ELSE
        DO 300 J=1,M
          EP=EP+E2(J)*Y(2+N+J)
          BP=BP+E2(M2+J)*Y(2+N+J)
          EDP=EDP+E2(J)*Y(4+N2+M+J)
          BDP=BDP+E2(M2+J)*Y(4+N2+M+J)
          UP(J)=ZERO
          CP(J)=ZERO
          GP(J)=ZERO
          NBMP(J)=ZERO

```

```

      BBP(J)=ZERO
      HP(J)=ZERO
      DDP(J)=ZERO
      DO 400 I=1,M
        UP(J)=UP(J)+BIJ2(I,J)*Y(2+N+I)
        CP(J)=CP(J)+BIJ2(M2+I,J)*Y(2+N+I)
        GP(J)=GP(J)+G2(I,J)*Y(2+N+I)
        NBMP(J)=NBMP(J)+COM(N2+I,J)*Y(2+N+I)
        BBP(J)=BBP(J)+G2(M2+I,J)*Y(2+N+I)
        HP(J)=HP(J)+G2(M+I,J)*Y(2+N+I)
        DDP(J)=DDP(J)+ET2(I,J)*Y(4+N2+M+I)
400      CONTINUE
        LCP(J)=CO(8)*CP(J)
300      CONTINUE
      ENDIF

C
C      This branch statement allows the omission of mass
C      matrix updates when UPDATE is called from the FORCING
C      routine by setting T<0.0.
C
      IF (T.LT.ZERO) GOTO 2000

C
C      Update the mass matrix.
C
      MU(2,2)=MF(2,2)
      SUM=(CO(1)*SB+CO(2)*CB)*AQ-CO(3)*SB*EP
      SUM=SUM-CO(4)*CO(3)*SB*BP+CO(1)*CO(3)*CAB
      SPEC=SUM-CO(2)*CO(3)*SAB
      MU(2,1)=SPEC+MF(2,1)
      MU(1,2)=MU(2,1)
      MU(1,1)=TWO*(SPEC+CO(5)*AQ-CO(5)*CO(3)*PQ)+MF(1,1)
      DO 500 J=1,N
        SUM=(CO(1)*SB+CO(2)*CB+CO(5))*E1(N3+J)*AQ
        SUM=SUM-CO(5)*CO(8+J)*PQ-CO(8+J)*SB*EP
        SUM=SUM-CO(4)*CO(8+J)*SB*BP
        SAV(1,J)=(CO(1)*SB+CO(2)*CB+CO(5))*CQ(J)
        SUM=SUM+(CO(1)*SB+CO(2)*CB+CO(5))*CQ(J)
        MU(2+J,1)=SUM+(CO(1)*CAB-CO(2)*SAB)*CO(8+J)+MF(2+J,1)
        MU(1,2+J)=(CO(1)*CB-CO(2)*SB)*CO(8+J)+MF(1,2+J)
C      MU(1,2+J)=MU(2+J,1)
        SUM=-E1(N2+J)*SB*EP-CO(4)*E1(N2+J)*SB*BP
        SAV(2,J)=(CO(1)*SB+CO(2)*CB)*CQ(J)
        SUM=SUM+(CO(1)*SB+CO(2)*CB)*CQ(J)
        MU(2+J,2)=SUM+(CO(1)*CAB-CO(2)*SAB)*E1(N2+J)+MF(2+J,2)
        MU(2,2+J)=(CO(1)*CB-CO(2)*SB)*E1(N2+J)+MF(2,2+J)
C      MU(2,2+J)=MU(2+J,2)
      DO 600 I=1,J
c changed cab to cb, sab to sb
        MU(2+J,2+I)=COM(J,I)*(CO(1)*CB-CO(2)*SB)+MF(2+J,2+I)
        IF (I .NE. J) THEN
          MU(2+I,2+J)=MU(2+J,2+I)
        ENDIF
600      CONTINUE
500      CONTINUE
      DO 700 J=1,M
        SAY(3,J)=CO(3)*SB*UP(J)
        SAV(4,J)=CO(4)*CO(3)*SB*CP(J)
        SUM=CO(8+N2+J)*SB*AQ-CO(3)*SB*UP(J)-CO(4)*CO(3)*SB*CP(J)
        MU(2+N+J,1)=SUM+CO(3)*CO(8+N2+J)*CAB+MF(2+N+J,1)
        MU(1,2+N+J)=CO(3)*CO(8+N2+J)*CB+MF(1,2+N+J)

```

```

C      MU(1,2+N+J)=MU(2+N+J,1)
      MU(2+N+J,2)=MF(2+N+J,2)
      MU(2,2+N+J)=MF(2,2+N+J)
      DO 800 I=1,N
C changed cb to cab. and back.
      MU(2+N+J,2+I)=E1(N2+I)*CO(8+N2+J)*CB+MF(2+N+J,2+I)
      MU(2+I,2+N+J)=MU(2+N+J,2+I)
800    CONTINUE
      DO 900 I=1,J
      MU(2+N+J,2+N+I)=MF(2+N+J,2+N+I)
      IF (I .NE. J) THEN
          MU(2+N+I,2+N+J)=MU(2+N+J,2+N+I)
      ENDIF
900    CONTINUE
700    CONTINUE
c      if ((t.gt.1.4684185).and.(t.lt.1.5)) then
c          print *, 'cb', cb
c          print *, 'y', y(1), y(2), y(3)
c          print *, 'y2', y(4), y(5), y(6)
c      endif
C
C      Update the offset vector b=tor+f-kx.
C
2000   CONTINUE
      OM3=Y(3+N+M)
      OOM3=Y(4+N+M)
      if ((abs(om3).gt.1.e15).or.(abs(oom3).gt.1.e15)) then
          print *, 'y from UPDATE', y
          singul=13
          goto 5000
      endif
      LOMB=OM3+OOM3
      LOMB2=OM3+OM3+TWO*OM3+OOM3+OOM3+OOM3
      LIFOM=LOMB2-OM3*OM3
C
C      FNT is a control variable used to allow the mass matrix
C      to be evaluated w/o q terms, while the non-linear vector is
C      evaluated consistently. FNT=1 does the above.
C
FNT=0
C
IF ((RLINE.EQ.1).AND.(FNT.EQ.1)) THEN
    DO 120 J=1,N
        AQ=AQ+E1(N2+J)*Y(2+J)
        PQ=PQ+E1(N3+J)*Y(2+J)
        ADQ=ADQ+E1(N2+J)*Y(4+N+M+J)
        PDQ=PDQ+E1(N3+J)*Y(4+N+M+J)
        CQ(J)=ZERO
        GQ(J)=ZERO
        NEMQ(J)=ZERO
        AAQ(J)=ZERO
        HQ(J)=ZERO
        DDQ(J)=ZERO
    DO 220 I=1,N
        CQ(J)=CQ(J)+BIJ1(N2+I,J)*Y(2+I)
        GQ(J)=GQ(J)+G1(I,J)*Y(2+I)
        NEMQ(J)=NEMQ(J)+COM(N+I,J)*Y(2+I)
        AAQ(J)=AAQ(J)+G1(N2+I,J)*Y(2+I)
        HQ(J)=HQ(J)+G1(N+I,J)*Y(2+I)
        DDQ(J)=DDQ(J)+ET1(I,J)*Y(4+N+M+I)

```

```

220      CONTINUE
          LCQ(J)=CO(3)*CQ(J)
120      CONTINUE
C        CAB=CB-SB*PQ
C        SAB=CB*PQ+SB
          CAB=COS(Y(2)+PQ)
          SAB=SIN(Y(2)+PQ)
          DO 320 J=1,M
            EP=EP+E2(J)*Y(2+N+J)
            BP=BP+E2(M2+J)*Y(2+N+J)
            EDP=EDP+E2(J)*Y(4+N2+M+J)
            BDP=BDP+E2(M2+J)*Y(4+N2+M+J)
            UP(J)=ZERO
            CP(J)=ZERO
            GP(J)=ZERO
            NBMP(J)=ZERO
            BBP(J)=ZERO
            HP(J)=ZERO
            DDP(J)=ZERO
            DO 420 I=1,M
              UP(J)=UP(J)+BIJ2(I,J)*Y(2+N+I)
              CP(J)=CP(J)+BIJ2(M2+I,J)*Y(2+N+I)
              GP(J)=GP(J)+G2(I,J)*Y(2+N+I)
              NBMP(J)=NBMP(J)+COM(N2+I,J)*Y(2+N+I)
              BBP(J)=BBP(J)+G2(M2+I,J)*Y(2+N+I)
              HP(J)=HP(J)+G2(M+I,J)*Y(2+N+I)
              DDP(J)=DDP(J)+ET2(I,J)*Y(4+N2+M+I)
420      CONTINUE
          LCP(J)=CO(8)*CP(J)
320      CONTINUE

```

```

ELSE
  IF (FOOL.EQ.1) THEN
    BU(1)=TOR(1)
    BU(2)=TOR(2)
    DO 1200 J=1,N
      BU(2+J)=-HQ(J)-DDQ(J)
1200    CONTINUE
    DO 1300 J=1,M
      BU(2+N+J)=-HP(J)-DDP(J)
1300    CONTINUE
    GOTO 5000
  ENDIF
ENDIF

```

C  
C The above IF statement allows the simulation of rate-linear  
C equations. 1/20/89- Modified to simulate rate-linear in small  
C elastic rates, but non-linear in rigid body rates.  
C

```

OMB=OM3+OOM3+PDQ
NOMB2=TWO*(OM3+OOM3)*PDQ
OMB2=LOMB2+NOMB2
DIFOM=LOMB2+NOMB2-OM3*OM3
COEF=(-CO(1)*CB+CO(2)*SB)*AQ+CO(3)*CB*EP
COEF=COEF+CO(4)*CO(3)*CB*BP+CO(3)*CO(1)*SAB
COEF=COEF+CO(3)*CO(2)*CAB
SUM=-TWO*OM3*((CO(1)*SB+CO(2)*CB+CO(5))*ADQ-CO(5)*CO(3)*PDQ)
SUM=SUM+LIFOM*COEF+NOMB2*(CO(3)*CO(1)*SB+CO(3)*CO(2)*CB)
SUM=SUM+TWO*LOMB*(CO(3)*SB*EDP+CO(4)*CO(3)*SB*BDP)
BU(1)=SUM+TOR(1)
SUM=-OM3*OM3*COEF-TWO*OM3*(CO(1)*SB+CU(2)*CB)*ADQ

```



```

C*****
C*****
C      These FORTRAN subroutines evaluate the constants to be used
C      by the INITIALIZE and UPDATE routines in the two-link flexible
C      arm simulation. Written by Carlos E. Padilla for his M.S.
C      thesis on 7-9-88.
C      DOUBLE PRECISION version.
C*****
C*****
      REAL*8 FUNCTION SINH(X)
      REAL*8 X
      SINH=(EXP(X)-EXP(-X))/2.0
      RETURN
      END

C
      REAL*8 FUNCTION COSH(X)
      REAL*8 X
      COSH=(EXP(X)+EXP(-X))/2.0
      RETURN
      END

C
C      As of now, given # of m.s. N, lambda1, length L, argument X,
C      the subroutine returns the modeshapes and the first three
C      derivatives J/dx in PHI(NMAX,4). Also the beta=lambda1/L
C      are returned in array BI(NMAX). Further, the signal are
C      returned in SI(NMAX).
C
      SUBROUTINE CMODES(N,LA,L,X,BI,PHI,SI)
      IMPLICIT REAL*8 (A-Z)
      INTEGER N,I,J,NMAX
      PARAMETER (NMAX=4)
      DIMENSION LA(NMAX),PHI(NMAX,4),BI(NMAX),SI(NMAX)

C
      DO 100 I=1,N
          SI(I)=(SINH(LA(I))-SIN(LA(I)))/(COSH(LA(I))+COS(LA(I)))
100    CONTINUE

C
      DO 200 J=1,N
          BI(J)=LA(J)/L
          BX=BI(J)*X
          SX=SIN(BX)
          CX=COS(BX)
          SINHX=SINH(BX)
          COSHX=COSH(BX)

C
          PHI(J,1)=(COSHX-CX-SI(J)*(SINHX-SX))
          PHI(J,2)=BI(J)*(SINHX+SX-SI(J)*(COSHX-CX))
          PHI(J,3)=BI(J)*BI(J)*(COSHX+CX-SI(J)*(SINHX+SX))
          PHI(J,4)=BI(J)*BI(J)*BI(J)*(SINHX-SX-SI(J)*(COSHX+CX))
200    CONTINUE
      RETURN
      END

C
C
C
      SUBROUTINE CONSTANT(CONL1,CONL2)
      IMPLICIT REAL*8 (A-Z)
      INTEGER N,M
      COMMON /PROP/ N,M,BM(8),RL(4)
C

```



```

C       This routine evaluates constants that do not depend on the
C       mode shapes. CONL1 on exit contains the constants for link 1
C       while CONL2 contains the constants for link2.
C
C       DIMENSION CONL1(6),CONL2(6)
C
C       Determine constants for link 1.
C
C       CONL1(1)=RL(1)*RL(3)
C       CONL1(2)=CONL1(1)*RL(3)/2.0
C       CONL1(3)=CONL1(2)*RL(3)*2.0/3.0
C       CONL1(4)=BM(1)+BM(2)+RL(3)
C       CONL1(5)=BM(5)*COS(BM(7))
C       CONL1(6)=BM(5)*SIN(BM(7))
C
C       Determine constants for link 2.
C
C       CONL2(1)=RL(2)*RL(4)
C       CONL2(2)=CONL2(1)*RL(4)/2.0
C       CONL2(3)=CONL2(2)*RL(4)*2.0/3.0
C       CONL2(4)=BM(3)+BM(4)+RL(4)
C       CONL2(5)=BM(6)*COS(BM(8))
C       CONL2(6)=BM(6)*SIN(BM(8))
C       RETURN
C       END
C
C
C
C       SUBROUTINE CONMOD(E1,G1,E2,G2)
C       IMPLICIT REAL*8 (A-Z)
C       INTEGER N,M,I,J,N2,N3,M2,M3,NMAX,NR
C       PARAMETER (ZERO=0.0,TWO=2.0,NMAX=4,SCALE=1.0)
C       COMMON /PROP/ N,M,BM(8),RL(4),LA(4),EI(4)
C
C       This routine evaluates constants that depend on the mode
C       shapes but that do not include foreshortening. N is the #
C       of modes for link 1. M is the # of modes for link 2. On exit
C       E1 contains the single-indexed mode constants for link 1 and
C       G1 contains the double-indexed mode constants for link 1.
C       Likewise for link 2.
C
C       DIMENSION E1(4*NMAX),G1(3*NMAX,NMAX),E2(4*NMAX),G2(3*NMAX,NMAX)
C       DIMENSION BI(NMAX),PHI(NMAX,4),SI(NMAX),KSIF(2+2*NMAX,2+2*NMAX)
C       DIMENSION MMASS(2+2*NMAX,2+2*NMAX)
C       L1=RL(3)
C       L2=RL(4)
C       NR=2+N+M
C       N2=2*N
C       M2=2*M
C       N3=3*N
C       M3=3*M
C       SCA2=SCALE*SCALE
C
C       Determine constants for link 1.
C
C       CALL CMODES(N,LA,L1,L1,BI,PHI,SI)
C       DO 100 I=1,N
C           E1(I)=SCALE*TWO*RL(1)*SI(I)/BI(I)
C           E1(N+I)=SCALE*TWO*RL(1)/(BI(I)*BI(I))
C           E1(N2+I)=SCALE*(PHI(I,1)+BM(2)*PHI(I,2))

```

```

E1(N3+I)=SCALE*PHI(I,2)
G1(I,I)=SCA2*RL(1)*RL(3)
G1(N+I,I)=SCA2*BI(I)*BI(I)*BI(I)*BI(I)*RL(3)*EI(1)*EI(2)

```

C  
C  
C  
C  
C

Note: KSIF is used to save the values of the constant flex. coordinates stiffness matrix. Mmass is used to save the values of the constant modal mass matrix.

```

MMASS(2+I,2+I)=G1(I,I)
KSIF(2+I,2+I)=G1(N+I,I)
G1(N2+I,I)=E1(N2+I)*E1(N2+I)
DO 200 J=1,I-1
  G1(I,J)=SCA2*ZERO
  G1(J,I)=G1(I,J)
  G1(N+I,J)=SCA2*ZERO
  G1(N+J,I)=G1(N+I,J)
  MMASS(2+I,2+J)=G1(I,J)
  MMASS(2+J,2+I)=G1(J,I)
  KSIF(2+I,2+J)=G1(N+I,J)
  KSIF(2+J,2+I)=G1(N+J,I)
  G1(N2+I,J)=E1(N2+I)*E1(N2+J)
  G1(N2+J,I)=G1(N2+I,J)

```

200 CONTINUE

100 CONTINUE

C  
C  
C

Determine constants for link 2.

```
CALL CMODES(M,LA,L2,L2,BI,PHI,SI)
```

C  
C  
C  
C

Note: LA is the same as for the above case in our special case of cantilever modes for both links.

```

DO 300 I=1,M
  E2(I)=SCALE*TWO*RL(2)*SI(I)/BI(I)
  E2(M+I)=SCALE*TWO*RL(2)/(BI(I)*BI(I))
  E2(M2+I)=SCALE*(PHI(I,1)+BM(4)*PHI(I,2))
  E2(M3+I)=SCALE*PHI(I,2)
  G2(I,I)=SCA2*RL(2)*RL(4)
  G2(M+I,I)=SCA2*BI(I)*BI(I)*BI(I)*BI(I)*RL(4)*EI(3)*EI(4)
  MMASS(2+N+I,2+N+I)=G2(I,I)
  KSIF(2+N+I,2+N+I)=G2(M+I,I)
  G2(M2+I,I)=E2(M2+I)*E2(M2+I)
  DO 400 J=1,I-1
    G2(I,J)=SCA2*ZERO
    G2(J,I)=G2(I,J)
    G2(M+I,J)=SCA2*ZERO
    G2(M+J,I)=G2(M+I,J)
    MMASS(2+N+I,2+N+J)=G2(I,J)
    MMASS(2+N+J,2+N+I)=G2(J,I)
    KSIF(2+N+I,2+N+J)=G2(M+I,J)
    KSIF(2+N+J,2+N+I)=G2(M+J,I)
    G2(M2+I,J)=E2(M2+I)*E2(M2+J)
    G2(M2+J,I)=G2(M2+I,J)

```

400 CONTINUE

300 CONTINUE

C  
C  
C  
C  
C

```

CALL WRMATRIX(NR,NR,MMASS,'MMAS','MMATT0')
CALL WRMATRIX(NR,NR,KSIF,'STIF','KWATT0')
CALL MATMATRIX(NR,NR,KSIF,'STIF','KWATT0')
RETURN
END

```

C  
C  
C

```
SUBROUTINE FOREST(BIJ1,BIJ2)
  IMPLICIT REAL*8 (A-Z)
  INTEGER N,M,I,J,N2,M2,NMAX,NR
  PARAMETER (ONE=1.0,TWO=2.0,NMAX=4,SCALE=1.0)
  COMMON /PROP/ N,M,BM(8),RL(4),LA(4)
```

C  
C  
C  
C  
C  
C  
C

This subroutine evaluates the modal constants that arise due to foresortening. N is the # of modes for link 1, and M is the # of modes for link 2. On return BIJ1 will contain the constants (all double indexed) pertaining to link 1. Likewise, BIJ2 will contain those of link 2.

```
DIMENSION BIJ1(3*NMAX,NMAX),BIJ2(3*NMAX,NMAX),BI(NMAX)
DIMENSION PHI(NMAX,4),SI(NMAX),BI3(NMAX),BI4(NMAX)
DIMENSION MUIJ(2+2*NMAX,2+2*NMAX),ETIJ(2+2*NMAX,2+2*NMAX)
DIMENSION CIJ1(2+2*NMAX,2+2*NMAX)
L1=RL(3)
L2=RL(4)
NR=2+N+M
N2=2*N
M2=2*M
SCA2=SCALE*SCALE
```

C  
C  
C

Determine constants for link 1.

```
CALL CMODES(N,LA,L1,L1,BI,PHI,SI)
L13=L1*L1*L1
L12=L1*L1/TWO
DO 100 I=1,N
  BI3(I)=BI(I)*BI(I)*BI(I)
  BI4(I)=BI(I)*BI3(I)
  SUM=3.0/TWO-11.0/8.0*SI(I)*BI(I)*L1
  SUM=SUM+ONE/TWO*(SI(I)*BI(I)*L1)**2
  BIJ1(I,I)=SCA2*RL(1)*SUM
  MUIJ(2+I,2+I)=BIJ1(I,I)
  SUM=5.0/4.0*L1+L13/(12.0*BI4(I))*PHI(I,4)*PHI(I,4)
  SUM=SUM-ONE/6.0*L13*PHI(I,1)*PHI(I,3)
  SUM=SUM+L13/12.0*PHI(I,2)*PHI(I,2)
  BIJ1(N+I,I)=SCA2*RL(1)*(SUM-L12*SI(I)*BI(I))
  ETIJ(2+I,2+I)=BIJ1(N+I,I)
  SUM=SI(I)*BI(I)*(TWO+SI(I)*BI(I)*L1)
  BIJ1(N2+I,I)=SCA2*(SUM+BM(2)*PHI(I,2)*PHI(I,2))
  CIJ1(2+I,2+I)=BIJ1(N2+I,I)
DO 200 J=1,I-1
  DIV=BI4(I)-BI4(J)
  COEF=RL(1)/DIV
  SUM=8.0*BI4(I)*(BI(I)*BI(J))**2/DIV
  SUM=SUM+8.0*BI4(J)*(BI(I)*BI(J))**2/DIV
  SUM=SUM-(-1.0)**(I+J)*16.0*BI4(I)*BI4(J)/DIV
  LAC1=4.0*BI(J)*BI(J)*BI3(I)*SI(I)
  LAC2=4.0*BI(I)*BI(I)*BI3(J)*SI(J)
  SUM=SUM-L1*LAC1+L1*LAC2
  BIJ1(I,J)=SCA2*COEF*SUM
  BIJ1(J,I)=BIJ1(I,J)
  MUIJ(2+I,2+J)=BIJ1(I,J)
  MUIJ(2+J,2+I)=BIJ1(J,I)
  SUM=-4.0*BI4(I)*BI4(J)/DIV*L1*PHI(I,1)*PHI(J,1)
```

```

FAC1=L1*PHI(I,2)*PHI(J,4)
FAC2=L1*PHI(I,4)*PHI(J,2)
FAC=-FAC1+L1*PHI(I,3)*PHI(J,3)-FAC2
SUM=SUM-TWO*(BI4(I)+BI4(J))/DIV*FAC
SUM=SUM+PHI(I,1)*PHI(J,4)-PHI(I,4)*PHI(J,1)
SUM=SUM-TWO*PHI(I,2)*PHI(J,3)+TWO*PHI(I,3)*PHI(J,2)
SUM=SUM-FAC2+FAC1-L12*LAC1
BIJ1(N+I,J)=SCA2*COEF*(SUM+L12*LAC2)
BIJ1(N+J,I)=BIJ1(N+I,J)
ETIJ(2+I,2+J)=BIJ1(N+I,J)
ETIJ(2+J,2+I)=BIJ1(N+J,I)
SUM1=SI(J)*BI4(I)*BI(J)-SI(I)*BI4(J)*BI(I)
SUM1=4.0*(-ONE)**(I+J)*SUM1/DIV
SUM=4.0*(BI(I)*BI(J))**2*(SI(I)*BI(I)-SI(J)*BI(J))/DIV
SUM=SUM1-SUM
BIJ1(N2+I,J)=SCA2*(SUM+BM(2)*PHI(I,2)*PHI(J,2))
BIJ1(N2+J,I)=BIJ1(N2+I,J)
CIJ1(2+I,2+J)=BIJ1(N2+I,J)
CIJ1(2+J,2+I)=BIJ1(N2+I,J)

```

```

200      CONTINUE
100      CONTINUE
C
C      Determine constants for link 2.
C

```

```

CALL CMODES(M,LA,L2,L2,BI,PHI,SI)
L23=L2*L2*L2
L22=L2*L2/TWO
DO 300 I=1,M
  BI3(I)=BI(I)*BI(I)*BI(I)
  BI4(I)=BI(I)*BI3(I)
  SUM=3.0/TWO-11.0/8.0*SI(I)*BI(I)*L2
  SUM=SUM+ONE/TWO*(SI(I)*BI(I)*L2)**2
  BIJ2(I,I)=SCA2*RL(2)*SUM
  MUJ(2+N+I,2+N+I)=BIJ2(I,I)
  SUM=5.0/4.0*L2+L23/(12.0*BI4(I))*PHI(I,4)*PHI(I,4)
  SUM=SUM-ONE/8.0*L23*PHI(I,1)*PHI(I,3)
  SUM=SUM+L23/12.0*PHI(I,2)*PHI(I,2)
  BIJ2(M+I,I)=SCA2*RL(2)*(SUM-L22*SI(I)*BI(I))
  ETIJ(2+N+I,2+N+I)=BIJ2(M+I,I)
  SUM=SI(I)*BI(I)*(TWO+SI(I)*BI(I)*L2)
  BIJ2(M2+I,I)=SCA2*(SUM+BM(4)*PHI(I,2)*PHI(I,2))
  CIJ1(2+N+I,2+N+I)=BIJ2(M2+I,I)
DO 400 J=1,I-1
  DIV=BI4(I)-BI4(J)
  COEF=RL(2)/DIV
  SUM=8.0*BI4(I)*(BI(I)*BI(J))**2/DIV
  SUM=SUM+8.0*BI4(J)*(BI(I)*BI(J))**2/DIV
  SUM=SUM-(-1.0)**(I+J)*16.0*BI4(I)*BI4(J)/DIV
  LAC1=4.0*BI(J)*BI(J)*BI3(I)*SI(I)
  LAC2=4.0*BI(I)*BI(I)*BI3(J)*SI(J)
  SUM=SUM-L2*LAC1+L2*LAC2
  BIJ2(I,J)=SCA2*COEF*SUM
  BIJ2(J,I)=BIJ2(I,J)
  MUJ(2+N+I,2+N+J)=BIJ2(I,J)
  MUJ(2+N+J,2+N+I)=BIJ2(J,I)
  SUM=-4.0*BI4(I)*BI4(J)/DIV*L2*PHI(I,1)*PHI(J,1)
  FAC1=L2*PHI(I,2)*PHI(J,4)
  FAC2=L2*PHI(I,4)*PHI(J,2)
  FAC=-FAC1+L2*PHI(I,3)*PHI(J,3)-FAC2
  SUM=SUM-TWO*(BI4(I)+BI4(J))/DIV*FAC

```

```

SUM=SUM+PHI(I,1)*PHI(J,4)-PHI(I,4)*PHI(J,1)
SUM=SUM-TWO*PHI(I,2)*PHI(J,3)+TWO*PHI(I,3)*PHI(J,2)
SUM=SUM-FAC2+FAC1-L22*LAC1
BIJ2(M+I,J)=SCA2*COEF*(SUM+L22*LAC2)
BIJ2(M+J,I)=BIJ2(M+I,J)
ETIJ(2+N+I,2+N+J)=BIJ2(M+I,J)
ETIJ(2+N+J,2+N+I)=BIJ2(M+J,I)
SUM1=SI(J)*BI4(I)*BI(J)-SI(I)*BI4(J)*BI(I)
SUM1=4.0*(-ONE)**(I+J)*SUM1/DIV
SUM=4.0*(BI(I)*BI(J))*2*(SI(I)*BI(I)-SI(J)*BI(J))/DIV
SUM=SUM1-SUM
BIJ2(M2+I,J)=SCA2*(SUM+BM(4)*PHI(I,2)*PHI(J,2))
BIJ2(M2+J,I)=BIJ2(M2+I,J)
CIJ1(2+N+I,2+N+J)=BIJ2(M2+I,J)
CIJ1(2+N+J,2+N+I)=BIJ2(M2+J,I)
400     CONTINUE
300     CONTINUE
c       CALL WRMATRIX(NR,NR,MUIJ,'MUIJ','MUIJT0')
c       CALL WRMATRIX(NR,NR,ETIJ,'ETIJ','METAT0')
C       CALL MATMATRIX(NR,NR,MUIJ,'MUIJ','MUIJT0')
C       CALL MATMATRIX(NR,NR,ETIJ,'ETIJ','METAT0')
CALL WRMATRIX(NR,NR,CIJ1,'CIJ1','CIJ1T0')
RETURN
END

```

```

C*****
C*****
C      This file contains the rest of the main subroutines for the
C      two-link flex. arm simulation. The following are all written
C      by Carlos E. Padilla. This file is included by the FORTRAN
C      command at the end of the file ARMAIN.FOR.
C      DOUBLE PRECISION version.
C*****
C*****
      SUBROUTINE DERIVS(T,Y,DYDT)
      IMPLICIT REAL*8 (A-Z)
      INTEGER N,M,I,J,NR,FORE,ANGMO,SINGUL,NMAX,COUNT
      PARAMETER (ZERO=0.0,NMAX=4)
      character dat*9,tim*9,AC(9)
      COMMON /CONTROL/ FORE,ANGMO,SINGUL
      COMMON /PROP/ N,M
      COMMON /DAMP/ DDQ(NMAX),DDP(NMAX)
      COMMON /ENER/ ME(2+2*NMAX,2+2*NMAX)

C
C      This is the user provided routine to determine the
C      time derivative of Y, DY/DT, used by the numerical recipes
C      ODEINT routine to solve the differential equations.
C
      DIMENSION Y(8+4*NMAX),DYDT(8+4*NMAX),MU(2+2*NMAX,2+2*NMAX)
      DIMENSION BU(2+2*NMAX),TOR(2)
      dimension be(2+2*nmax)
      NR=2+N+M

C
      DYDT(1)=Y(1+NR)
      DYDT(2)=Y(2+NR)
      DO 100 I=1,N
         DYDT(2+I)=Y(2+NR+I)
100  CONTINUE
      DO 200 I=1,M
         DYDT(2+N+I)=Y(2+NR+N+I)
200  CONTINUE

C
      CALL FORCING(T,Y,TOR)
      CALL UPDATE(T,Y,TOR,MU,BU)
      c  if ((t.gt.0.5993199).and.(t.lt.0.6)) then
      c      print *,t
      c      print *,y(2)
      c      do 110 i=1,nr
      c          print *,(mu(i,j)),j=1,nr
      c 110  continue
      c      endif
      IF (SINGUL.NE.0) GOTO 3000

C
C      This is to output MU and BU for a small number of times.
C
      DATA AC/'1','2','3','4','5','6','7','8','9'/
      IF (T.GE.0.5993211) THEN
      IF (COUNT.LE.8) THEN
      PRINT *,T,y(2),Y(nr+2)
      COUNT=COUNT+1
      CALL MATMATRIX(NR,NR,MU,'MUSI','MUSIM'//AC(COUNT))
      CALL MATMATRIX(NR,1,BU,'BUSI','BUSIM'//AC(COUNT))
      ENDIF
      ENDIF
C

```

```

C      Derivatives for "Integration checks." Angular momentum,
C      energy due to torques, and energy dissipation due to damping.
C
      DYDT(1+2*NR)=TOR(1)
      DYDT(2+2*NR)=TOR(1)*Y(1+NR)
      DYDT(3+2*NR)=TOR(2)*Y(2+NR)
      SUM=ZERO
      DO 800 I=1,N
          SUM=SUM+DDQ(I)*Y(2+NR+I)
800    CONTINUE
      DO 900 I=1,M
          SUM=SUM+DDP(I)*Y(2+NR+N+I)
900    CONTINUE
      DYDT(4+2*NR)=SUM

C
C      If checking of energy is on, save MU in ME.
C
C      If (t.eq.zero) then
      IF (ANGMO.EQ.1) THEN
          DO 400 I=1,NR
              be(I)=bu(I)
              DO 500 J=1,I
                  ME(I,J)=MU(I,J)
                  IF (I.NE.J) ME(J,I)=MU(J,I)
500          CONTINUE
400    CONTINUE
      ENDIF
      else
          do 600 I=1,nr
              do 700 J=1,I
                  mu(I,J)=me(I,J)
                  if (I.ne.J) mu(J,I)=me(J,I)
700          continue
600    continue
      endif

C
C      The following lines do row scaling of the system MUa=BU
C      so as to improve the conditioning of the mass matrix by
C      setting the infinity norms of the rows to 1.
C
      DO 1100 I=1,NR
          SON=MU(I,1)
          DO 1200 J=2,NR
              IF (SON.LT.MU(I,J)) SON=MU(I,J)
1200    CONTINUE
          DO 1300 J=1,NR
              MU(I,J)=1.0/SON*MU(I,J)
1300    CONTINUE
          BU(I)=1.0/SON*BU(I)
1100    CONTINUE

C
C      Invert the mass matrix to obtain the acceleration vector.
C
      If (t.eq.zero) call matmatrix(nr,nr,mu,'MUT0','MUMATX')
      If (t.eq.zero) call wrmatrix(nr,nr,mu,'mut0','MWRIT')
      CALL LUDEC(NR,NR,MU)
      If (singul.ne.0) then
          open (1,file='[user.avf.carios.thesis]overflow',status='unknown',
&             access='append',form='formatted')
          call date(dat)

```

```

      call time(tim)
      write(1,*)dat,' ',tim
      write(1,*)'t=',t
      write(1,*)'y=',y
      close (1)
c      if (angmo.eq.1) then
c          call matmatrix(nr,nr,me,'MUSI','MUMATX')
c          call wrmatrix(nr,nr,me,'musi','MUWRIT')
c      endif
      endif
      IF (SINGUL.NE.0) GOTO 1000
      CALL LUSOLVE(NR,NR,MU,BU)
      IF (SINGUL.NE.0) GOTO 2000
C
      DO 300 I=1,NR
          DYDT(NR+I)=BU(I)
300  CONTINUE
C
C      The following two lines are to be used to freeze the
C      shoulder link for purposes of spinning of second link only.
C      They should be commented out during normal simulations.
C
c      dydt(1)=zero
c      dydt(1+nr)=zero
      GOTO 5000
1000  PAUSE 'Mass matrix non-positive-definite. Aborting.'
      call matmatrix(nr,nr,me,'musi','musimx')
      GOTO 5000
2000  PAUSE 'State vector growing without bound. Aborting.'
      call matmatrix(nr,nr,me,'musi','musimx')
      call matmatrix(nr,1,be,'besi','besimx')
      call matmatrix(nr,1,bu,'busi','busimx')
      GOTO 5000
3000  PAUSE 'Rates too large in UPDATE. Aborting.'
      call matmatrix(nr,nr,mu,'musi','musimx')
5000  CONTINUE
      RETURN
      END
C
C
C
      SUBROUTINE INITIME(T)
      IMPLICIT REAL*8 (A-Z)
      INTEGER N,M,NMAX
      PARAMETER (ONE=1.0,TWO=2.0,NMAX=4,API=3.141592654,SAFETY=0.9)
      COMMON /PROP/ N,M,BM(8),RL(4),LA(NMAX),EI(4)
C
C      This subroutine determines a trial initial time step 'H1'
C      which is returned in T. It is based on the highest freq.
C      mode shape times a safety factor.
C
      L1=RL(3)
      L2=RL(4)
      F1=LA(N)**2/(TWO*API*L1*L1)*SQRT(EI(1)*EI(2)/RL(1))
      F2=LA(M)**2/(TWO*API*L2*L2)*SQRT(EI(3)*EI(4)/RL(2))
      IF (F1 .GT. F2) THEN
          F=F1
      ELSE
          F=F2
      ENDIF

```



T=ONE/10.0\*SAFETY\*ONE/F

RETURN

END

C  
C  
C

```
SUBROUTINE AMOMENTUM(T,Y,H,DELH)
  IMPLICIT REAL*8 (A-Z)
  INTEGER N,M,I,J,FORE,ANGMO,N2,NMAX,NR,SING,RLINE,FNT
  PARAMETER (ZERO=0.0,TWO=2.0,NMAX=4)
  COMMON /CONTROL/ FORE,ANGMO,SING,RLINE
  COMMON /PROP/ N,M
  COMMON /FIX/ MF(2+2*NMAX,2+2*NMAX),CO(3*NMAX+8),COM(3*NMAX,NMAX)
  COMMON /FIX/ E1(4*NMAX),G1(3*NMAX,NMAX),E2(4*NMAX),G2(3*NMAX,NMAX)
  COMMON /ANG1/ AN(3*NMAX+4)
  COMMON /ANG2/ AQ,ADQ,PQ,PDQ,EP,EDP,BP,BDP,FNT
  COMMON /ANG3/ HREF
```

C  
C  
C  
C  
C  
C  
C  
C  
C

This routine determines the angular momentum of the arm. It is called by ODEINT if the control variable ANGMO is set to 1 by the input program. It uses the constants CO and AN evaluated in the INITIALIZE routine and the time variables evaluated in the UPDATE routine placed in the COMMON block ANG2.

```
DIMENSION Y(8+4*NMAX)
N2=2*N
NR=2+N+M
```

C  
C  
C

Determine time dependent factors not in COMMON block.

```
LB=COS(Y(2))
SB=SIN(Y(2))
OM3=Y(3+N+M)
OOM3=Y(4+N+M)
LOMB=OM3+OOM3
C IF ((RLINE.EQ.1).AND.(FNT.NE.1)) THEN
C   DO 300 J=1,N
C     AQ=AQ+E1(N2+J)*Y(2+J)
C     PQ=PQ+E1(N3+J)*Y(2+J)
C     ADQ=ADQ+E1(N2+J)*Y(4+N+M+J)
C     PDQ=PDQ+E1(N3+J)*Y(4+N+M+J)
C 300   CONTINUE
C     DO 400 J=1,M
C       EP=EP+E2(J)*Y(2+N+J)
C       BP=BP+E2(M2+J)*Y(2+N+J)
C       EDP=EDP+E2(J)*Y(4+N2+M+J)
C       BDP=BDP+E2(M2+J)*Y(4+N2+M+J)
C 400   CONTINUE
C   ENDOF
C   CAB=CB-SB*PQ
C   SAB=CB*PQ+SB
C   CAB=CGS(Y(2)+PQ)
C   SAB=SIN(Y(2)+PQ)
C   OMB=OM3+OOM3+PDQ
C   FBEQ=ZERO
C   FBEP=ZERO
C   PDP=ZERO
C   DO 100 I=1,N
C     FBEQ=FBEQ+AN(4+I)*Y(4+N+M+I)
```

```

100 CONTINUE
    DO 200 I=1,M
        PDP=PDP+AN(4+N+M+I)*Y(4+N2+M+I)
        FBEP=FBEP+AN(4+N+I)*Y(4+N2+M+I)
200 CONTINUE
    SUM=OM3*(AN(1)+TWO*CO(5)*AQ-TWO*CO(3)*CO(5)*PQ)
    SUM=SUM+OMB*AN(2)
    FAC=CO(1)*CO(3)*CAB-CO(2)*CO(3)*SAB-CO(3)*SB*EP
    FAC=FAC+(CO(1)*SB+CO(2)*CB)*AQ-CO(4)*CO(3)*SB*BP
C
C     On 1/23/89 changed omb to lomb to linearize consistently.
C
    SUM=SUM+(OM3+LOMB)*FAC+AN(3)*PDQ
    SUM=SUM+PDQ*(CO(1)*CO(3)*CB-CO(2)*CO(3)*SB)
    SUM=SUM+(CO(6)*CO(3)+CO(7)+CO(1)*CB-CO(2)*SB)*ADQ
    SUM=SUM+CO(3)*CB*EDP+(CO(8)+CO(3)*CB)*CO(4)*BDP
    H=SUM+AN(4)*PDP+FBEP+FBEP
    IF (T.EQ.ZERO) HREF=H
    DELH=H-(Y(1+2*NR)+HREF)
    RETURN
    END
C
C
C
SUBROUTINE ENERGY(Y,TENER)
    IMPLICIT REAL*8 (A-Z)
    INTEGER N,M,I,J,NR,NMAX
    PARAMETER (ZERO=0.0,TWO=2.0,NMAX=4)
    COMMON /PROP/ N,M
    COMMON /FIX/ MF(2+2*NMAX,2+2*NMAX),CO(3*NMAX+8),COM(3*NMAX,NMAX)
    COMMON /FIX/ E1(4*NMAX),G1(3*NMAX,NMAX),E2(4*NMAX),G2(3*NMAX,NMAX)
    COMMON /ENER/ MU(2+2*NMAX,2+2*NMAX)
C
C     This routine is determines the total energy of the arm.
C     It is called by ODEINT if the control variable ANGMO is set
C     to 1 by the input program. It uses the constants G1 and G2
C     evaluated in the INITIALIZE routine and the variable MU
C     evaluated in the UPDATE routine placed in the COMMON block
C     ENER in the subroutine DERIVS.
C
    DIMENSION Y(8+4*NMAX)
    NR=2+N+M
C
C     Determine the arm Kinetic Energy.
C
    KE=ZERO
    DO 100 I=1,NR
        SUM=ZERO
        DO 200 J=1,NR
            SUM=SUM+MU(I,J)*Y(NR+J)
200 CONTINUE
        KE=KE+SUM*Y(NR+I)
100 CONTINUE
C
C     Determine the arm Potential Energy.
C
    PE1=ZERO
    PE2=ZERO
    DO 300 I=1,N
        SUM=ZERO

```

```

        DO 400 J=1,N
            SUM=SUM+G1(N+I,J)*Y(2+J)
400     CONTINUE
        PE1=PE1+SUM*Y(2+I)
300     CONTINUE
        DO 500 I=1,M
            SUM=ZERO
            DO 600 J=1,M
                SUM=SUM+G2(M+I,J)*Y(2+N+J)
600     CONTINUE
            PE2=PE2+SUM*Y(2+N+I)
500     CONTINUE
C
C         Return the total energy of the arm.
C
        TENER=1.0/TWO*(KE+PE1+PE2)
        RETURN
        END
C
C
C
SUBROUTINE OUTPUT
IMPLICIT REAL*8 (A-Z)
INTEGER N,M,KMAX,KOUNT,NR,I,J,N2,NMAX
PARAMETER (ZERO=0.0,NMAX=4,SCALE=1.0)
COMMON /PROP/ N,M,BM(8),RL(4),LA(NMAX),EI(4),MM(4)
COMMON /PATH/ KMAX,KOUNT,DXSAV,XP(500),YP(24,500),HP(500),EP(500)
COMMON /PATH/ ME(500,15),DHP(500),TOR(2,500),SFOR(500),STIC(500)
C
C         This routine takes care of the output from the simulation.
C         It does any necessary calculations to the raw output from
C         ODEINT and stores it in MATRIXx format in MATPLOT.DAT. It
C         will also be able to store output data in tabular form in
C         DATFILE.DAT. Both files will be stored in the THESIS sub-
C         directory.
C
        DOUBLE PRECISION X(500,21),XM(500,16)
        DIMENSION Y1(500),Y2(500),DY1(500),DY2(500),PDQ(500)
        DIMENSION BI(NMAX),PHI(NMAX,4),SI(NMAX),PHI2(NMAX,4)
        OPEN (1,FILE='[USER.AVF.CARLOS.THESIS]MATPLOT',STATUS='NEW',
&           FORM='FORMATTED')
        OPEN (3,FILE='[USER.AVF.CARLOS.THESIS]DATFILE',STATUS='NEW',
&           FORM='FORMATTED')
        OPEN (4,FILE='[USER.AVF.CARLOS.THESIS]BUGFILE',STATUS='NEW',
&           FORM='FORMATTED')
        NR=2+N+M
        N2=2*N
        L1=RL(3)
        L2=RL(4)
C
C         Determine small tip deflections of both links from the
C         output modal amplitudes and the mode shapes evaluated at the
C         tip.
C
        CALL CMODES(N,LA,L1,L2,BI,PHI,SI)
        CALL CMODES(M,LA,L2,L2,BI,PHI2,SI)
        DO 100 J=1,KOUNT
            Y1(J)=ZERO
            DY1(J)=ZERO
            PDQ(J)=ZERO

```

```

      Y2(J)=ZERO
      DY2(J)=ZERO
      DO 200 I=1,N
        Y1(J)=Y1(J)+SCALE*PHI(I,1)*YP(2+I,J)
        DY1(J)=DY1(J)+SCALE*PHI(I,1)*YP(4+N+M+I,J)
        PDQ(J)=PDQ(J)+SCALE*PHI(I,2)*YP(4+N+M+I,J)
200    CONTINUE
      DO 300 I=1,M
        Y2(J)=Y2(J)+SCALE*PHI2(I,1)*YP(2+N+I,J)
        DY2(J)=DY2(J)+SCALE*PHI2(I,1)*YP(4+N2+M+I,J)
300    CONTINUE
100    CONTINUE
C
C      Copy values to MATRIXx-ready array, and store.
C
      DO 400 I=1,KOUNT
        X(I,1)=XP(I)
        X(I,2)=YP(1,I)
        X(I,3)=YP(2,I)
        X(I,4)=Y1(I)
        X(I,5)=Y2(I)
        X(I,6)=YP(3+N+M,I)
        X(I,7)=YP(4+N+M,I)
        X(I,8)=DY1(I)
        X(I,9)=DY2(I)
        X(I,10)=+P(I)
        X(I,11)=EP(I)
        X(I,12)=DHP(I)
        X(I,13)=TOR(1,I)
        X(I,14)=TOR(2,I)
        X(I,15)=YP(2*NR+1,I)
        X(I,16)=YP(2*NR+2,I)
        X(I,17)=YP(2*NR+3,I)
        X(I,18)=YP(2*NR+4,I)
        X(I,19)=PDQ(I)
        X(I,20)=SFOR(I)
        X(I,21)=STIC(I)
        XM(I,1)=X(I,1)
C      DO 800 J=1,15
C          XM(I,J+1)=ME(I,J)
C 800    CONTINUE
400    CONTINUE
      CALL MATSAV(1,'DATAx',500,KOUNT,21,0,X,DUMMY,'(1P2E24.15)')
      CLOSE (1)
C      CALL MATSAV(4,'DATAx',500,KOUNT,16,0,XM,DUMMY,'(1P2E24.15)')
C      CLOSE (4)
C
C      Copy raw data to file.
C
      NR=2+N+M
      WRITE(3,*)N,M,KOUNT,RL(3),RL(4)
      WRITE(3,*)MM(1),MM(2),MM(3),MM(4)
      WRITE(3,*)LA(1),LA(2),LA(3),LA(4)
      DO 500 I=1,KOUNT
        WRITE(3,*)XP(I),YP(1,I),YP(2,I)
        DO 600 J=1,N
          WRITE(3,*)YP(2+J,I),YP(2+NR+J,I)
600    CONTINUE
        DO 700 J=1,M
          WRITE(3,*)YP(2+N+J,I),YP(2+NR+N+J,I)

```

```
700      CONTINUE
500      CONTINUE
      CLOSE (3)
      RETURN
      END
```

C  
C  
C

```
SUBROUTINE OUT_DIAGNOSTICS
IMPLICIT REAL*8 (A-Z)
INTEGER NOK,NBAD,NSAV,N,M,NR,MCOUNT,FORE,ANGMO,SINGUL
INTEGER NCO
PARAMETER (AMIN=60.0)
CHARACTER*9 DAT,TIM
REAL TINIT,TODE,TOUT
COMMON /CONTROL/ FORE,ANGMO,SINGUL
COMMON /PROP/ N,M
COMMON /DIAG/ HSAV,TSAV
COMMON /DIAG/ NOK,NBAD,HISAV,DAT,TIM,TINIT,TODE,TOUT
COMMON /DIA2/ NCO
COMMON /BUG/ HMIN,DXSAV,SAVPTS,DX,TIM2,BETA,NSAV,EPS,THETA
COMMON /BUG/ MCOUNT,Y(24)
```

C  
C  
C  
C

```
      This routine outputs diagnostics messages to the file
      ARMDIAG.DAT in the subdirectory THESIS.
```

```
      OPEN (1,FILE='[USER.AVF.CARLOS.THESIS]ARMDIAG',STATUS='UNKNOWN',
&          ACCESS='APPEND',FORM='FORMATTED')
      WRITE(1,*)'Date and time of start of simulation:',DAT,' ',TIM
      WRITE(1,*)'Number of good steps taken:', NOK
      WRITE(1,*)'Number of bad but retried steps taken:',NBAD
      WRITE(1,*)'Initial time step tried:',HISAV
      WRITE(1,*)'Final time step used:',HSAV
      WRITE(1,*)'# of loops in RKQC for last time step:',NCO
      WRITE(1,*)'Time at end of simulation:',TSAV
      IF (TINIT .GE. AMIN) THEN
          TINIT=TINIT/AMIN
          WRITE(1,*)'Time to complete initialization (min.):',TINIT
      ELSE
          WRITE(1,*)'Time to complete initialization (sec.):',TINIT
      ENDIF
      IF (TODE .GE. AMIN) THEN
          TODE=TODE/AMIN
          WRITE(1,*)'Time to solve O.D.E. (min.):',TODE
      ELSE
          WRITE(1,*)'Time to solve O.D.E. (sec.):',TODE
      ENDIF
      IF (TOUT .GE. AMIN) THEN
          TOUT=TOUT/AMIN
          WRITE(1,*)'Time to complete output sequences (min.):',TOUT
      ELSE
          WRITE(1,*)'Time to complete output sequences (sec.):',TOUT
      ENDIF
      IF (SINGUL.NE.0) THEN
          WRITE(1,*)'*****'
          WRITE(1,*)'Simulation aborted.'
          WRITE(1,*)'See .LOG file for error message.'
          WRITE(1,*)'*****'
      ENDIF
```

C

C  
C

Debugging diagnostics.

```
WRITE(1,*)'DEBUGGING DIAGNOSTICS:'
WRITE(1,*)'SINGUL= ',SINGUL
WRITE(1,*)'HMIN= ',HMIN
WRITE(1,*)'Number of HMIN exceeds: ',MCOUNT
WRITE(1,*)'DXSAV= ',DXSAV
WRITE(1,*)'T2= ',TIM2
WRITE(1,*)'THETA DOT= ',THETA
WRITE(1,*)'BETA DOT= ',BETA
WRITE(1,*)'N= ',NSAV
WRITE(1,*)'M= ',M
WRITE(1,*)'EPS= ',EPS
NR=2+NHM
WRITE(1,*)'Y(I)      Y(NR+I)'
DO 100 I=1,NR
  WRITE(1,*)Y(I),Y(NR+I)
100 CONTINUE
CALL DATE(DAT)
CALL TIME(TIM)
WRITE(1,*)'Date and time of end of simulation:',DAT,' ',TIM
WRITE(1,*)' '
CLOSE (1)
RETURN
END
```

```

C*****
C*****
C      This file contains subroutines written for the two-link
C      arm simulation from 4-29-89 on. It is written by Carlos E.
C      Padilla as part of his M.S. thesis.
C      DOUBLE PRECISION version.
C*****
C*****

```

```

SUBROUTINE STABCHK(Y,DYDT,OUT)
IMPLICIT REAL*8 (A-Z)
INTEGER N,M,I,J,NR,N2,NMAX,FORE
PARAMETER (ZERO=0.0,NMAX=4)
COMMON /PROP/ N,M,BM(8)
COMMON /CONTROL/ FORE
COMMON /FIX/ MF(2+2*NMAX,2+2*NMAX),CO(3*NMAX+8),COM(3*NMAX,NMAX)
COMMON /FIX/ E1(4*NMAX),G1(3*NMAX,NMAX),E2(4*NMAX),G2(3*NMAX,NMAX)
COMMON /FIX/ BIJ1(3*NMAX,NMAX),BIJ2(3*NMAX,NMAX)
COMMON /FIX/ ET1(NMAX,NMAX),ET2(NMAX,NMAX)
COMMON /ANG2/ AQ,ADQ,PQ,PDQ

```

```

C
C      This subroutine checks the dynamic parameters of link
C      two of the two-link manipulator, to see if the stability
C      boundary for the consistent model predictions is exceeded.
C      If M=2, then the "exact" dynamic stiffness eigenvalues are
C      checked for non-positive definiteness. A time trace of the
C      lowest eigenvalue is returned on output.
C      If M>2, then a first order approx. is used using the stab.
C      boundary derived in Ch. 3 of my M.S. thesis. The relative
C      distance
C      of u2 to the boundary (given u1dot and u3) is returned on
C      output.
C

```

```

DIMENSION Y(8+4*NMAX),DYDT(8+4*NMAX)
IF (FORE.EQ.1) GOTO 5000
IF (M.EQ.0) GOTO 5000
N2=2*N
NR=2+N+M
BETA=Y(2)
DTHE=Y(1+NR)
DDTHE=DYDT(1+NR)
DBE=Y(2+NR)
SB=SIN(BETA)
CB=COS(BETA)
SAB=PQ*CB+SB
CAB=CB-PQ*SB
L1=CO(3)
B22=BM(3)
DADQ=ZERO
DO 100 I=1,N
    DADQ=DADQ+E1(N2+I)*DYDT(2+NR+I)

```

100

```

CONTINUE
U3=DTHE+DBE+PDQ
U2=DTHE*AQ*SB+ADQ*CB+L1*DTHE*CAB
U1DOT=-(DDTHE*AQ+2*DTHE*ADQ)*CB-DTHE*DTHE*L1*CAB
U1DOT=U1DOT+DDTHE*L1*SAB+(DADQ-DTHE*DTHE*AQ)*SB
IF (M.EQ.2) THEN
    COE1=U2*U3+U3*U3*B22-U1DOT
    A=G2(M+1,1)+COE1*BIJ2(1,1)+U3*U3*(BIJ2(M+1,1)-G2(1,1))
    B=G2(M+1,2)+COE1*BIJ2(1,2)+U3*U3*(BIJ2(M+1,2)-G2(1,2))
    D=G2(M+2,2)+COE1*BIJ2(2,2)+U3*U3*(BIJ2(M+2,2)-G2(2,2))

```

```

S1=0.5*(A+D+SQRT((A-D)**2+4*B*B))
S2=0.5*(A+D-SQRT((A-D)**2+4*B*B))
IF (S1.LT.S2) THEN
  OUT=S1
ELSE
  OUT=S2
ENDIF
ELSE
  H11=G2(M+1,1)
  MU11=BIJ2(1,1)
  ETA11=BIJ2(M+1,1)
  G11=G2(1,1)
  IF (U3.NE.ZERO) THEN
    CECK=-1/U3*(H11/MU11-U1DOT)
    CECK=CECK-U3*(B22+ETA11/MU11-G11/MU11)
    IF (CECK.NE.ZERO) THEN
      OUT=(CECK-U2)/CECK
    ELSE
      OUT=ZERO
    ENDIF
  ELSE
    OUT=0
  ENDIF
ENDIF
5000 CONTINUE
RETURN
END

```



```

C*****
C*****
C       These subroutines were written by Carlos E. Padilla for
C       18.335 P.S. #6. They are used here for his M.S. thesis arm
C       simulation in order to invert the symmetric mass matrix
C       using Cholesky decomposition for maximum savings in execution
C       time.
C       DOUBLE PRECISION version.
C       On 9/9/88 routines were added to allow PA=LU decomposition,
C       i.e., LU decomposition with partial pivoting, to handle mass
C       matrices that are asymmetric due to linearization.
C*****
C*****
C
C       Use Cholesky factorization. Overwrites lower A with G - Cholesky
C       triangle.
C
C       SUBROUTINE CHOLESKY(M,N,A)
C       INTEGER NRA,NRE,NSING,NMAX
C       REAL*8 ZERO
C       PARAMETER (ZERO=0.0,NMAX=10)
C       COMMON /CONTROL/ NRA,NRE,NSING
C       INTEGER M,N,K,P,I
C       REAL*8 A(NMAX,NMAX),S
C
C       IF (M .NE. N) THEN
C           PRINT *, 'Matrix not square - Cholesky aborted'
C           RETURN
C       ENDIF
C       DO 10 K=1,N
C           S=0.0
C           DO 15 P=1,K-1
C               S=S+A(K,P)*A(K,P)
15          CONTINUE
C           IF ((A(K,K)-S).LE.ZERO) GOTO 1000
C           A(K,K)=SQRT(A(K,K)-S)
c          if (a(k,k).lt.3.4e-3) print *, 'chol',k,a(k,k)
C           DO 20 I=K+1,N
C               S=0.0
C               DO 25 P=1,K-1
C                   S=S+A(I,P)*A(K,P)
25          CONTINUE
C           A(I,K)=(A(I,K)-S)/A(K,K)
20          CONTINUE
10          CONTINUE
C           GOTO 5000
1000         NSING=1
5000         CONTINUE
C           RETURN
C           END
C
C       Solve for y s.t. Ly=b, L n-by-n lower triangular. Overwrites b with y.
C
C       SUBROUTINE FORWARD(NDIM,N,L,B)
C       INTEGER NMAX
C       PARAMETER (NMAX=10)
C       INTEGER NDIM,N,I,J
C       REAL*8 L(NMAX,NMAX),B(NMAX)
C
C       DO 40 I=1,N

```

```

      DO 45 J=1,I-1
        B(I)=B(I)-L(I,J)*B(J)
45     CONTINUE
      B(I)=B(I)/L(I,I)
40     CONTINUE
      RETURN
      END

```

```

C
C Solve for x s.t. Ux=y, U n-by-n upper triangular. Overwrites y with x.
C

```

```

      SUBROUTINE BACKWARD(NDIM,N,U,Y)
      INTEGER NMAX,NRA,NRE,NSING
      PARAMETER (NMAX=10,HUGE=1.0E35)
      COMMON /CONTROL/ NRA,NRE,NSING
      INTEGER NDIM,N,I,J
      REAL*8 U(NMAX,NMAX),Y(NMAX)

```

```

C
      DO 50 I=N,1,-1
        DO 55 J=I+1,N
          Y(I)=Y(I)-U(I,J)*Y(J)
55     CONTINUE
        Y(I)=Y(I)/U(I,I)
        IF (ABS(Y(I)).GT.HUGE) THEN
          NSING=2
          GOTO 5000
        ENDIF

```

```

50     CONTINUE
5000    CONTINUE
      RETURN
      END

```

```

C
C
C

```

```

      SUBROUTINE TRANSPOSE(M,N,A,B)
      INTEGER NMAX
      PARAMETER (NMAX=10)
      INTEGER M,N,I,J
      REAL*8 A(NMAX,NMAX),B(NMAX,NMAX)

```

```

C
      DO 30 I=1,M
        DO 35 J=1,N
          B(J,I)=A(I,J)
35     CONTINUE
30     CONTINUE
      RETURN
      END

```

```

C
C
C

```

```

      SUBROUTINE LUDEC(NDIM,N,A)
      IMPLICIT REAL*8 (A-Z)
      INTEGER NDIM,N,NMAX,I,J,K,P,IPVT
      INTEGER NRA,NRE,NSING
      PARAMETER (ZERO=0.0,ONE=1.0,NMAX=10,TINY=1.0E-12)
      COMMON /CONTROL/ NRA,NRE,NSING
      COMMON /LUBLOC/ IPVT(NMAX)
      DIMENSION A(NMAX,NMAX),W(NMAX)

```

```

C
C This subroutine determines the LU decomposition
C of matrix A using partial pivoting. It is based on
C

```

C algorithm from Golub and von Loan. The subroutine returns  
 C the permutation vector IPVT(N) (used in LUSOLVE), and  
 C a unit lower triangular matrix in A(I>J) and an upper  
 C triangular matrix in A(I<=J).

```

C
IPVT(N)=1
DO 100 K=1,N-1
  P=K
  DO 200 I=K+1,N
    IF (ABS(A(I,K)).GT.ABS(A(P,K))) P=I
200  CONTINUE
  IPVT(K)=P
  IF (P.NE.K) IPVT(N)=-IPVT(N)
  IF (ABS(A(P,K)).LE.TINY) GOTO 1000
  DO 300 J=1,N
    T=A(P,J)
    A(P,J)=A(K,J)
    A(K,J)=T
    W(J)=T
300  CONTINUE
  DO 400 I=K+1,N
    T=A(I,K)/A(K,K)
    A(I,K)=T
    DO 500 J=K+1,N
      A(I,J)=A(I,J)-T*W(J)
500  CONTINUE
400  CONTINUE
100  CONTINUE
  DET=IPVT(N)
  DO 600 I=1,N
    DET=DET*A(I,I)
600  CONTINUE
  IF (ABS(DET).GT.TINY*TINY) GOTO 5000
1000 NSING=1
5000 CONTINUE
  RETURN
  END

```

C  
 C  
 C

```

SUBROUTINE LUSOLVE(NDIM,N,A,B)
  IMPLICIT REAL*8 (A-Z)
  INTEGER NDIM,N,NMAX,I,J,K,P,IPVT
  PARAMETER (ZERO=0.0,ONE=1.0,NMAX=10)
  COMMON /LUBLOC/ IPVT(NMAX)
  DIMENSION A(NMAX,NMAX),B(NMAX),DIAG(NMAX)

```

C  
 C  
 C  
 C  
 C

This subroutine solves the matrix equation  
 $PAx=Pb$ , where A is LU=PA from subroutine LUDEC.  
 It returns the value of x in B.

```

DO 100 K=1,N-1
  P=IPVT(K)
  T=B(P)
  B(P)=B(K)
  B(K)=T
100  CONTINUE
DO 200 I=1,N
  DIAG(I)=A(I,I)
  A(I,I)=ONE

```

```

200 CONTINUE
C
C     Ensure  $L=A(i>=j)$  is unit lower triangular, then
C     solve  $Ly=Pb$ .
C
CALL FORWARD(NDIM,N,A,B)
DO 300 I=1,N
    A(I,I)=DIAG(I)
300 CONTINUE
C
C     Ensure  $U=A(i<=j)$  is upper triangular again, then
C     solve  $Ux=y$ .
C
CALL BACKWARD(NDIM,N,A,B)
RETURN
END

C
C
C
SUBROUTINE MATMATRIX(N,M,A,NAM,NFIL)
IMPLICIT REAL*8 (A-Z)
INTEGER NMAX
PARAMETER (NMAX=10)
INTEGER N,M,I,J
DIMENSION A(NMAX,NMAX)
DOUBLE PRECISION X(NMAX,NMAX)
CHARACTER*4 NAM
CHARACTER*6 NFIL

C
C     This subroutine writes the matrix A to the MATRIXx data
C     file FILE.DAT in the subdirectory THESIS.
C
OPEN (1,FILE='[USER.AVF.CARLOS.THESIS]//NFIL,STATUS='NEW',
&      FORM='FORMATTED')
DO 100 I=1,N
    DO 200 J=1,M
        X(I,J)=A(I,J)
200 CONTINUE
100 CONTINUE
CALL MATSAV(1,NAM,NMAX,N,M,0,X,DUMMY,'(1P2E24.15)')
CLOSE (1)
RETURN
END

C
C
C
SUBROUTINE WRMATRIX(N,M,A,NAM,NFIL)
IMPLICIT REAL*8 (A-Z)
INTEGER NMAX
PARAMETER (NMAX=10)
INTEGER N,M,I,J
DIMENSION A(NMAX,NMAX)
CHARACTER*4 NAM
CHARACTER*6 NFIL

C
C     This subroutine writes the matrix A to the ouput file
C     FILE.DAT in the subdirectory THESIS.
C
OPEN (1,FILE='[USER.AVF.CARLOS.THESIS]//NFIL,STATUS='NEW',
&      FORM='FORMATTED')

```

```
WRITE (1,1100) NAM,N,M
DO 100 I=1,N
  WRITE (1,1000) I,(A(I,J),J=1,INT(M/2))
  WRITE (1,1000) I,(A(I,J),J=M-INT(M/2)+1,M)
100 CONTINUE
1000 FORMAT (I3,<M/2>(D18.10))
1100 FORMAT (' MATRIX ',A4,'(',I2,' BY',I3,')')
CLOSE (1)
RETURN
END
```

```
C*****
C*****
C      This file contains INCLUDE commands that ensures all the
C      necessary files are compiled in order to solve the ODE's for
C      the two-link flex. arm using Runge-Kutta fourth order with
C      variable step-size. (See Numerica Recipes for reference.)
C      This was written as part of the simulation package for
C      Carlos E. Padilla's M.S. thesis.
C      DOUBLE PRECISION version.
C*****
C*****
      INCLUDE '[USER.AVF.CARLOS.FORTRAN]DRK4.FOR'
      INCLUDE '[USER.AVF.CARLOS.FORTRAN]DRKQC.FOR'
      INCLUDE '[USER.AVF.CARLOS.FORTRAN]DODEINT.FOR'
```

```

SUBROUTINE OEINT(YSTART,NVAR,X1,X2,EPS,H1,HMIN,NOK,NBAD)
  IMPLICIT INTEGER (I-N)
  IMPLICIT REAL*8 (A-H,O-Z)
  PARAMETER (MAXSTP=35000,NMAX=24,TWO=2.0,ZERO=0.0,TINY=1.D-30,
&           API=3.141592654)
  COMMON /PATH/ KMAX,KOUNT,DXSAV,XP(500),YP(24,500),HP(500),EP(500)
  COMMON /PATH/ SM(500,15),DHP(500),DOR(2,500),SFOR(500),STIC(500)
  COMMON /ENER/ SME(10,10)
  COMMON /CONTROL/ NFORE,NANG,NSING
  COMMON /PROP/ N,M
  COMMON /DIAG/ HSAV,TSAV
  COMMON /BUG/ TRA,TRE,TRI,TRO,TRU,CRA,NRE,CRI,CRO
  COMMON /BUG/ MCOUNT,YW(NMAX)
  COMMON /OUS/ FORT(12,4)
  DIMENSION YSTART(NMAX),YSCAL(NMAX),Y(NMAX),DYDX(NMAX),TOR(2)
  X=X1
  H=SIGN(H1,X2-X1)
  XFRAC=0.0
  XSTE=(X2-X1)/10.0
  NCHECK=0
  MPREV=0
  NOK=0
  NBAD=0
  KOUNT=0
  NR=2+N+M
  NSING=0
  YMAX=ZERO
  DO 11 I=1,NVAR
    Y(I)=YSTART(I)
11  CONTINUE
  XSAV=X-DXSAV*TWO
  DO 10 NSTP=1,MAXSTP
    IF (X.GE.XFRAC) THEN
      PRINT *, 'Current time:',x,'out of:',x2
      XFRAC=XFRAC+XSTE
    ENDIF
    IF (NSTP.GE.NCHECK) THEN
      PRINT *, '# of steps so far:',NSTP,' HMIN exceeds:',MCOUNT
      MDIF=MCOUNT-MPREV
      MPREV=MCOUNT
      NCHECK=NCHECK+1000
      IF (1000-MDIF.LE.300) THEN
        NSING=14
        PRINT *, 'HMIN exceeds 70% of last 1000 steps taken.'
        print *, 'yscal=',yscal
        print *, 'y=',y
        GOTO 5000
      ENDIF
    ENDIF
    CALL DERIVS(X,Y,DYDX)
    IF(NSING.NE.0) GOTO 5000
c   DO 300 I=1,NVAR
c     IF ((I.GT.2).AND.(I.NE.NR+1).AND.(I.NE.NR+2)) THEN
c       IF ((ABS(Y(I))+ABS(H*DYDX(I))).GT.YMAX) THEN
c         YMAX=ABS(Y(I))+ABS(H*DYDX(I))+TINY
c       ENDIF
c     ENDIF
c 300 CONTINUE
  DO 12 I=1,NVAR
    IF ((I.GT.2).AND.(I.NE.NR+1).AND.(I.NE.NR+2)) THEN

```

```

c      IF (I.NE.(1+2*NR)) THEN
          YSCAL(I)=ABS(Y(I))+ABS(H*DYDX(I))+TINY
      ELSE
c      IF (ABS(Y(I)).GT.API) THEN
          YSCAL(I)=ABS(Y(I))+ABS(H*DYDX(I))+TINY
c      ELSE
c      YSCAL(I)=API
c      ENDIF
      ENDIF
C
12     CONTINUE
      IF(KMAX.GT.0)THEN
          IF(ABS(X-XSAV).GT.ABS(DXSAV)) THEN
              IF(KOUNT.LT.KMAX-1)THEN
                  KOUNT=KOUNT+1
                  XP(KOUNT)=X
                  DO 13 I=1,NVAR
                      YP(I,KOUNT)=Y(I)
13             CONTINUE
                      IF(NANG.EQ.1) THEN
                          SFOR(KOUNT)=FORT(2,1)
                          CALL AMOMENTUM(X,Y,AMOM,DAM)
                          CALL ENERGY(Y,ENER)
                          CALL FORCING(X,Y,TOR)
                          CALL STABCHK(Y,DYDX,STAB)
                          DOR(1,KOUNT)=TOR(1)
                          DOR(2,KOUNT)=TOR(2)
                          HP(KOUNT)=AMOM
                          DHP(KOUNT)=DAM
                          EP(KOUNT)=ENER
                          STIC(KOUNT)=STAB
c                          SM(KOUNT,1)=SME(1,1)
c                          SM(KOUNT,2)=SME(2,1)
c                          SM(KOUNT,3)=SME(3,1)
c                          SM(KOUNT,4)=SME(3,2)
c                          SM(KOUNT,5)=SME(3,3)
c                          SM(KOUNT,6)=SME(4,1)
c                          SM(KOUNT,7)=SME(4,2)
c                          SM(KOUNT,8)=SME(4,3)
c                          SM(KOUNT,9)=SME(4,4)
c                          SM(KOUNT,10)=SME(5,1)
c                          SM(KOUNT,11)=SME(5,3)
c                          SM(KOUNT,12)=SME(5,4)
c                          SM(KOUNT,13)=SME(6,1)
c                          SM(KOUNT,14)=SME(6,3)
c                          SM(KOUNT,15)=SME(6,4)
                      ENDIF
                      XSAV=X
                  ENDIF
              ENDIF
          ENDIF
          IF((X+H-X2)*(X+H-X1).GT.ZERO) H=X2-X
          CALL RKQC(Y,DYDX,NVAR,X,H,EPS,YSCAL,HDID,HNEXT)
          IF(NSING.NE.0) THEN
              print *, 'yscal', yscal
              GOTO 5000
          ENDIF
          IF(HDID.EQ.H)THEN
              NOK=NOK+1
          ELSE

```



```

      NBAD=NBAD+1
    ENDIF
    DO 100 I=1,NVAR
      YW(I)=Y(I)
100  CONTINUE
      IF((X-X2)*(X2-X1).GE.ZERO)THEN
        DO 14 I=1,NVAR
          YSTART(I)=Y(I)
14  CONTINUE
          IF(KMAX.NE.0)THEN
            KOUNT=KOUNT+1
            XP(KOUNT)=X
            DO 15 I=1,NVAR
              YP(I,KOUNT)=Y(I)
15  CONTINUE
              IF(NANG.EQ.1) THEN
                SFOR(KOUNT)=FORT(2,1)
                CALL AMOMENTUM(X,Y,AMOM,DAM)
                CALL ENERGY(Y,ENER)
                CALL FORCING(X,Y,TOR)
                CALL STABCHK(Y,DYDX,STAB)
                DOR(1,KOUNT)=TOR(1)
                DOR(2,KOUNT)=TOR(2)
                HP(KOUNT)=AMOM
                DHP(KOUNT)=DAM
                EP(KOUNT)=ENER
                STIC(KOUNT)=STAB
                C      SM(KOUNT,1)=SME(1,1)
                C      SM(KOUNT,2)=SME(2,1)
                C      SM(KOUNT,3)=SME(3,1)
                C      SM(KOUNT,4)=SME(3,2)
                C      SM(KOUNT,5)=SME(3,3)
                C      SM(KOUNT,6)=SME(4,1)
                C      SM(KOUNT,7)=SME(4,2)
                C      SM(KOUNT,8)=SME(4,3)
                C      SM(KOUNT,9)=SME(4,4)
                C      SM(KOUNT,10)=SME(5,1)
                C      SM(KOUNT,11)=SME(5,3)
                C      SM(KOUNT,12)=SME(5,4)
                C      SM(KOUNT,13)=SME(6,1)
                C      SM(KOUNT,14)=SME(6,3)
                C      SM(KOUNT,15)=SME(6,4)
              ENDIF
            ENDIF
            HSAV=H
            TSAV=X
            RETURN
          ENDIF
          IF (ABS(HNEXT).LT.HMIN) THEN
            HNEXT=HMIN
            MCOUNT=MCOUNT+1
          ENDIF
          C      IF(ABS(HNEXT).LT.HMIN) GOTO 1000
          H=HNEXT
16  CONTINUE
          PAUSE 'Too many steps.'
          GOTO 5000
1000 PAUSE 'Stepsize smaller than minimum.'
5000 CONTINUE
      HSAV=HNEXT

```

TSAV=X

DO 200 I=1,NVAR

YW(I)=Y(I)

200 CONTINUE

RETURN

END

```

SUBROUTINE RKQC(Y,DYDX,N,X,HTRY, EPS, YSCAL, HDID, HNEXT)
  IMPLICIT INTEGER (I-N)
  IMPLICIT REAL*8 (A-H,O-Z)
  PARAMETER (NMAX=24,FCOR=.0666666667,PGROW=0.20,PSHRNK=0.25,
  * ONE=1.,SAFETY=0.9,ERRCON=6.D-4)
  EXTERNAL DERIVS
  COMMON /CONTROL/ NRA,NRE,NSING
  COMMON /DIA2/ NCO
  DIMENSION Y(NMAX),DYDX(NMAX),YSCAL(NMAX)
  DIMENSION YTEMP(NMAX),YSAV(NMAX),DYSAV(NMAX)
C   PGROW=0.20
C   PSHRNK=0.25
  XSAV=X
  DO 11 I=1,N
    YSAV(I)=Y(I)
    DYSAV(I)=DYDX(I)
11  CONTINUE
  H=HTRY
  NCO=0
1   HH=0.5*H
  CALL RK4(YSAV,DYSAV,N,XSAV,HH,YTEMP,DERIVS)
  IF(NSING.NE.0) THEN
    NSING=NSING+3
    GOTO 5000
  ENDIF
  X=XSAV+HH
  CALL DERIVS(X,YTEMP,DYDX)
  IF(NSING.NE.0) THEN
    NSING=3
    GOTO 5000
  ENDIF
  CALL RK4(YTEMP,DYDX,N,X,HH,Y,DERIVS)
  IF(NSING.NE.0) THEN
    NSING=NSING+6
    GOTO 5000
  ENDIF
  X=XSAV+H
  IF(X.EQ.XSAV) GOTO 1000
  CALL RK4(YSAV,DYSAV,N,XSAV,H,YTEMP,DERIVS)
  IF(NSING.NE.0) THEN
    NSING=NSING+9
    GOTO 5000
  ENDIF
  ERRMAX=0.
  DO 12 I=1,N
    YTEMP(I)=Y(I)-YTEMP(I)
    ERRMAX=MAX(ERRMAX,ABS(YTEMP(I)/YSCAL(I)))
12  CONTINUE
  ERRMAX=ERRMAX/EPS
  IF(ERRMAX.GT.ONE) THEN
    H=SAFETY*H*(ERRMAX**PSHRNK)
    NCO=NCO+1
    GOTO 1
  ELSE
    HDID=H
    IF(ERRMAX.GT.ERRCON)THEN
      HNEXT=SAFETY*H*(ERRMAX**PGROW)
    ELSE
      HNEXT=4.*H
    ENDIF
  
```

```
ENDIF
DO 13 I=1,N
  Y(I)=Y(I)+YTEMP(I)*FCOR
13 CONTINUE
GOTO 5000
1000 PAUSE 'Stepsize not significant in RKQC.'
5000 CONTINUE
RETURN
END
```

```

SUBROUTINE RK4(Y,DYDX,N,X,H,YOUT,DERIVS)
  IMPLICIT INTEGER (I-N)
  IMPLICIT REAL*8 (A-H,O-Z)
  PARAMETER (NMAX=24)
  COMMON /CONTROL/ NRA,NRE,NSING
  DIMENSION Y(NMAX),DYDX(NMAX),YOUT(NMAX)
  DIMENSION YT(NMAX),DYT(NMAX),DYM(NMAX)
  HH=H*0.5
  H6=H/6.
  XH=X+HH
  DO 11 I=1,N
    YT(I)=Y(I)+HH*DYDX(I)
11  CONTINUE
    CALL DERIVS(XH,YT,DYT)
    IF(NSING.NE.0) THEN
      NSING=1
      GOTO 5000
    ENDIF
    DO 12 I=1,N
      YT(I)=Y(I)+HH*DYT(I)
12  CONTINUE
      CALL DERIVS(XH,YT,DYM)
      IF(NSING.NE.0) THEN
        NSING=2
        GOTO 5000
      ENDIF
      DO 13 I=1,N
        YT(I)=Y(I)+H*DYM(I)
        DYM(I)=DYT(I)+DYM(I)
13  CONTINUE
        CALL DERIVS(X+H,YT,DYT)
        IF(NSING.NE.0) THEN
          print *,'rk4 x and h:',x,h
          print *,'rk4 state vector:',yt
          NSING=3
          GOTO 5000
        ENDIF
        DO 14 I=1,N
          YOUT(I)=Y(I)+H6*(DYDX(I)+DYT(I)+2.*DYM(I))
14  CONTINUE
5000 CONTINUE
      RETURN
      END

```

```
C.....
C.....
C      This file contains the INCLUDE commands that ensures that
C      the appropriate files are compiled for solving the ODE's for
C      the two-link flex. arm simulation using Runge-Kutta fourth order
C      with no variable step size. This was written as part of the
C      simulation package for Carlos E. Padilla's M.S. thesis.
C      DOUBLE PRECISION version.
C.....
C.....
      INCLUDE '[USER.AVF.CARLOS.FORTRAN]DRK4.FOR'
      INCLUDE '[USER.AVF.CARLOS.FORTRAN]DRKDUMB.FOR'
```

```

SUBROUTINE RKDUMB(VSTART,NVAR,X1,X2,NSTEP)
  IMPLICIT INTEGER (I-N)
  IMPLICIT REAL*8 (A-H,O-Z)
  PARAMETER (ZERO=0.0,TWO=2.0,NMAX=24)
  COMMON /PROP/ N,M
  COMMON /PATH/ KMAX,KOUNT,DXSAV,XP(500),YP(24,500),HP(500),EP(500)
  COMMON /PATH/ SM(500,15),DHP(500),DOR(2,500),SFOR(500)
  COMMON /ENER/ SME(10,10)
  COMMON /CONTROL/ NFORE,NANG,NSING
  COMMON /DIAG/ HSAV,TSAV
  COMMON /BUG/ TRA,TRE,TRI,TRO,TRU,CRA,NRE,CRI,CRO
  COMMON /BUG/ MCOUNT,YW(NMAX)
  COMMON /OUS/ FORT(12,4)
  DIMENSION VSTART(NVAR),V(NMAX),DV(NMAX),TOR(2)
  KOUNT=0
  DO 10 I=1,NVAR
    V(I)=VSTART(I)
10  CONTINUE
  X=X1
  XSAV=X-DXSAV*TWO
  H=(X2-X1)/NSTEP
  XFRAC=0.0
  XSTE=(X2-X1)/10.0
  NCHECK=0
  NSING=0
  NR=2+H*M
  DO 13 K=1,NSTEP
    IF (X.GE.XFRAC) THEN
      PRINT *, 'Current time:',x, 'out of:',x2
      XFRAC=XFRAC+XSTE
    ENDIF
    IF (K.GE.NCHECK) THEN
      PRINT *, '# of steps so far:',K
      NCHECK=NCHECK+1000
    ENDIF
    CALL DERIVS(X,V,DV)
    IF (NSING.NE.0) GOTO 5000
    IF (KMAX.GT.0) THEN
      IF (ABS(X-XSAV).GT.ABS(DXSAV)) THEN
        IF (KOUNT.LT.KMAX-1) THEN
          KOUNT=KOUNT+1
          XP(KOUNT)=X
          DO 11 I=1,NVAR
            YP(I,KOUNT)=V(I)
11          CONTINUE
          IF (NANG.EQ.1) THEN
            SFOR(KOUNT)=FORT(2,1)
            CALL AMOMENTUM(X,V,AMOM,DAM)
            CALL ENERGY(V,ENER)
            CALL FORCING(X,V,TOR)
            DOR(1,KOUNT)=TOR(1)
            DOR(2,KOUNT)=TOR(2)
            HP(KOUNT)=AMOM
            DHP(KOUNT)=DAM
            EP(KOUNT)=ENER
            SM(KOUNT,1)=SME(1,1)
            SM(KOUNT,2)=SME(2,1)
            SM(KOUNT,3)=SME(3,1)
            SM(KOUNT,4)=SME(3,2)
            SM(KOUNT,5)=SME(3,3)
          ENDIF
        ENDIF
      ENDIF
    ENDIF
  END DO

```

```

        SM(KOUNT,6)=SME(4,1)
        SM(KOUNT,7)=SME(4,2)
        SM(KOUNT,8)=SME(4,3)
        SM(KOUNT,9)=SME(4,4)
        SM(KOUNT,10)=SME(5,1)
        SM(KOUNT,11)=SME(5,3)
        SM(KOUNT,12)=SME(5,4)
        SM(KOUNT,13)=SME(6,1)
        SM(KOUNT,14)=SME(6,3)
        SM(KOUNT,15)=SME(6,4)
    ENDIF
    XSAV=X
  ENDIF
ENDIF
ENDIF
CALL RK4(V,DV,NVAR,X,H,V,DERIVS)
IF (NSING.NE.0) GOTO 5000
IF(X+H.EQ.X)PAUSE 'Stepsize not significant in RKDUMB.'
TSAV=X
IF (K.EQ.NSTEP)THEN
  KOUNT=KOUNT+1
  XP(KOUNT)=X
  DO 12 I=1,NVAR
    YP(I,KOUNT)=V(I)
12  CONTINUE
    IF(NANG.EQ.1) THEN
      SFOR(KOUNT)=FORT(2,1)
      CALL AMOMENTUM(X,V,AMOM,DAM)
      CALL ENERGY(V,ENER)
      CALL FORCING(X,V,TOR)
      DOR(1,KOUNT)=TOR(1)
      DOR(2,KOUNT)=TOR(2)
      HP(KOUNT)=AMOM
      DHP(KOUNT)=DAM
      EP(KOUNT)=ENER
      SM(KOUNT,1)=SME(1,1)
      SM(KOUNT,2)=SME(2,1)
      SM(KOUNT,3)=SME(3,1)
      SM(KOUNT,4)=SME(3,2)
      SM(KOUNT,5)=SME(3,3)
      SM(KOUNT,6)=SME(4,1)
      SM(KOUNT,7)=SME(4,2)
      SM(KOUNT,8)=SME(4,3)
      SM(KOUNT,9)=SME(4,4)
      SM(KOUNT,10)=SME(5,1)
      SM(KOUNT,11)=SME(5,3)
      SM(KOUNT,12)=SME(5,4)
      SM(KOUNT,13)=SME(6,1)
      SM(KOUNT,14)=SME(6,3)
      SM(KOUNT,15)=SME(6,4)
    ENDIF
  ENDIF
  X=X+H
13  CONTINUE
5000 CONTINUE
  TSAV=X
  DO 100 I=1,NVAR
    YW(I)=V(I)
100  CONTINUE
  RETURN

```



END

```

C.....
C.....
C      This file contains the routine that determines the form of
C      the forcing functions for the two-link flex. arm simulation.
C      That is, it determines the joint torques. This was written by
C      Carlos E. Padilla as part of his M.S. thesis work.
C      DOUBLE PRECISION version.
C.....
C.....
      SUBROUTINE FORCING(T,Y,TOR)
      IMPLICIT REAL*8 (A-Z)
      INTEGER N,M,I,J,NMAX,NR,FORE,ANGMO,SING,RLINE,SRLINE
      PARAMETER (ZERO=0.0,NMAX=4,PI=3.141592654)
      COMMON /CONTROL/ FORE,ANGMO,SING,RLINE
      COMMON /PROP/ N,M

C
C      This subroutine determines the joint torques given the
C      time T and the state vector Y (for use in feedback control
C      laws). The values of the torques are returned in TOR(2).
C
      COMMON /FORC/ A0,A1,A2,A3,A4,A5,B0,B1,B2,B3,B4,B5

C
C      The above common block is for use in this subroutine ex-
C      clusively to avoid recalculation of constants.
C
      DIMENSION Y(8+4*NMAX),YD(8+4*NMAX),TOR(2),DUM(2)
      DIMENSION MD(2+2*NMAX,2+2*NMAX),BD(2+2*NMAX)

C
      NR=2+N*M

C
      X=-1.0

C
      If x .lt. zero, the mass matrix is not updated.
C
      X=1.0
      DUM(1)=ZERO
      DUM(2)=ZERO

C
C      The following variable determines the time scaling of the
C      trajectory.
C
      AL=2.0

C
C      The following assumes angular rates and accelerations
C      are desired zero at t=0 and t=tf.
C
      IF (T.EQ.ZERO) THEN
          THEI=0.0
          THEF=PI
          BEI=0.0873
          BEF=0.0
          TF=8.0
          TF2=TF*TF
          TF3=TF*TF2
          TF4=TF*TF3
          TF5=TF*TF4
          A0=THEI
          A1=ZERO
          A2=ZERO
          A3=(20.*THEF-20.*THEI)/(2.*TF3)

```

```

A4=(30.*HEI-30.*HEI)/(2.*TF4)
A5=(12.*THEF-12.*THEI)/(2.*TF5)
B0=BEI
B1=ZERO
B2=ZERO
B3=(20.*BEF-20.*BEI)/(2.*TF3)
B4=(30.*BEI-30.*BEF)/(2.*TF4)
B5=(12.*BEF-12.*BEI)/(2.*TF5)
ENDIF
TA=AL*T
TA2=TA*TA
TA3=TA*TA2
TA4=TA*TA3
TA5=TA*TA4
IF (TA.LE.TF) THEN
  YD(1)=A0+A1*TA+A2*TA2+A3*TA3+A4*TA4+A5*TA5
  YD(2)=B0+B1*TA+B2*TA2+B3*TA3+B4*TA4+B5*TA5
  YD(1+NR)=AL*(A1+2.*A2*TA+3.*A3*TA2+4.*A4*TA3+5.*A5*TA4)
  YD(2+NR)=AL*(B1+2.*B2*TA+3.*B3*TA2+4.*B4*TA3+5.*B5*TA4)
  AC1=AL*AL*(2.*A2+6.*A3*TA+12.*A4*TA2+20.*A5*TA3)
  AC2=AL*AL*(2.*B2+6.*B3*TA+12.*B4*TA2+20.*B5*TA3)
  THETA=YD(1)
  BETA=YD(2)
ELSE
  YD(1)=THETA
  YD(2)=BETA
  YD(1+NR)=ZERO
  YD(2+NR)=ZERO
  AC1=ZERO
  AC2=ZERO
ENDIF
DO 100 I=1,N
  YD(2+I)=zero
  YD(2+NR+I)=zero
100 CONTINUE
DO 200 J=1,M
  YD(2+N+J)=zero
  YD(2+NR+N+J)=zero
200 CONTINUE
C
CALL UPDATE(X,YD,DUM,MD,BD)
TOR(1)=MD(1,1)*AC1+MD(1,2)*AC2-BD(1)
TOR(2)=MD(2,1)*AC1+MD(2,2)*AC2-BD(2)
C
RETURN
END
C
C
C

```

```

C*****
C*****
C      This file contains the routine that determines the form of
C      the forcing functions for the two-link flex. arm simulation.
C      That is, it determines the joint torques. This was written by
C      Carlos E. Padilla as part of his M.S. thesis work.
C      DOUBLE PRECISION version.
C*****
C*****
      SUBROUTINE FORCING(T,Y,TOR)
      IMPLICIT REAL*8 (A-Z)
      INTEGER N,M,I,J,NMAX,NR,FORE,ANGMO,SING,RLINE,SRLINE
      PARAMETER (ZERO=0.0,NMAX=4,PI=3.141592654)
      COMMON /CONTROL/ FORE,ANGMO,SING,RLINE
      COMMON /PROP/ N,M
C
C      This subroutine determines the joint torques given the
C      time T and the state vector Y (for use in feedback control
C      laws). The values of the torques are returned in TOR(2).
C
      COMMON /FORC/ A0,A1,A2,A3,A4,A5,B0,B1,B2,B3,B4,B5
C
C      The above common block is for use in this subroutine ex-
C      clusively to avoid recalculation of constants.
C
      DIMENSION Y(8+4*NMAX),YD(8+4*NMAX),TOR(2),DUM(2)
      DIMENSION MD(2+2*NMAX,2+2*NMAX),BD(2+2*NMAX)
C
      NR=2+N*M
C
      X=-1.0
C
      If x .lt. zero, the mass matrix is not updated.
C
      X=1.0
      DUM(1)=ZERO
      DUM(2)=ZERO
C
      The following variable determines the time scaling of the
      trajectory.
C
      AL=2.0
C
      The following assumes angular rates and accelerations
      are desired zero at t=0 and t=tf.
C
      IF (T.EQ.ZERO) THEN
          THEI=-1.570796
          THEF=0.2617994
          BEI=2.967060
          BEF=0.8726646
          TF=4.0
          TF2=TF*TF
          TF3=TF*TF2
          TF4=TF*TF3
          TF5=TF*TF4
          A0=THEI
          A1=ZERO
          A2=ZERO
          A3=(20.*THEF-20.*THEI)/(2.*TF3)

```

```

A4=(30.*THEI-30.*THEF)/(2.*TF4)
A5=(12.*THEF-12.*THEI)/(2.*TF5)
B0=BEI
B1=ZERO
B2=ZERO
B3=(20.*BEF-20.*BEI)/(2.*TF3)
B4=(30.*BEI-30.*BEF)/(2.*TF4)
B5=(12.*BEF-12.*BEI)/(2.*TF5)
ENDIF
TA=AL*T
TA2=TA*TA
TA3=TA*TA2
TA4=TA*TA3
TA5=TA*TA4
IF (TA.LE.TF) THEN
  YD(1)=A0+A1*TA+A2*TA2+A3*TA3+A4*TA4+A5*TA5
  YD(2)=B0+B1*TA+B2*TA2+B3*TA3+B4*TA4+B5*TA5
  YD(1+NR)=AL*(A1+2.*A2*TA+3.*A3*TA2+4.*A4*TA3+5.*A5*TA4)
  YD(2+NR)=AL*(B1+2.*B2*TA+3.*B3*TA2+4.*B4*TA3+5.*B5*TA4)
  AC1=AL*AL*(2.*A2+6.*A3*TA+12.*A4*TA2+20.*A5*TA3)
  AC2=AL*AL*(2.*B2+6.*B3*TA+12.*B4*TA2+20.*B5*TA3)
  THETA=YD(1)
  BETA=YD(2)
ELSE
  YD(1)=THETA
  YD(2)=BETA
  YD(1+NR)=ZERO
  YD(2+NR)=ZERO
  AC1=ZERO
  AC2=ZERO
ENDIF
DO 100 I=1,N
  YD(2+I)=zero
  YD(2+NR+I)=zero
100 CONTINUE
DO 200 J=1,M
  YD(2+NR+J)=zero
  YD(2+NR+NR+J)=zero
200 CONTINUE
C
CALL UPDATE(X,YD,DUM,MD,BD)
TOR(1)=MD(1,1)*AC1+MD(1,2)*AC2-BD(1)
TOR(2)=MD(2,1)*AC1+MD(2,2)*AC2-BD(2)
C
RETURN
END
C
C
C

```

```

C*****
C*****
C      This file contains the routine that determines the form of
C      the forcing functions for the two-link flex. arm simulation.
C      That is, it determines the joint torques. This was written by
C      Carlos E. Padilla as part of his M.S. thesis work.
C      DOUBLE PRECISION version.
C*****
C*****
      SUBROUTINE FORCING(T,Y,TOR)
      IMPLICIT REAL*8 (A-Z)
      INTEGER N,M,I,J,NMAX,NR,FORE,ANGMO,SING,RLINE,SRLINE
      PARAMETER (ZERO=0.0,NMAX=4,PI=3.141592654)
      COMMON /CONTROL/ FORE,ANGMO,SING,RLINE
      COMMON /PROP/ N,M

C
C      This common block is for use in this subroutine exclusively,
C      in order to prevent repetition of constants from call to call.
C
C      COMMON /FSAVE/ BESAVE,OMSAVE,TSAVE,IB,MB,LB

C      This subroutine determines the joint torques given the
C      time T and the state vector Y (for use in feedback control
C      laws). The values of the torques are returned in TOR(2).
C
      DIMENSION Y(8+4*NMAX),YD(8+4*NMAX),TOR(2),DUM(2)
      DIMENSION MD(2+2*NMAX,2+2*NMAX),BD(2+2*NMAX)

C
      NR=2+N+M

C
      X=-1.0

C      If x .lt. zero, the mass matrix is not updated.
C
      X=1.0
      TORM1=1.5
      SCAL1=SQRT(1.0/(TORM1/15.962871))
      TORM2=(TORM1/(15.962871+1.9225763))*1.9225768
      SCAL2=SCAL1
      INC=1.2

C
C      Switch control of shoulder torque.
C
      TS1=1.13*SCAL1*INC
      TS2=1.44*SCAL1*INC
      TS3=1.77*SCAL1*INC
      TF1=2.91*SCAL1*INC
      IF (T.LE.TS1) THEN
        TOR(1)=-TORM1
      ELSE
        IF (T.LE.TS2) THEN
          TOR(1)=TORM1
        ELSE
          IF (T.LE.TS3) THEN
            TOR(1)=-TORM1
          ELSE
            IF (T.LE.TF1) THEN
              TOR(1)=TORM1
            ELSE
              TOR(1)=ZERO
            
```

```
ENDIF
ENDIF
ENDIF
ENDIF
```

```
C
C
C
```

```
Switch control of elbow torque.
```

```
TE1=1.42*SCAL2*INC
TF2=2.84*SCAL2*INC
IF (T.LE.TE1) THEN
TOR(2)=TORM2
```

```
ELSE
IF (T.LE.TF2) THEN
TOR(2)=-TORM2
ELSE
TOR(2)=ZERO
```

```
ENDIF
ENDIF
print *,t,tor(1),tor(2)
tor(1)=zero
tor(1)=zero
```

```
C
c
e
C
```

```
RETURN
END
```

```
C
C
C
```

```

C*****
C      This file contains the routine that determines the form of
C      the forcing functions for the two-link flex. arm simulation.
C      That is, it determines the joint torques. This was written by
C      Carlos E. Padilla as part of his M.S. thesis work.
C      DOUBLE PRECISION version.
C*****
C*****
      SUBROUTINE FORCING(T,Y,TOR)
      IMPLICIT REAL*8 (A-Z)
      INTEGER N,M,I,J,NMAX,NR,FORE,ANGMO,SING,RLINE,SRLINE
      PARAMETER (ZERO=0.0,NMAX=4,PI=3.141592654)
      COMMON /CONTROL/ FORE,ANGMO,SING,RLINE
      COMMON /PROP/ N,M

C
C      This common block is for use in this subroutine exclusively,
C      in order to prevent repetition of constants from call to call.
C
C      COMMON /FSAVE/ BESAVE,OMSAVE,TSAVE,IB,MB,LB

C
C      This subroutine determines the joint torques given the
C      time T and the state vector Y (for use in feedback control
C      laws). The values of the torques are returned in TOR(2).
C
      DIMENSION Y(8+4*NMAX),YD(8+4*NMAX),TOR(2),DUM(2)
      DIMENSION MD(2+2*NMAX,2+2*NMAX),BD(2+2*NMAX)

C
C      This forcing scheme is used to do smooth spin-up maneuver of elbow
C      link with "Kane's" formula. Two statements in DARMSEC.FOR are
C      used to freeze the shoulder angle.
C
      NR=2+N*M

C
C      X=-1.0

C
C      If x .lt. zero, the mass matrix is not updated.
C
      DUM(1)=ZERO
      DUM(2)=ZERO
      X=1.0
      BEI=0.0
      TF=15.0
      OMF=6.0
      OM=2.0*PI/TF
      FAC=OMF/TF
      IF (T.LE.TF) THEN
        YD(2)=FAC*(T*T/2.+1./(OM*OM)*(COS(OM*T)-1.))+BEI
        YD(2+NR)=FAC*(T-1./OM*SIN(OM*T))
        AC2=FAC*(1.-COS(OM*T))
        BETA=YD(2)
        TB=T
      ELSE
        YD(2)=OMF*T+BETA-OMF*TB
        YD(2+NR)=OMF
        AC2=ZERO
      ENDIF
      YD(1)=ZERO
      YD(1+NR)=ZERO

```



```
AC1=ZERO
DO 100 I=1,N
  YD(2+I)=ZERO
  YD(2+NR+I)=ZERO
100 CONTINUE
DO 200 I=1,M
  YD(2+NI)=ZERO
  YD(2+NR+NI)=ZERO
200 CONTINUE
CALL UPDATE(X,YD,DUM,MD,BD)
TOR(1)=MD(1,1)*AC1+MD(1,2)*AC2-BD(1)
TOR(2)=MD(2,1)*AC1+MD(2,2)*AC2-BD(2)

C
RETURN
END

C
C
C
```

```

C*****
C*****
C      This FORTRAN program acts as a post-processor for the
C      tabulated data from the two-link flex. arm simulation. It was
C      written by Carlos E. Padilla as part of his M.S. thesis work in
C      order to prepare data to be transferred to an IBM PC to be
C      used in a graphics demonstration of the arm motion.
C      This program takes raw data from the file DATFILE.DAT and
C      translates it into BASIC compatible data in the file ARMGAT.DAT
C      which is transferred to the PC.
C*****
C*****
      INCLUDE '[USER.AVF.CARLOS.FORTRAN]CMODES.FOR'
C
C      FAC establishes the scaling of the flex. deflections
C      for max. visibility in graphics animation.
C
      PROGRAM POST_PROCESS
      PARAMETER (ZERO=0.0,NMAX=4,FAC=1.0,SCAP=1.0)
      IMPLICIT REAL (A-Z)
      INTEGER N,M,KOUNT,I,J,K,NR
      DIMENSION T(500),YP(20,500),XR(20),YR(20),X2R(20),Y2R(20)
      DIMENSION LA(NMAX),BI(NMAX),PHI(NMAX,4),SI(NMAX)
      OPEN (1,FILE='[USER.AVF.CARLOS.THESIS]DATFILE',STATUS='OLD',
&        FORM='FORMATTED')
      OPEN (3,FILE='[USER.AVF.CARLOS.GRAF]ARMGAT',STATUS='NEW',
&        FORM='FORMATTED')
C
C      Read in data from DATFILE.DAT.
C
      READ(1,*)N,M,KOUNT,L1,L2
      READ(1,*)M1,M2A,M2B,M3
      READ(1,*)LA(1),LA(2),LA(3),LA(4)
      NR=2+N*M
      DO 100 I=1,KOUNT
        READ(1,*)T(I),YP(1,I),YP(2,I)
        DO 200 J=1,N
          READ(1,*)YP(2+J,I),YP(2+NR+J,I)
200      CONTINUE
        DO 300 J=1,M
          READ(1,*)YP(2+N+J,I),YP(2+NR+N+J,I)
300      CONTINUE
100      CONTINUE
      CLOSE (1)
C
C      Manipulate data.
C
      XC=0.
      YC=0.
      LENG=1.5
      M2=M2A+M2B
      CH=M1
      IF (M2.GT.CH) CH=M2
      IF (M3.GT.CH) CH=M3
      IF (CH.EQ.ZERO) THEN
        R1=.025
        R2=.025
        R3=.025
      ELSE
c      Changed from .25 to .13 on Jan. 11,1989.

```

```

MR=.13/CH
R1=MR*M1
IF (R1.EQ.ZERO) R1=.025
R2=MR*M2
R3=MR*M3
IF (R3.LE.0.025) R3=.025
ENDIF
CH=L1
IF (L2.GT.CH) CH=L2
LR=1.0/CH
WRITE(3,*) FAC
WRITE(3,*) KOUNT,R1,R2,R3
DO 400 I=1,KOUNT
  STH=SIN(YP(1,I))
  CTH=COS(YP(1,I))
  AL=ZERO
  TY1=ZERO
  CALL CMODES(N,LA,L1,L1,BI,PHI,SI)
  DO 800 K=1,N
    AL=AL+SCAP*PHI(K,2)*YP(2+K,I)
    TY1=TY1+SCAP*PHI(K,1)*YP(2+K,I)
800  CONTINUE
    TY1=FAC*TY1
    AL=FAC*AL
    XR(20)=LR*(L1*CTH-TY1*STH)
    YR(20)=LR*(L1*STH+TY1*CTH)
    BETA=YP(1,I)+AL+YP(2,I)
    SBE=SIN(BETA)
    CBE=COS(BETA)
    AL2=ZERO
    TY2=ZERO
    CALL CMODES(M,LA,L2,L2,BI,PHI,SI)
    DO 900 K=1,M
      AL2=AL2+SCAP*PHI(K,2)*YP(2+M+K,I)
      TY2=TY2+SCAP*PHI(K,1)*YP(2+M+K,I)
900  CONTINUE
      TY2=FAC*TY2
      AL2=FAC*AL2
      X2R(20)=LR*(L2*CBE-TY2*SBE)
      Y2R(20)=LR*(L2*SBE+TY2*CBE)
      X=XC+R1*CTH
      Y=YC+R1*STH
      DLX=LENG*CTH
      DLY=LENG*STH
      DX1=1./20.*L1
      TX1=DX1
      DX2=1./20.*L2
      TX2=DX2
      DO 500 J=1,10
        CALL CMODES(N,LA,L1,TX1,BI,PHI,SI)
        TY1=ZERO
        DO 600 K=1,N
          TY1=TY1+SCAP*PHI(K,1)*YP(2+K,I)
600  CONTINUE
          TY1=FAC*TY1
          XR(J)=LR*(TX1*CTH-TY1*STH)
          YR(J)=LR*(TX1*STH+TY1*CTH)
          TX1=TX1+DX1
          CALL CMODES(M,LA,L2,TX2,BI,PHI,SI)
          TY2=ZERO

```

```

      DO 700 K=1,M
      TY2=TY2+SCAP*PHI(K,1)*YP(2+N+K,I)
700  CONTINUE
      TY2=FAC*TY2
      X2R(J)=LR*(TX2*CBE-TY2*SBE)
      Y2R(J)=LR*(TX2*SBE+TY2*CBE)
      TX2=TX2+DX2
500  CONTINUE
      XC2=X+XR(20)+R2*COS(YP(1,I)+AL)
      YC2=Y+YR(20)+R2*SIN(YP(1,I)+AL)
      X2=XC2+R2*CBE
      Y2=YC2+R2*SBE
      DLX2=LENG*CBE
      DLY2=LENG*SBE
      XC3=X2+X2R(20)+R3*COS(BETA+AL2)
      YC3=Y2+Y2R(20)+R3*SIN(BETA+AL2)
      WRITE(3,*)T(I)
      WRITE(3,*)X,Y,DLX,DLY
      WRITE(3,*)XC2,YC2,X2,Y2
      WRITE(3,*)DLX2,DLY2,XC3,YC3
      DO 1000 J=1,20
      WRITE(3,*)XR(J),YR(J),X2R(J),Y2R(J)
1000 CONTINUE
400  CONTINUE
      CLOSE (3)
      END

```

## PROGRAM ANIMATE\_ARM

C  
C This animation program is written by Carlos E. Padilla as part  
C of his M.S. thesis to enact an animation of a two-link flexible  
C arm. It is based on the example set by the CUBE.FOR program  
C in the VWSDEMO directory in the microvax.  
C

```

IMPLICIT INTEGER (A-Z)
EXTERNAL ENABLE_WINDOW_RESIZE
INTEGER UIS$CREATE_DISPLAY,UIS$CREATE_WINDOW
REAL VP_WIDTH,VP_HEIGHT,WC_X1,WC_Y1,WC_X2,WC_Y2
REAL RETX,RETY,x1
REAL XC1,YC1,R1,R2,R3,S,XS,YS,XD,YD
REAL X(500),Y(500),XR(20,500),YR(20,500),XC2(500),YC2(500)
REAL X2(500),Y2(500),X2R(20,500),Y2R(20,500),DLX2(500)
REAL XC3(500),YC3(500),T(500),DLX(500),DLY(500),DLY2(500)
PARAMETER (TINY=0.02)
CHARACTER*12 TIME(500),FAC
COMMON WC_X1,WC_Y1,WC_X2,WC_Y2,VP_WIDTH,VP_HEIGHT
COMMON NEW_ABS_X,NEW_ABS_Y,WD_ID,VD_ID

```

C  
C  
C

```

VP_WIDTH=50.
VP_HEIGHT=50.

```

C

```

WC_X1=-3.
WC_Y1=-3.
WC_X2=3.
WC_Y2=3.

```

C

```

XC1=0.0
YC1=0.0

```

C  
C  
C

Input data from ARMGAT.DAT.

```

OPEN (1,FILE='[USER.AVF.CARLOS.GRAF]ARMGAT',STATUS='OLD',
&      FORM='FORMATTED')
READ(1,3000) FAC
READ(1,*) KOUNT,R1,R2,R3
DO 600 I=1,KOUNT
  READ(1,3000) TIME(I)
  READ(1,*) X(I),Y(I),DLX(I),DLY(I)
  READ(1,*) XC2(I),YC2(I),X2(I),Y2(I)
  READ(1,*) DLX2(I),DLY2(I),XC3(I),YC3(I)
  DO 700 J=1,20
    READ(1,*) XR(J,I),YR(J,I),X2R(J,I),Y2R(J,I)
700   CONTINUE
600   CONTINUE
CLOSE(1)
3000  FORMAT (A12)

```

C  
C  
C

Create display.

```

6000  VD_ID=UIS$CREATE_DISPLAY(WC_X1,WC_Y1,WC_X2,WC_Y2,
&      VP_WIDTH,VP_HEIGHT)
CALL UIS$DISABLE_DISPLAY_LIST(VD_ID)
WD_ID=UIS$CREATE_WINDOW(VD_ID,'SYS$WORKSTATION',
&      'TWO-LINK FLEXIBLE ARM')

```

C

```

C
C
CALL UIS$SET_RESIZE_AST(VD_ID,WD_ID,ENABLE_WINDOW_RESIZE,,
& NEW_ABS_X,NEW_ABS_Y,VP_WIDTH,VP_HEIGHT)
CALL UIS$SET_WRITING_MODE(VD_ID,0,1,9)
CALL UIS$SET_WRITING_MODE(VD_ID,0,2,3)

C
C      Write permanent text to window.
C

CALL UIS$TEXT(VD_ID,2,'Time (sec):',-2.8,-2.8)
CALL UIS$GET_ALIGNED_POSITION(VD_ID,1,RETX,RETY)
CALL UIS$TEXT(VD_ID,2,'Flex. scale: '//FAC,1.6,-2.8)

C
C      Draw crosshairs.
C

CALL UIS$PLOT(VD_ID,2,XC1-0.5,0.,XC1+0.5,0.)
CALL UIS$PLOT(VD_ID,2,0.,YC1-0.5,0.,YC1+0.5)

C
C      Enter arm loop.
C

PRINT *,'Leave trace? (0-No,1-Yes)'
READ *,TRACE
IF (TRACE.EQ.0) THEN
    PRINT *,'Plot guides? (0-No,1-Yes)'
    READ *,GUID
    STEP=75
ELSE
    GUID=0
    STEP=1
ENDIF
CALL UIS$CIRCLE(VD_ID,2,XC1,YC1,R1)
JM=1
DO 2000 J=1,KOUNT
    CALL UIS$TEXT(VD_ID,2,TIME(J),RETX,RETY)
    XS=X(J)
    YS=Y(J)
    XD=X2(J)
    YD=Y2(J)
    CALL UIS$CIRCLE(VD_ID,2,XC1,YC1,R1)
    IF (GUID.EQ.1) THEN
        call uis$plot(vd_id,2,xs,ys,xs+d1x(j),ys+d1y(j))
    ENDIF
    CALL UIS$PLOT(VD_ID,2,XS,YS,XS+XR(1,J),YS+YR(1,J))
    DO 200 I=2,20
        CALL UIS$PLOT(VD_ID,2,XS+XR(I-1,J),YS+YR(I-1,J),
& XS+XR(I,J),YS+YR(I,J))
        CALL UIS$PLOT(VD_ID,2,XS+XR(I-1,J),YS+YR(I-1,J))
200    CONTINUE
    CALL UIS$CIRCLE(VD_ID,2,XC2(J),YC2(J),R2)
    IF (GUID.EQ.1) THEN
        call uis$plot(vd_id,2,xd,yd,xd+d1x2(j),yd+d1y2(j))
    ENDIF
    CALL UIS$PLOT(VD_ID,2,XD,YD,XD+X2R(1,J),YD+Y2R(1,J))
    DO 300 I=2,20
        CALL UIS$PLOT(VD_ID,2,XD+X2R(I-1,J),YD+Y2R(I-1,J),
& XD+X2R(I,J),YD+Y2R(I,J))
        CALL UIS$PLOT(VD_ID,2,XD+X2R(I-1,J),YD+Y2R(I-1,J))
300    CONTINUE
    CALL UIS$CIRCLE(VD_ID,2,XC3(J),YC3(J),R3)
    IF (TRACE.EQ.1) GOTO 5000

```

```

C
C      The following three lines draw the tip trajectory.
C
      if (j.ne.1) then
          call uis$plot(vd_id,2,xc3(j-1),yc3(j-1),xc3(j),yc3(j))
      endif
      IF ((J.NE.1).AND.(J.NE.JM).AND.(J.NE.KOUNT)) THEN
c      CALL UIS$CIRCLE(VD_ID,2,XC1,YC1,R1)
      IF (GUID.EQ.1) THEN
          call uis$plot(vd_id,2,xs,ys,xs+d1x(j),ys+d1y(j))
      ENDIF
      CALL UIS$PLOT(VD_ID,2,XS,YS,XS+XR(1,J),YS+YR(1,J))
      DO 400 I=2,20
          CALL UIS$PLOT(VD_ID,2,XS+XR(I-1,J),YS+YR(I-1,J),
&              XS+XR(I,J),YS+YR(I,J))
          CALL UIS$PLOT(VD_ID,2,XS+XR(I-1,J),YS+YR(I-1,J))
400      CONTINUE
      CALL UIS$CIRCLE(VD_ID,2,XC2(J),YC2(J),R2)
      IF (GUID.EQ.1) THEN
          call uis$plot(vd_id,2,xd,yd,xd+d1x2(j),yd+d1y2(j))
      ENDIF
      CALL UIS$PLOT(VD_ID,2,XD,YD,X2(J)+X2R(1,J),
&              YD+Y2R(1,J))
      DO 500 I=2,20
          CALL UIS$PLOT(VD_ID,2,XD+X2R(I-1,J),YD+Y2R(I-1,J),
&              XD+X2R(I,J),YD+Y2R(I,J))
          CALL UIS$PLOT(VD_ID,2,XD+X2R(I-1,J),YD+Y2R(I-1,J))
500      CONTINUE
      CALL UIS$CIRCLE(VD_ID,2,XC3(J),YC3(J),R3)
      ELSE
          JM=JM+STEP
      ENDIF

      5000      CONTINUE
          CALL UIS$TEXT(VD_ID,2,TIME(J),RETX,RETY)
      2000      CONTINUE
          CALL UIS$TEXT(VD_ID,2,TIME(KOUNT),RETX,RETY)
c      CALL UIS$CIRCLE(VD_ID,2,XC1,YC1,R1)
          PRINT *, 'Repeat? (0-No,1-Yes)'
          READ *,A
          IF (A.EQ.1) THEN
              CALL UIS$DELETE_DISPLAY(VD_ID)
              GOTO 6000
          ENDIF
          CALL UIS$SOUND_BELL('SYS$WORKSTATION')
          END
  
```

```

C
C
C
C
C
C
C
C
C
  
```

#### SUBROUTINE enable\_window\_resize

This routine will allow the user to change the size of the window. The user may not specify a window width or height of less than 3/10 of a centimeter. This routine is called from the resize ast routine.

```

COMMON wc_x1,wc_y1,wc_x2,wc_y2,vp_width,vp_height
COMMON new_abs_x,new_abs_y,wd_id,vd_id
  
```

```

IF (vp_width .LT. .30) vp_width = .30
  
```

```
IF (vp_height .LT. .30) vp_height = .30
CALL UIS$RESIZE_WINDOW(vd_id,wd_id,new_ubs_x,new_ubs_y,
1      vp_width,vp_height,
2      wc_x1,wc_y1,wc_x2,wc_y2)
```

```
RETURN
END
```